

ScholarWorks@GSU

Cellular responses to Rubella virus infection of neural progenitors derived from human embryonic stem cells

Authors	Xu, Jie
Citation	Xu, Jie. 2013. "Cellular responses to Rubella virus infection of neural progenitors derived from human embryonic stem cells." Georgia State University. https://doi.org/10.57709/4859069
DOI	https://doi.org/10.57709/4859069
Download date	2026-03-10 19:21:45
Link to Item	https://hdl.handle.net/20.500.14694/1933

CELLULAR RESPONSES TO RUBELLA VIRUS INFECTION OF NEURAL PROGENITORS
DERIVED FROM HUMAN EMBRYONIC STEM CELLS

by

JIE XU

Under the Direction of Dr. Teryl K. Frey

ABSTRACT

Rubella virus (RUBV) is a significant human pathogen. RUBV infection takes an enormous toll due to congenital rubella syndrome (CRS), a constellation of birth defects including blindness, hearing defects and mental retardation. Little is known about RUBV-induced teratogenesis due to the absence of useful models. This research is now enabled by the availability of human embryonic stem cells (hESCs) and hESC-derived precursor cell lines. Human neural progenitor cells (hNPCs) serve as a particularly relevant model due to the symptoms and complications of CRS related to neural system development. The overarching question addressed in this dissertation is: what is the mechanism underlying the development of neurological abnormalities seen in CRS? In this context, we investigated the cellular responses of hNPCs to RUBV infection comprehensively by: 1) assessing susceptibility of the cells to RUBV infection; 2) analyzing the effect of infection on cell proliferation; and 3) examining the impact of RUBV infection on differentiation of hNPCs into neuronal and astroglial lineages. We found that hNPCs are susceptible to RUBV infection and that the percentage of infected cells closely mimics CRS in which few cells har-

bor virus. The virus was able to persist in culture for up to one month without significant alteration of cell morphology and stemness marker expression. In addition, RUBV infection moderately attenuated the proliferation of undifferentiated hNPCs by triggering cell cycle arrest, but not apoptosis or other cell death events commonly seen upon virus infection. This lack of apoptosis appeared to be due in part to virus-induced anti-apoptotic suppression. Interestingly, the virus only had a marginal effect on the induction of cell differentiation into both neuronal and astroglial phenotypes. In fact, RUBV infection promoted terminal differentiation of the culture due to depletion of precursor cells. With differentiation, viral replication was suppressed. We thus propose a model for RUBV-induced neurological defects in which the virus acts by depleting precursor cell pools. The results of this study provide clues for elucidating the mechanisms of RUBV teratogenicity at the cellular level and serves as a potential reference study for elucidating mechanisms of teratogenesis induced by other infectious agents.

INDEX WORDS: Rubella virus, Congenital rubella syndrome, Teragoten, Central nervous system, Brain, Stem cells, Neural progenitors

CELLULAR RESPONSES TO RUBELLA VIRUS INFECTION OF NEURAL PROGENITORS DE-
RIVED FROM HUMAN EMBRYONIC STEM CELLS

by

JIE XU

A Dissertation Submitted in Partial Fulfillment of the Requirements for the Degree of

Doctor of Philosophy

in the College of Arts and Sciences

Georgia State University

2013

Copyright by

Jie Xu

2013

CELLULAR RESPONSES TO RUBELLA VIRUS INFECTION OF NEURAL PROGENITORS DERIVED FROM HUMAN EMBRYONIC STEM CELLS

by

JIE XU

Committee Chair: Teryl K. Frey

Committee: William Walthall

Yuan Liu

Rodney Nash

Electronic Version Approved:

Office of Graduate Studies

College of Arts and Sciences

Georgia State University

December 2013

DEDICATION

To my parent, Qingji Xu and Xiaohui Xu; my grandparents, Sheng Xu and Manwen Chen and my sister Xiaoxu Wang and Zheng Xu, with love.

ACKNOWLEDGEMENTS

I would like to thank my mentor, Dr. Teryl Frey, for providing me all possible guidance to attain this degree. I thank him for his encouragement throughout my time in this lab and his allowance for my research freedom as I have grown as a scientist; Dr. William Walthall, Drs. Yuan Liu and Dr. Rodney Nash, for their valuable input that has added to this work, and also for their support all the time towards my professional career development. I have enjoyed learning from my committee members, coursework, and the MBD program. I would like to thank Dr. Yumei Zhou for her assistance and guidance in all the projects I've been through during my Ph.D years, she fostered my scientific thinking and adjective attitude toward research. I would also like to thank Dr. Jason Mathews, for his patient mentorship and encouragement; he always saw something when I saw nothing from my negative results. I would like to thank Dr. Heather Mousa, for her patients with my writing , for her sentences in e-mail and hours of talk with me that gradually build up my self-confidence, for just being their all the times. I would also like to thank my lab mate Nadia Hunte and Christie Sleigher, for giving me so much wonderful and unforgettable memories in the lab. I would like to thank all of the members in Frey lab, for their technical assistance, encouragement, and especially friendship. I would lastly like to thank my GSU friends, who have become like family to me. You have all have seen me through the highest and lowest moments of my personal and professional life and I am grateful for your friendship through it all. Finally, special thanks to Zhiqi Yu, for your support technically and emotionally through my Ph.D year, for your unchanging patience to my routinely complains, for your warmest and kindest resolution towards every of our ups and downs.

TABLE OF CONTENTS

ACKNOWLEDGEMENTS	V
LIST OF TABLES.....	XI
LIST OF FIGURES.....	XII
LIST OF ABBREVIATION	XIV
CHAPTER 1 : GENERAL INTRODUCTION.....	1
1.1 RUBELLA VIRUS CLASSIFICATION AND RELATED VIRUSES	1
1.2 RUBELLA VIRUS STRUCTURE, LIFE CYCLE, AND CODING STRATEGY	2
1.3 RUBELLA: A BRIEF OVERVIEW	4
1.4 RUBELLA: THE DISEASE.....	5
1.4.1 Acute infection.....	5
1.4.2 Congenital Rubella Syndrome	6
1.4.3 Teratogenesis of rubella: mechanistic studies	8
1.5 NEUROLOGICAL ASPECTS OF RUBELLA VIRUS.....	11
1.5.1 Postacute Rubella encephalitis.....	12
1.5.2 CRS associated neurological anomalies.....	12
1.5.3 Progressive Rubella Panecephalitis.....	13
1.6 HUMAN EMBRYONIC STEM CELL DERIVED PROGENITOR CELLS AS A MODEL .	15
1.7 VIRUS INFECTION OF PROGENITOR CELLS: REVIEW OF PREVIOUS WORKS	18
1.8 RESEACH OVERVIEW	20
CHAPTER 2 : CHARACTERIZATION OF RUBV INFECTION OF HUMAN NEURAL PROGENITOR CELLS	35

2.1 INTRODUCTION	35
2.2 MATERIAL AND METHODS	36
2.2.1 Cell culture	36
2.2.2 Virus stock preparation and infection	37
2.2.3 RUBV growth curve characterization (infection strategy and plaque assay).....	37
2.2.4 Virus genome detection by reverse-transcription PCR (RT-PCR) and quantitative reverse-transcription PCR (qRT-PCR)	38
2.2.5 Live-cell morphology changes	38
2.2.6 Immunofluorescent assay (IFA)	39
2.2.7 Flow cytometry	39
2.2.8 Western Blot.....	40
2.3 RESULTS	41
2.3.1 hNPCs are permissive for RUBV infection	41
2.3.2 Infected hNPCs support a modest-level of replication of RUBV	41
2.3.3 RUBV undergoes genetic modifications during infection in hNPCs.....	42
2.3.4 RUBV infected hNPCs did not develop CPE	43
2.3.5 RUBV infected cells exhibit hNPC stemness marker	43
2.3.6 Influence of long-term RUBV infection on biological features of hNPCs	43
2.4 DISCUSSION.....	46
CHAPTER 3 : RUBV ATTENUATES HUMAN NEURAL PROGENITOR CELL GROWTH BY MITOTIC INHIBITION INSTEAD OF TRIGGERING CELL DEATH.....	60
3.1 INTRODUCTION	60

3.2 MATERIAL AND METHODS	61
3.2.1 Cell culture	61
3.2.2 Cell growth curve characterization	61
3.2.3 EdU incorporation assay	61
3.2.4 Apoptosis assays	62
3.2.5 Cell death assay by propidium iodide staining.....	62
3.2.6 Proliferation assays	63
3.2.7 Image processing by Cell Profiler	63
3.3 RESULTS	64
3.3.1 RUBV slightly decreases hNPC proliferation.....	64
3.3.2 RUBV did not induce apoptosis and other cell death events in infected hNPCs	65
3.3.3 RUBV induces mitotic inhibition (cell senescence) in hNPCs	66
3.3.4 The ability of RUBV to alter cell adhesion may contribute to the reduction of hNPC proliferation.....	66
3.3.5 RUBV did not induce inflammatory cytokine responses in hNPCs cultures	67
3.4 DISCUSSION	68
 CHAPTER 4 : CHARACERIZATION OF THE EFFECT OF RUBV INFECTION ON HUMAN NEURAL PROGENITOR CELL DIFFERENTIATION INTO NEURONS AND GLIAL CELLS 82	
4.1 INTRODUCTION	82
4.2 MATERIAL AND METHODS	83
4.2.1 Cell culture and differentiation	83
4.2.2 Monitoring the stage of differentiation and the loss of multipotency by flow cytometry..	85

4.2.3 Cell differentiation marker expression profiling by qRT-PCR	85
4.2.4 Immunofluorescence staining of differentiated hNPCs	86
4.2.5 Viral susceptibility studies	86
4.3 RESULT	87
4.3.1 Effect of RUBV infection on hNPCs neurogenesis	87
4.3.2 Effect of RUBV infection on hNPC gliogenesis.....	91
4.4 DISCUSSION	95
CHAPTER 5 : SINDBIS VIRUS INFECTION INDUCES APOPTOSIS AND TRIGGERS PREMATURE DIFFERENTIATION OF HUMAN NEURAL PROGENITORS.....	121
5.1 INTRODUCTION	121
5.2 MATERIAL AND METHODS	122
5.2.1 Cell culture	122
5.2.2 Virus stock preparation and infection	122
5.2.3 SINV growth curve characterization.....	123
5.2.4 Live-cell morphology changes.....	123
5.2.5 Immunofluorescent assay (IFA)	123
5.2.6 Proliferation assay	124
5.2.7 Flow cytometry	124
5.2.8 Western Blot.....	124
5.3 RESULTS	125
5.3.1 hNPCs are fully permissive to SINV infection	125

5.3.2 SINV inhibits hNPCs proliferation by inducing apoptosis but not cell cycle arrest	126
5.3.3 Proliferating hNPCs lost cellular multipotency/stemness upon SINV infection.....	127
5.3.4 SINV modulates multiple cell signaling pathways of hNPCs during infection	127
5.4 DISCUSSION.....	128
CHAPTER 6 : GENERAL CONCLUSION, SIGNIFICANCE AND FUTURE DIRECTION	137
6.1 GENERAL CONCLUSIONS AND SIGNIFICANCE.....	137
6.1.1 Working model for CRS and RUBV induced neurological diseases	137
6.1.2 hESC derived neural progenitors as a model to study viral teratogenesis	138
6.1.3 Significance.....	139
6.2 FUTURE DIRECTIONS	140
REFERENCES.....	142
APPENDICES.....	158
APPENDIX A. HYPOTHETICAL STATISTIC TEST	158

LIST OF TABLES

Table 1.1 Teratogenesis of HCMV and RUBV.....	22
Table 1.2 In vitro studies of RUBV infection in embryonic, fetal and neuronal cultures.	25
Table 1.3 Characteristics features of neurotropic viruses and their effects on the hNPCs.....	27
Table 4.1 List of target genes and primers used in gene expression profiling study	104
Table 4.2 Description of markers used in this study.....	105

LIST OF FIGURES

Figure 1.1 Cryo-electron micrograph of rubella virion.....	29
Figure 1.2 Schematic representation of the RUBV genome, translation and processing strategy of the RUBV nonstructural and structural proteins.	30
Figure 1.3 Schematic representation of the RUBV replication cycle.	31
Figure 1.4 Proposed pathogenesis of congenital rubella.....	32
Figure 1.5 Embryonic neural development and the timing of NPC differentiation.	33
Figure 1.6 Embryonic neural stem cell (NSC and/or NPC) pathway in vitro and major markers for identification of each cell type before and after differentiation.....	34
Figure 2.1 Viral antigen detection and percentage of infected cell determination by indirect immunoflorescent assay.....	53
Figure 2.2 Viral RNA detection at early and late times of infection..	54
Figure 2.3 RUBV growth curve in proliferating hNPCs.	55
Figure 2.4 Plaque size comparison between stock RUBV and hNPCs produced RUBV.	56
Figure 2.5 Infected cells display the hNPC stemness marker Nestin.	57
Figure 2.6 RUBV persists in hNPCs without altering their morphology and undifferentiated phenotype.....	59
Figure 3.1 hNPC growing kinetics in presence and absence of RUBV.	75
Figure 3.2 Proliferation of hNPC vs A549 after RUBV infection as measured by EdU incorporation assay.	76

Figure 3.3 RUBV did not induce apoptosis in infected hNPCs.....	78
Figure 3.4 RUBV induce cell senescence to hNPCs.	79
Figure 3.5 RUBV infection of hNPCs did not increase the number of "Floaters".	80
Figure 3.6 RUBV did not induce inflammatory responses in hNPCs.	81
Figure 4.1 hNPC spontaneous differentiation is primarily into neurons.....	108
Figure 4.2 Effect of RUBV infection on spontaneous differentiation of hNPCs.	110
Figure 4.3 RUBV infection did not impair hNPC neurogenesis.	112
Figure 4.4 Lack of permissivity to the RUBV infection of hNPCs under spontaneous differentiation.	114
Figure 4.5 Differentiation of hNPCs into astroglial cells.....	116
Figure 4.6 Effect of RUBV infection on hNPCs astroglial differentiation.....	117
Figure 4.7 Effect of RUBV infection of gene expression during hNPC astroglial differentiation. ..	118
Figure 4.8 Lack of permissivity to RUBV infection of hNPCs following astroglial differentiation..	120
Figure 5.1 hNPCs are highly susceptible to SINV infection.....	134
Figure 5.2 Effect of SINV infection on hNPCs proliferation and undifferentiated phenotype.....	136
Figure 6.1 Proposed model for RUBV teratogenesis in the central nervous system.....	141

LIST OF ABBREVIATION

BDV: Borna Disease virus

CHIKV: Chikungunya virus

CMV: Cytomegalovirus

CVB3: Coxsackie virus B3

HCMV: Human Cytomegalovirus

HIV-1: Human Immunodeficiency virus Type I

HSV: Herpes simplex virus

JEV: Japanese Encephalitis virus

RRV: Ross River virus

RUBV: Rubella virus

RV: Rabies virus

SINV: Sindbis virus

VEEV: Venezuelan equine encephalitis virus

WNV: West Nile virus

ORF: Open reading frame

Envelope: E

Capsid: C

RCs: Replication complexes

NSP: Nonstructural protein

IFN: Interferon

CRS: Congenial Rubella Syndrome

PRP: Progressive Rubella Panecephalitis

CNS: Central nervous system

SGZ: Subgranular zone

SVZ: Subventricular zone

hESC: Human embryonic stem cell

hNPC: Human neural progenitor cell

hMPro: Human mesenchymal progenitor cell

CHAPTER 1 : GENERAL INTRODUCTION

1.1 RUBELLA VIRUS CLASSIFICATION AND RELATED VIRUSES

Rubella virus (RUBV) is the sole member of the genus *Rubivirus* in the family *Togaviridae* [1]. This family includes animal viruses with ribonucleic acid (RNA) genomes of positive-polarity (mRNA sense) of ~10,000 nt in length. Togaviruses have small round virions that consist of a quasispherical nucleocapsid surrounded by a lipid bilayer envelope. All members of this family replicate in the host cell cytoplasm within a membranous replication complex (RC) derived from host structures and do not integrate into the genome of the host.

The other 26 members of the *Togaviridae* family, such as the well studied Sindbis virus (SINV), Semliki forest virus (SFV), Chikungunya virus (CHIKV), Venezuelan equine encephalitis virus (VEEV), and Ross River virus (RRV), all belong to the genus *Alphavirus* [2]. Alphaviruses are classified into Old World and New World viruses dependent on their geographical distribution. Diseases symptoms can range from rash and fever with Old World viruses to encephalitis with New World viruses. The alphavirus and rubivirus genera mainly differ in following two respects. First, all alphaviruses are arthropod (mosquito)-borne and infect humans, mammals, and birds. RUBV does not circulate through arthropods and humans are the only host. Secondly, the alphavirus and rubivirus genera share no homology at either the nucleotide or amino acid level and exhibit no antigenic cross reactivity. However, due to the similarities in their genomic coding strategies and replication cycles between the two genera of *Togaviridae*, important parallels may be drawn between RUBV and the alphaviruses. SINV, for example, causes rash and fever in humans but age-dependent encephalitis in mice, therefore serving as a model to study viral encephalitis induced by viruses in the *Togaviridae* family [3, 4]. Another example is SFV, which infects developing fetuses in mice and is used as a model to study viral teratogenic effects due to its broad tropism [5]. However, unlike RUBV, which replicates slowly and asynchronously in host cells, most alpha-

viruses replicate quickly and induce a lytic cycle. This has to be taken into consideration in comparative virology studies.

1.2 RUBELLA VIRUS STRUCTURE, LIFE CYCLE, AND CODING STRATEGY

In electron micrographs rubella virions generally appear round with a mean diameter of 70 nm (Figure 1.1). The virion is surrounded by an envelope derived from host lipid membranes. Embedded in this envelope are two viral glycoproteins, E1 (58 kDa) and E2 (44-52 kDa), which can be resolved as spikes on the surface of the envelope. The quasispherical core inside the envelope is made up of the viral capsid protein, C (34 kDa), in the form of disulfide-linked homodimers. The viral RNA genome contained within the core is considered as an integral component of the core structure [6].

RUBV has a 5'-capped and 3'-poly (A)-tailed RNA genome of almost 10 kb in length. The genome has a G+C content of 69%, which is among the highest of all of the RNA viruses identified to date. The genome is comprised of two polycistronic open reading frames (ORFs) separated by a nontranslated region [7]. The 5' ORF encodes two nonstructural replicase proteins, P150 and P90, which are proteolytically processed from one precursor called P200. The 3' ORF encodes three proteins, E1, E2 and C, that form the virion structure and are similarly processed from a single precursor, but translated from a subgenomic RNA that consists of sequences from the 3' terminal third of the genome RNA (Figure 1.2) [8].

The RUBV life cycle begins with the attachment of the virion to the host cell; this process is rapid with adhesion occurring anywhere from 30 minutes to 3 hours post-infection [9]. The only known RUBV receptor is myelin oligodendrocyte glycoprotein (MOG) [10]. Next, the virus enters the cell through low pH-mediated endocytosis. Release of the viral genetic material into the cytoplasm is thought to be triggered by low pH-mediated conformational changes to the viral glycoproteins that allow the fusion of the viral and endosomal membranes. Once the RUBV genetic material has been released, replication of the genome begins. During viral replication, the genomic RNA serves as the mRNA for the nonstructural protein precursor and as the template for the synthesis of a full-length negative-polarity RNA strand. The

minus strand in turns acts as the template for the transcription of both the genomic and subgenomic RNAs, with the subgenomic RNA serving as the mRNA for the translation of structural proteins. The replication process was thought to take place in replication complexes (RCs), vacuoles which form on the surface of viral-modified endosomes and lysosomes. The converted organelles, known as “cytopathic vacuoles”, recruit other cellular structures such as the rough endoplasmic reticulum (RER), Golgi, and mitochondria to the site of replication, thus providing the RCs with all the energy, ribosomes, and protein processing required for successful replication [11]. Following the replication of the genome RNA and synthesis of the structural proteins, the RNA and capsid protein coalesce to form capsids. Following this encapsidation process, de novo virions are formed by budding of the capsid through membranes of the Golgi in which the glycoproteins have accumulated. Virions are eventually released from the cell via the exocytotic pathway (Figure 1.3).

In terms of kinetics, both the genomic and subgenomic RNA are detectable at the end of the viral latent period of 12-24 hours, with the viral structural proteins appearing 4 hours later. Peak virus production usually occurs during the period from 36 to 48 hours post infection (h.p.i) in permissive cell lines such as Vero and BHK/21. Infection of culture cells is asynchronous (meaning that the cells in the culture do not become infected at the same time), even when high multiplicities of infection (MOIs) are used, and relatively noncytopathic [12].

As noted above, SINV shares a similar virus life cycle with RUBV. The viral 11.7 kb RNA genome serves as an mRNA for the nonstructural polyproteins P123 and P1234. The structural proteins, capsid, E1, and E2 are translated from a subgenomic RNA. E2 is synthesized as a precursor, pE2 that is cleaved to E2 and E3 late in replication to produce the mature E2 necessary for virions to be infectious. Heterodimers of E1 and E2 trimerize to form the spikes of the mature virion. Virion formation is by budding of the capsid through the cytoplasmic membrane [13]. In contrast to RUBV, SINV replication is rapid (completed within 24 hours in permissive cell lines), high titer (100 X titers achieved by RUBV), and lytic in nature.

1.3 RUBELLA: A BRIEF OVERVIEW

RUBV is the causative agent of the disease rubella. The disease was initially recognized by two German physicians, Bergen and Orlow in 1752 and 1758, respectively [14]. It was not until 1866 that the then “German Measles” was termed rubella by Scottish physician Veale, who further elaborated on its clinical characteristics [15]. The cornerstone for rubella as a disease of significance, rather than a benign illness, was the discovery of its role in causing congenital birth defects. This was achieved in 1940 by Australian ophthalmologist Norman Gregg, who observed that there was resounding evidence of pregnant mothers with rubella transmitting congenital defects to her offspring, including cataracts, deafness, small size, low birth weight, and heart defects [16]. The term congenital rubella syndrome (CRS) was given to describe the collection of birth defects caused by RUBV.

Rubella is endemic worldwide, with regular seasonal peaks occurring in the spring months in temperate climates. Before the introduction of vaccine, epidemics of rubella occurred at the interval of 6 to 9 years in the United States. Rubella and CRS became nationally notifiable disease in 1966. The largest annual total of cases of rubella in US was in 1969, when 57,686 cases were reported. Following vaccine licensure in 1969, rubella incidence declined rapidly in the United States and the reported cases since the 1990s are mostly among the foreign-born and unvaccinated Hispanics and Latin Americans, with elimination of indigenous rubella in the United States achieved in 2004 [17-19]. However, given that there is no treatment for CRS, rubella is still a major concern in most developing countries where vaccination is rarely provided [20, 21].

Rubella vaccination is accomplished by parenteral injection of live attenuated rubella strains grown in human diploid fibroblast cells [22]. The first rubella vaccine was the HPV-77 strain, licensed in 1969, seven years after the isolation of the virus [23]. Today, with the exception of Japan, the vaccine in use is the RA 27/3 virus [24], which was attenuated and produced in cultures of fetal human diploid fibroblast cells during the early 1960s in the Stanley Plotkin laboratory [25]. The immunogenicity of the RA 27/3

virus is high, leading to seroconversion in close to 100% of vaccinees [26]. It is important to note that RA 27/3 is available in combination with measles, mumps and varicella vaccines. The current vaccination strategy utilizes the measles-mumps-rubella (MMR) vaccine with one dose at 12-15 months of age and a second at 5-10 years of age [27]. However, despite vaccination programs it is believed that 10% to 20% of post pubescent individuals are still susceptible to rubella in developed countries and up to 68% are susceptible in developing countries, allowing for the continued transmission of RUBV among women of reproductive age, the group at risk [28-30]. The addition of the rubella vaccine to their 2008 initiatives by the Global Alliance for Vaccines and Immunization (GAVI) further emphasized rubella and CRS as major public health issues worldwide and further asserts the importance of the study of this virus [31].

1.4 RUBELLA: THE DISEASE

1.4.1 Acute infection

RUBV is transmitted by the respiratory route, resulting in mild disease (acute or acquired rubella) that typically exhibits in symptoms such as rash, low-grade fever, lymphadenopathy, and conjunctivitis [29]. The disease has a general incubation period of 12 to 22 days before the onset of rash. The virus replicates first in the nasopharynx and then in regional lymph nodes, resulting in viremia 7 days before the rash. A second round of viremia is thought to be generated from virus replication in target organs such as the spleen and distant lymph nodes [32]. Immune responses such as generation of neutralizing antibodies, cessation of viremia, and appearance of transformed lymphocytes can be seen 2 to 3 days after the onset of rash [33]. The end of the disease state occurs with the resolution of the rash. Complications of rubella such as arthralgia, thrombocytopenia, encephalopathy, and hemorrhagic manifestations are not common, but occur more often in adults than in children [34, 35]. The most devastating effect of RUBV infection is CRS, which is caused by the infection of the placenta and fetus during viremia.

1.4.2 Congenital Rubella Syndrome

While infection with RUBV only causes mild disease when contracted postnatally, it can cause severe birth defects in a developing fetus during pregnancy. The term congenital rubella syndrome (CRS) is defined by South and Sever to denote any combination of the complications known to result from gestational rubella [36].

The range of defects, before and after birth, caused by RUBV infection has been well documented and they almost exclusively result from infection in the first trimester [37]. The main defects associated with CRS are deafness, cataracts, cardiovascular defects, particularly patent ductus arteriosus, and CNS damage including to mental retardation. Neonatal manifestations that result from infection include a wide range of transient symptoms, but growth retardation and failure to thrive are the most severe. Postnatal defects, which were found by monitoring of CRS survivors for up to 50 years, include insulin-dependent diabetes, thyroid dysfunction, and a rare neurodegenerative disorder- progressive-rubella panencephalitis (or PRP) [38, 39]. The incidence of above mentioned defects are: intrauterine growth retardation such as microcephaly (62%), cardiac disease (52%), deafness (48%), cataracts (18%), and mental deficiency (5%) [33]. Despite the difference in the frequency of each type of defect, two common features of CRS fetuses are reduced size of affected organs and angiopathy of early placental and embryonic tissues. Microscopic analysis of aborted RUBV infected fetuses revealed cellular damage in multiple sites, with non-inflammatory necrosis being common in the eyes, heart, brain, and ears [40, 41].

The two most important features of CRS from a virological point of view are as follows. First, the efficiency of fetal infection and degree of severity of CRS symptoms are most pronounced when infection occurs during early pregnancy. During the first trimester of pregnancy, the rate of fetal infection approaches 80% and most of the infants exhibit symptoms. The risk of fetal infection and the severity of congenital abnormalities decreases after first trimester; after 17 weeks gestation the risk of developing any defects is low (25-35%) [9, 42-44]. This is partially due to changes in the placenta during second tri-

mester which allows sufficient transfer of maternal RUBV-specific IgG antibodies to the fetus [41]. Meanwhile, fetal IgG as well as alpha-interferon (IFN) is readily detectable in the sera of midgestational RUBV- infected fetuses, implying that fetus starts producing its own immune responses after the first trimester to combat RUBV infection [45, 46]. The second important feature is the persistence of RUBV in CRS patients, making congenital rubella a contagious disease. Children born after exposure to RUBV *in utero* continue to shed virus in the nasopharynx and urine for months after birth and the virus has been shown to persist in human tissues for several years [47]. In one case, RUBV was cultured from cataract material as late as three years after birth [48]. *In vitro* study of RUBV carrier cultures derived from congenitally infected abortuses also demonstrated recovery of the virus in most organs including brain, which rarely can be infected due to the presence of blood-brain barrier [49]. Serological testing has demonstrated persistence of RUBV antibody in congenitally infected patients and many have elevated titers for over twenty years [50, 51]. Therefore, the persistence of RUBV infection may play a significant role in the development of late onset manifestations of CRS [52].

Currently there is no cure for CRS. RUBV has long been recognized as teratogen [53] and furthermore was among the initial group of infectious teratogen that were categorized as TORCH agents (toxoplasmosis, other virus such as varicella zoster virus and syphilis, rubella, cytomegalovirus, and herpes simplex virus) a medical acronym for a set of perinatal infections that lead to severe fetal anomalies and even fetal death [54, 55]. Of these, RUBV was the most efficient in terms of incidence of defects following maternal infection. Early on, RUBV was one of the best model systems to study viral teratogenesis due to sufficient numbers of aborted CRS fetal specimens and such studies date back to early 1940s[56]. However, with the decline of the disease after institution of vaccination programs ~1970, such studies ceased. Despite the elimination or near elimination of rubella and CRS in developed countries, the fact that the incidence of CRS remains very high in developing countries emphasizes the continued importance of the study of RUBV-induced teratogenicity. Additionally, there are likely common mechanisms that RUBV shares with other teratogenic agents..

1.4.3 Teratogenesis of rubella: mechanistic studies

Following congenital RUBV infection, the explicit pathways leading to teratogenesis remain to be elucidated. While the consequences of CRS are well documented, exactly how the virus causes this dramatic effect has been the subject of much speculation. In fact, the study of RUBV as a teratogen can be dated back to late 1960s when scientists examined clinical specimens, which were still available, and used different animal models to simulate CRS, without success [57, 58]. Recently with advanced techniques, insights into RUBV-induced teratogenicity at the cellular level have been gained. Several hypotheses have been posed by the findings of this research, based both on the virus' replication and ability to establish persistence in culture cells, which mimics the persistent infection established by the virus in the infected fetus. The major hypotheses are summarized as follows:

(a) Noncytopathic RUBV infection of selected embryonic cell types upsets the delicate balance of proliferation and differentiation with a profound effect on organogenesis. RUBV generally establishes a chronic nonlytic infection in the fetus and has the potential to infect any organ [59]. *In vivo*, examination of RUBV-induced cataractous eye lenses from first-trimester fetuses revealed lens development was retarded [40]. A recent clinical study of CRS patients with motor deficiencies revealed the most serious motor deficits are associated with first 4 weeks of gestation, when the structures that will be involved in a particular motor activity are in their most crucial stage of organization and differentiation [60]. *In vitro*, RUBV multiplication has been demonstrated in murine embryonic cells, human embryo derived cultures as well as human fibroblasts [5, 49, 61-63]. Human mesenchymal stem cells derived from embryonic cells persistently infected with RUBV display an altered responsiveness to the growth-promoting properties of epidermal growth factors as well as a decreased capacity for collagen synthesis, a sign of abnormal differentiation [64]. Therefore, RUBV infection may contribute to the development of CRS by affecting cell differentiation and the following organogenesis.

(b) RUBV infection in early fetal cells, including progenitor cells, is able to cause a cell-growth inhibition, by slowing down or halting the cell cycle. A constant feature of CRS is fetal growth retardation, perhaps due to reduced or slower cell division in infected cells [36, 65]. A number of *in vitro* studies have shown that the RUBV infected cells divide more slowly than do uninfected cells [7, 66]. Cell strains derived from different fetal human organs, although demonstrated no sign of cell death and morphological changes, exhibited tissue specific responses to RUBV. Those diploid cells derived from human fetal lung, kidney or pituitary ceased growth within a few passages; while this effect is inapparent in skin and muscle, a high percentage of chromosome breakage was observed [61, 63, 67]. *In vitro* growth inhibition has been attributed to a protein present in the culture fluid which inhibited mitosis [68]. Moreover, it has been reported that the RUBV nonstructural protein P90 associated with the cellular citron-K kinase, potentially causing cell cycle aberrations [69, 70]. “Clones of infected cells” isolated from CRS abortuses indicated that only 1 in 10^3 to 10^5 of cells from the infected fetal organs harbored the virus and these infected cells always clustered in infected organs. Thus, the growth retardation effect of RUBV infection is restricted so that infected fetus can still be born and serve as a vector for spread of the virus [52].

(c) Destruction of formed organs seen in CRS is partially due to cell death such as apoptosis and necrosis. Microscopic analysis of aborted infected fetuses revealed non-inflammatory necrosis being common in the structure of the eyes, heart, brain, and ears [71, 72]. Cell necrosis may occur at the time of initial infection or at a later stage in development. For this to happen the virus still has to gain entry into susceptible cells, but the damage may not occur until later due to growth of virus which has persisted in infected cells [33]. High multiplicity RUBV infection induces apoptosis in many types of cells, including Vero, BHK21 and RK13, although there are discrepancies among the proposed mechanisms of induction among these studies [73-77]. Moreover, multiplication of RUBV induced apoptosis in both rat neural and glial cells, both of which are representative of terminally differentiated cells [78-80]. It has been proposed that during congenital rubella infection, RUBV destroys precursor cells by induction of apoptosis [76]

Thus, inhibition of cell growth and cell death, alone or in concert, could be contribute to the pathogenesis of CRS.

(d) In addition to these direct effects of RUBV replication in host tissue, there is evidence that perinatal and also postnatal damage is, at least in part, immune mediated. Pathological signs in infants who die at some interval after birth usually include mononuclear inflammatory infiltrates in one or more organs, particularly the lung and brain [81]. Although *in vitro* studies have shown that RUBV is a poor inducer of IFN compared to other teratogenic viruses, a substantially higher amount of IFN is detected in placenta during midgestational stage [36, 82, 83]. A cytokine storm model has also been proposed recent years considering the failure of multiple organs in CRS infants [84]. Circulating immune complexes containing RUBV antigens are found in the serum of nearly half of all infants with CRS and there is an increased likelihood of finding rubella-specific immune complexes in the serum of CRS children with active clinical problems [85]. In addition, immune mediated responses have long been considered involved in the pathogenesis of late-onset complications. A molecular mimicry between RUBV peptides with cellular myelin oligodendrocyte glycoprotein is thought to contribute development of neurological anomalies seen in mice infected with RUBV

(e) Persistent RUBV infection in the developing fetus contributes to the CRS symptoms both at birth and late onset. A number of studies have investigated the cellular effects of a persistent RUBV infection in tissue culture, a persistence that can be correlated to persistent fetal infection by RUBV [64, 86]. RUBV persistence is maintained without a proviral DNA intermediate, as seen in latent retroviral infections, even in the presence of neutralizing antibodies in the culture medium, which also correlates with persistence in the infected fetus from late in gestation when the fetus develops the ability to make antibodies [87]. Joklik proposed several mechanisms which could play a role in the maintenance of persistent virus infections [88]. These included the presence of endogenous interferon, defective interfering (DI) particles, and temperature-sensitive (ts) mutants. These mechanisms have been examined in an attempt to explain persistent RUBV infections.

(f) The ongoing RUBV replication can impact normal host cell function, notably, mitochondrial abnormalities and disruption of the host cell cytoskeleton [8, 89, 90]. The mitochondrial dysfunction is proposed because RUBV replicates in close association with the mitochondria [91, 92]. Mitochondria are also related to cell death since they contain and release proteins that are an integral part of the apoptotic cascade. As for the cytoskeleton, infection with RUBV has a profound effect on the organization of actin in both Vero and BHK21 cells. Actin microfilaments were observed to disintegrate progressively into amorphous aggregates as the infection proceeds [8, 89]. In addition, the observation of actin assembly inhibition in RUBV infected cells strongly suggests that attenuated mitosis as well as abnormal size of RUBV-infected cells could cause some of the pathology of CRS [93].

Apparently, the mechanism underlying RUBV teratogenesis is likely to be multifactorial and the routes are not limited to above discussed aspects, since many other cellular events that could be affected by RUBV infection still remain unknown in both precursor and differentiated cell lines. A summary of the pathogenesis of maternal and congenital rubella is provided (Figure. 1.4).

1.5 NEUROLOGICAL ASPECTS OF RUBELLA VIRUS

RUBV was one of the first viruses demonstrated to cause congenital anomalies after gestational exposure, and, more than 50 years since this discovery; it remains a model for viral teratogenic effects on the central nervous system [16, 94]. Of particular relevance to psychiatric disorders, CRS has clear developmental manifestations involving the nervous system, including hearing defects, mental retardation, ventriculomegaly, encephalitis, cataracts, and childhood psychiatric disorders such as schizophrenia, autism, separation anxiety, and impaired social relations [95]. Relating to the CNS, sequelae of RUBV infection include three distinct neurological syndromes: a post-infectious encephalitis following acute infection (acute encephalitis and Guillian Barr Syndrome), a spectrum of neurological manifestations following congenital infection (microcephaly, mental retardation, schizophrenia, etc.) and a rare neurodegenerative disorder following either postnatal and perinatal infection, progressive rubella panencephalitis (PRP)

[78, 96, 97]. Although virus invasion and replication in the brain has been demonstrated in CRS and appears to account for the majority of neurological lesions observed, the pathogenesis of these other syndromes is incompletely understood [33, 98, 99]. The following paragraphs will describe each syndrome in detail.

1.5.1 Postacute Rubella encephalitis

Although post-acute rubella encephalitis is relatively rare (1 in 5,000-10,000 cases), prior to the advent of vaccination programs, rubella was a leading cause of encephalitis among children [100]. The average onset of encephalitis is 4 days after the appearance of a rubella rash; in fatal cases, death usually ensues within 3 days. In fatal cases, autopsy reveals diffuse nonspecific neural degeneration, edema, the presence of perivascular lymphocytes, but neither demyelination nor pronounced inflammatory damage [101]. The presence of rubella antibodies has been demonstrated in most patients; however, positive detection of virus by PCR has been rarely successful [102, 103]. Therefore, it is generally thought that the pathogenesis is immunological in nature, either due to a hypersensitive reaction or to a molecular mimicry between RUBV and host antigens that triggers an autoimmune response [103, 104]. However, all of these hypotheses are contradictory to the lack of inflammation in most cases. Thus, the pathogenesis of post-acute rubella encephalitis is unresolved. In addition to encephalitis, acute RUBV infection has occasionally been associated with cases of Guillain-Barre syndrome [105].

1.5.2 CRS associated neurological anomalies

It is estimated that as many as 80% of CRS patients exhibit neurological disorders, which can be devastating in the most severe forms. Microcephaly, motor deficits, mental retardation, autism and schizophrenia are commonly encountered with development of affected individuals [94]. CRS brain examinations exhibit rare gross structural malformations. The most notable lesions are: (a) vascular abnormalities including focal destructions of blood vessels, defects of internal elastic lamina, deposition of granular material and endothelial proliferations; (b) reduced cortical width with enlarged ventricles; (c) necrosis in

white matter with decreased number of oligodendrocytes [36, 40, 65]. Inflammatory changes in the brain were described as minimal at the most [106]. RUBV has been recovered from CSF and brain tissue of infants with clinical CRS, strongly indicating a direct involvement of the virus in CNS complications [60]. As far as how the virus induces damage in brain, different mechanisms have been proposed. The microcephaly in CRS infants would be consistent with the concept that the virus can infect the neuroepithelium and reduce cell proliferation. Despite a wealth of experimental evidence showing RUBV induces mitotic arrest (see part 1.4.3), cultures of CRS brain derived cells also display poor growth and stop to proliferating within 3 passages [98]. RUBV triggered apoptosis of neuronal cells, especially oligodendrocytes, has been shown in multiple studies using a rat model [80, 107]. In human cell culture, the virus selectively and heavily infects astrocytes, but such specificity has not been described *in vivo* [108]. Since the primary time in gestation when RUBV exhibits profound teratogenicity (i.e first trimester) coincides with organogenesis in the developing fetus, another favored hypothesis is that alterations induced in infected fetal progenitor cells ultimately affects organ development. This idea is further supported by the recently developed “schizophrenia hypothesis” after a strong correlation was observed between infection by a number of viruses, both congenital and peripheral, and the development of late onset psychiatric diseases [96, 97]. The schizophrenia hypothesis states that schizophrenia results from a disruption in programmed maturation of the brain in prenatal and early neonatal life [109]. Therefore, susceptibility of fetal progenitor cells to RUBV infection should be investigated. However, one should not ignore that vascular damage may also play a role in the overall pathogenesis of CRS. Additionally, the involvement of viral persistence may be implicated as infants who exhibit prolonged persistence do not fare as well medically as those who clear the virus.

1.5.3 Progressive Rubella Panencephalitis

Progressive rubella panencephalitis (PRP) was first described by Weil et al., in 1975 as a chronic, inflammatory, and progressive CNS disorder associated with either delayed reaction to congenital rubella or acute postnatal rubella infection [110]. PRP is universally fatal and only a few cases have been reported

[111, 112]. Patients usually develop PRP in their second decade of life, undergoing a period of several years of a protracted clinical course consisting of intellectual deterioration, seizure, myoclonus, cerebellar ataxia, and cortical spinal tract signs. Laboratory tests revealed high titers of rubella antibodies in serum and CSF and the occurrence of oligoclonal CSF IgG, suggesting a local production of immunoglobulin in the CNS [113, 114]. The neuropathological investigation showed meningeal and perivascular plasma cells and lymphocytes, gliosis, and glial nodules as well as diffuse neuronal loss. Inclusion bodies and/or virus structures, as seen in subacute sclerosing panencephalitis (SSPE), a disease associated with measles virus, or other virus infections of the CNS, were not detected. In contrast to SSPE, amorphous deposits similar to those seen in children dying with PRP were present in the blood vessel walls throughout different regions of brain [111, 115]. *In vitro* characterization of PRP brain derived cell cultures showed very few cells were RUBV positive although isolation of infectious RUBV could be achieved [98]. Related to these observations, it has been hypothesized that PRP is caused by a systemic persistent virus infection and somehow pathogenesis is concentrated in the brain, mostly by immunopathological mechanism. Considering the similarities in the symptoms of SSPE, which is caused by measles viruses, one parallel hypothesis of the PRP pathogenesis is that RUBV present in the brain is in the form of defective virus. However, considering the different coding strategies and replication cycles between RUBV and measles, this hypothesis is less favored. Also, as PRP shares similarities with multiple sclerosis (MS), a progressive autoimmune disease, the molecular mimicry mechanism may apply in the developing of such disease. It has been proposed that RUBV induces the death of oligodendrocytes and those dead cells would release otherwise sequestered myelin proteins that would serve as a trigger for such an immune attack. Due to the slow progressive properties of PRP, RUBV was added to the growing list of “slow virus” infections of the CNS [116].

Kemper et.,al proposed two mechanism involved in CRS encephalopathy: one, an inhibition of cell replication affecting the number of oligodendrocyte and glial cells; the other is the non-specific effect of delayed maturation conceivably due to the persistence of the viral infection [117]. It is necessary to reit-

erate here that RUBV, although eradicated in most developing countries, remains to be one of the best models to study teratogen induced CNS complications. Despite different mechanisms proposed, including immunological ones, it is still of great importance to examine how the virus affects authentic neuronal cells during development.

1.6 HUMAN EMBRYONIC STEM CELL DERIVED PROGENITOR CELLS AS A MODEL

Laboratory models have an important role in identifying agents with teratogenic potential, supporting or refuting the biological plausibility of teratogenic associations identified in human studies, and determining mechanisms of abnormal development [118]. The key processes that control development appear to be very highly conserved across species. Therefore, human teratogens have traditionally been studied by establishing animal models. There have been many attempts to develop animal models for CRS despite that fact that humans are the only host to RUBV. Birth defects following congenital RUBV infection only identified in limited studies using animal models such as rats, rabbits and monkeys [119-121]. Other studies using the same models did not successfully reproduce these defects [122-125]. Therefore, unlike most human teratogens, animal models of CRS are not particularly useful and have not contributed significantly to the understanding of the pathogenesis of the defects. Alternative models that well mimic human fetal development are needed for the future study of the mechanisms of pathogenesis of CRS.

Human embryonic stem cells (hESCs) are pluripotent stem cells derived from the inner cell mass of a blastocyst, an early-stage embryo [126]. They are distinguished by two distinctive properties: their pluripotency, which means they have the potential to differentiate into other cell types, and their ability to self-renewal, which means they can replicate indefinitely [127]. hESCs and their derived progenitor cells are now used widely in clinical therapies (such as human genetic disorders), cosmetics development, and most relevant to our discussion, as a laboratory model for various types of studies including viral teratogenicity research [128-130].

Neuroepithelial stem cells or neural progenitor cells (NPCs) are self-renewing multipotent cells that can differentiate into neurons, oligodendrocytes, and astrocytes, the three main types of cells composing the CNS [131]. Neurons transmit information through action potentials and neurotransmitters; astrocytes and oligodendrocytes, which are collectively called glial cells, play important roles of their own in the CNS in addition to providing a critical role in the support of optimal neuronal functioning and survival, such as providing the myelin sheath. NPCs naturally exist during development and also in the mature CNS. Very early in mammalian development, the CNS begins to develop with the induction of the neuroectoderm, which forms the neural plates and then folds to give rise to the neural tube. In humans, this process is estimated to occur in the 3rd to 4th week of gestation. Within these primitive neural structures, NPCs exist. From then on, NPCs undergo either symmetric division to expand their pools or asymmetric division to generate more restricted progenitors that eventually give rise to neuronal and glial cells (Figure. 1.5)[132]. It was believed that once CNS was complete, it was incapable of mitotic divisions to generate new brain cells due to the mitotic incapability of neurons. However, there is now well-established evidence that multipotent NPCs do exist in the mature mammalian CNS and that they play a role in neuroregeneration [133]. Important cell signaling pathways involved in temporal events during neural differentiation are the WNT, BMP, FGF, and RA pathways[134]. Besides mimicking the development of the CNS, another feature that makes hNPC's a good model for the study of teratogenicity is the controllable and quantifiable cell differentiation of this cell type that can be induced *in vitro*. (a) Spontaneous hNPC differentiation can be easily achieved by removing growth factors such as EGF and bFGF provided in basal culturing medium, whereas directed differentiation requires additional culturing supplements, such as ciliary neurotrophic factor (CNTF) for the derivation of astroglial and 3T3 for the derivation of pure oligodendrocytes. The differentiation process usually takes about 14-21 days [135-137]. (b) A typical way to quantify the differentiation of progenitor, as well as stem, cells is by examining the expression of intracellular as well as cell surface markers to identify specific types of cells [138]. To monitor the differentiation stages of hNPCs, different cell markers may be used (Figure. 1.6), for example, Nestin, CD133 and

SOX2, which have a high level expression in undifferentiated progenitors cells but not in terminally differentiated neurons [135]. Many markers can be used to detect specific differentiation, e.g. A2B5 is an early astroglial lineage marker, beta-tubulin-III (Tuj-1) and neurofilament-M (NF-M) are markers in terminally differentiated neurons, and GFAP and MOG serve as markers for astrocytes and oligodendrocytes, respectively [136, 137]. Additional quantification methods may also be used, including microscopic analysis of morphological changes as well as transcriptional profiling.

There are three sources of human neural progenitors: neural tissues from fetuses, immortalized cell lines, and hESCs. hESC-derived NPCs have advantages over the other two in that: there are no concerns about tumorigenesis and genetic instability ; the outcomes are consistent and do not depend on the gestational age of the cells as with those isolated from fetal tissue ; and hESC- derived hNPCs exhibit no decrease in plasticity during passaging [132]. Laboratory generation of hESC- derived hNPCs can be achieved using either an embryoid body model or adherent culture model, the latter ensures a more homogenous hNPC population. Although cultured hNPCs do not require mouse embryonic feeder (MEF) like hESCs do, other factors are still required to maintain proper growth and self-renewal including a proper extracellular matrix which can be provided by laminin or Matrigel and supplying nutrient and mitotic factors such as basal fibroblast growth factors (bFGF) [132].

Recently hNPCs have been developed commercially as a model to study developmental neurotoxicity and teratogenicity [139]. The model we utilized in this study, hNP1 (ArunA Biomedical), are an hNPC line derived from the NIH-approved H9 human embryonic stem cell line, which has a normal female (46XX) karyotype [126]. hNP1 cells express the NPC markers nestin and SOX2. According to the supplier, hNP1 cells also differentiate into multiple neuronal subtypes, including cholinergic, dopaminergic, and GABAergic neurons, glia, and oligodendrocytes, and maintain a stable karyotype for at least 10 passages. hNP1 cells have not been immortalized or otherwise transformed, and therefore the potential caveats of transformation are not at an issue when using these cells. They also grow as a monolayer without fibroblast support. hNP1 cells have been successfully used in radiation sensitivity testing, neurotoxicity

ty screening, neurophysiology, tissue engineering, and translational medicine [135, 140-145]. Thus, there is every reason to expect hNPC/hNP1 could be used as a model for studying neurodegenerative diseases and the vast majority of CNS abnormalities, including those caused by RUBV infection in CRS.

1.7 VIRUS INFECTION OF PROGENITOR CELLS: REVIEW OF PREVIOUS WORKS

Viral infections in the prenatal and perinatal period are a common cause of brain malfunctions. Besides the immediate neurological dysfunctions, virus infections may critically affect CNS development that culminates in long-term sequelae such as cognitive deficits. Most of these neurotropic viruses are most damaging at a critical stage when the brain is in a dynamic stage of development. As one of the mitotically active populations in the postnatal brain, hNPCs have emerged as the potential targets of neurotropic viruses. Numerous studies have focused on how viruses affect such cell populations and review of this work is relevant in terms of how RUBV infection causes neural anomalies during development [146]. Teratogenic viruses such as cytomegalovirus (CMV), human immunodeficiency viruses (HIV), Borna disease viruses (BDV), and Coxsackie virus, were among the first to be used in hNPC infection studies (see Table 1.3 for detail). Human cytomegalovirus (HCMV), a DNA virus belonging to *Herpesvirus* family, is currently the second most common cause of congenital brain deficiencies (after Down's syndrome) and a detailed comparison of the teratogenic aspects of HCMV and RUBV infection is summarized in Table 1.1. HCMV is highly tropic to hNPCs, even in the adult brain, particularly in the subventricular zone (SVZ) [147]. *In vitro* study showed that hNPCs are highly susceptible to virus infection; however, cells were not dead following infection but rather displayed slowed proliferation [148-150]. A similar impact on hNPCs proliferation is seen with BDV, HIV, and Japanese encephalitis virus (JEV), where virus infection results in insignificant cell death but promotes cell quiescence [151-153]. Therefore, hNPCs are resistant to virus induced cell death. The only exceptions were Coxsackie virus and a SINV vector expressing HIV-gp120, both of which induced significant cell death [120]. The effect of virus infection on hNPC multipotency or differentiation potential varies. HIV-1 infection promotes hNPCs to prematurely and preferentially differentiate into astrocytes *in vivo* and *in vitro* after a long-term infection

[154, 155]. BDV, on the other hand, significantly impairs hNPC neurogenesis instead of gliogenesis [151]. Contradictory results have been found with HCMV: in one study, the virus inhibited hNPC neuronal differentiation by triggering cell death while in another the virus induced premature differentiation of hNPC [119, 149]. The difference in these results may be caused by different sources of hNPCs used in each study. It is worth pointing out, however, that these other studies were done using hNPCs derived directly from aborted human fetuses and thus our use of hNPCs derived from hESCs is novel.

Hepatitis B virus (HBV), another classical teratogenic virus, triggers hepatic encephalopathy as a result of liver failure at late-decades of infected individuals. These neurological anomalies result from an increased level of toxic chemicals in the blood (such as ammonia) released from hepatocytes that are incapable of metabolizing the waste products. Small molecule toxins interfere with neuronal transmission and glial cell osmotic pressure within the brain and nervous system, thus resulting in abnormal psychomotor behaviors. However, it is intriguing why HBV does not trigger CNS defects in the fetus during pregnancy? It was proposed that HBV does not have the ability to cross blood-brain barrier of fetus, or alternatively, does not have access to brain/nervous cells due to lack of proper cell surface receptors [156]. It was reported that the hepatitis B vaccine induced CNS inflammation and demyelination. A molecular mimicry mechanism between MBP and hepatitis B antigen was suggested as an explanation of the onset of disease. However, the correlation between the HBV vaccine and demyelination is still debatable [157].

As for RUBV, teratogenic studies related to CNS malfunctions have been limited to few studies. Hearne et al., showed RUBV has activated replication when the blastocyst came to the embryonic stages in mouse; however, the virus titer achieved is only moderate and no cytopathic effects (CPE) were observed [5]. Noncytolytic infections of RUBV have also been reported in human embryos where infected cells demonstrated strong growth attenuation and became insensitive to the addition of growth factor to the medium [62, 64, 66, 67, 158, 159]. Studies focused on CNS malfunctions have only been carried out in mature neuronal culture. RUBV replication in glial cells, especially oligodendrocytes, has been reported extensively in a rat model, which showed a varied teratogenic response to RUBV infection [78-80,

107]. The only human study reported that RUBV replicated selectively and heavily in astrocytes, however, this is not seen *in vivo* [36, 108]. Research on the topic was done either on terminally differentiated neuronal and glial cultures or primary embryonic cultures (see Table 1.2 for detail). None of the experiments were carried out on the intermediate progenitor stages where the virus could exert the most damage. Thus, it is necessary to investigate the susceptibility of hNPCs to RUBV infection as well as its neurotoxicity to the same population.

Besides RUBV, many other viruses in *Togaviridae* family are teratogenic, such as Semliki forest viruses (SFV). In addition, SINV causes age-dependent encephalitis in mice and therefore is a very useful model to study viral encephalitis for the family [3, 4]. Viruses with such properties can be used as a control in this study. SINV infection to NPCs has been characterized: Undifferentiated murine NPCs were permissive for SINV and susceptible to virus-induced cell death. With differentiation, cells exhibited reduced virus replication and became progressively resistant to virus-induced cell death, resulting in prolonged virus replication [160, 161]. Mechanisms governing pathogenic outcome and extent of SINV replication in human cells are not sufficiently characterized [162].

1.8 RESEACH OVERVIEW

This dissertation is focused on the study the mechanism behind the development of CRS. Currently there are three type of models utilized in our lab to address this issue: (i) hESC derived progenitor cells including hNPC and human mesenchymal progenitors (hMPro) as a model to study the effect of RUBV on the development of different organs and tissues in the fetus; (ii) human lung epithelial cells (A549) as a model to characterize innate cellular responses to acute RUBV infection in mature individuals; (iii) a RUBV-replicon harboring Vero cell line (925-IN) as a model to study viral persistence. Three seemingly separate models unite together in the sense that all contribute to a more complete picture of how RUBV impacts the human body from embryo to fetuses to the developed individual. Work has been carried out on all three systems during research towards the PhD. This dissertation only describes the hNPC studies,

with the 925-IN studies, which have been completed [163]. The A549 studies are currently being written up for publication by another author.

The overarching question addressed in this dissertation is what is the mechanism underlying the development of neurological abnormalities seen in CRS? By using hNPCs as a model cell line, we approached the question with respect to neurogenesis. Based on previous studies, the general hypothesis is that infection of neural progenitor cells by RUBV leads to the disruption of the proliferation and differentiation of these cells, which is a primary mechanism underlying the development of CRS.

Since none of the previous research has been done on virus infection of hESC- derived hNPCs, and we thus approached the project in a comprehensive manner. **Project I, Cellular responses to RUBV infection in hNPCs.** The susceptibility of hNPCs to RUBV infection and the virus effect on properties of undifferentiated hNPCs is described in Chapter 2. Virus effect on undifferentiated hNPC proliferation, with a focus on whether and how RUBV induces cell death and growth attenuation, is presented in Chapter 3. One advantage of using hNPCs as a model is that the cells can into all three lineages of cells that compose adult CNS system and thus the effect of RUBV infection on hNPCs differentiation into both neuronal and glial cells were studied and are reported in Chapter 4. In **project II, Cellular responses to SINV infection in hNPCs**, we utilize SINV, a model Togavirus for viral encephalitis studies, as a control model for RUBV studies. Studies on this project are reported in Chapter 5.

The significance of studying cellular responses to RUBV infection in hNPCs is threefold: (a) this is the first time RUBV infection has been studied in stem and precursor cells which mimic the stage at which is critical to CRS development; (b) the result of this study provides direct clues for elucidating the cellular mechanisms of RUBV-induced teratogenicity during the progression of CRS, and (c) the project serves as reference study with the potential to inform corresponding research in the stem cell infection field and possibly provide unifying mechanisms of teratogenesis induced by infectious agent.

Table 1.1 Teratogenesis of HCMV and RUBV

Fact	HCMV	RUBV
Incidence of disease	5-10% microcephaly, periventricular calcification [164], Optic nerve pathology [165] (most common cause of birth defect) 10% subclinical congenital infection, but will subsequently develop brain disorders including mental retardation, sensorineural hearing loss, visual defects, seizure and epilepsy (reviewed in [147])	5-10% microcephaly, mental retardation periventricular calcification, Optic nerve pathology (most common cause of birth defect), hearing loss 10% subclinical congenital infection, but will subsequently develop brain disorders including mental retardation, psychomotor retardation, visual defects, seizure and epilepsy. Progressive Rubella Panencephalitis (PRP, very rare)
Transmission	Contact with body fluid of person who are infected with virus [56], Congenital	Respiratory route; body fluid? Congenital
Fetal infection Rate Risk of develop disease after congenital infection	50% (at first trimester) The risk of fetal transmission appears to increase with gestational age, but neurological outcomes are more severe when infection occurs during the first trimester [166]	80% (at first trimester) Most severe at first trimester of pregnancy with decreased likelihood of developing congenital disease thereafter, no sequelae after 16 weeks of gestation.
Immune responses	Adaptive: IgG; The presence of maternal antibodies has been shown to be associated with a decreased incidence of CMV and with improved neurological outcomes in the setting of congenital infection Innate: Robust CD8+ cell but few CD4+ Mild inflammation agents	Adaptive: IgG, IgM Rubella specific immune complexes present in CRS patients Innate: Both CD8+ and CD4+ Mononuclear inflammatory infiltration in brain Inflammation in acute encephalitis and PRP but not CRS brain [167] Mild Inflammation agent
Pathology in brain		
Isolation of virus	CSF, brain	CSF, brain
Acute infection	White matter abnormalities, necrosis, gliosis	Diffuse non-specific neural degeneration, No sign of demyelination and inflammation (or delayed myelination process)
Chronic lesions	1. Atrophy (volume loss), parenchymal and ependymal cysts, 2. Structural brain abnormalities 3. Abnormal periventricular hyper/hypoechoogenicity, ventricular adhesions, cystic formation around the ventricles, ependymal protrusions; vascular necrosis	Atrophy (due to reduced cell number) Free of morphological malformations Abnormal in blood vessels: focal destruction of veins and arteries, patchy defects of the internal elastic lamina, deposition of granular material, endothelial proliferation; vascular necrosis.

	4. White matter gliosis, 5. Cortical malformations? 6. Cranial calcifications	Whiter matter necrosis, oliodendroglial cell depletion Reduced cortical gray matter Calcification? *In PRP: destruction of white matter, loss of myelin, sever gliosis
Cell type infected	Preferentially infect cells in VZ and SVZ	Preferentially infection epithelial cells
Proposed mechanism of teratogenic effects[168]	1) Virus penetrated the placenta and infected fetus 2) A cytopathic infection to cells within infected fetuses. 3) Clones of differentiating cell s may be destroyed, and this may have either a direct or indirect effect on developing tissues and organs. 4) The indirect effect may be exerted through interference with cellular interactions during development.	1) Virus penetrated the placenta and infected fetus 2) A systemic infection of the fetus occurs with most types of cells are persistently infected 3) Teratogenesis is induced by inhibition of cell division and/or differentiation in cells involved in morphogenesis and organogenesis as well as by cell lysis. 4) Immune tolerance my facilitate viral persistency
Mechanisms	HCMV	RUBV
Molecular Virology	DNA virus, <i>Herpesviridae</i> Family	RNA virus, <i>Togaviridae</i> Family
Persistent infection Latency	Yes	Yes
Reinfection & reactivation	Life-long latency and Periodical reactivation	No
Receptor [169]	EGFR, IL10RA	MOG
Cell type infected <i>in vitro</i> ⁽²⁾	Neural progenitors (Highly susceptible) [170] In differentiated glial but not neuron Astrocyte Rarely show replication in neuron Rarely show replication in oligodendrocytes[171] Brain microvascular epithelial cells Does not replication in ES cells [172] PBML	Not known Astrocyte, microglia [108]; No replication in rat neuron Poor replication in rat oligodendrocytes[78, 107] Embryonic vascular epithelial cells [173] Infect mouse embryo[5] Embryonic cells derived from abortuses PBML [174]
Effect to cells		
Chromosome injury	Yes Chromosomal breakage [175]	Yes Chromosomal abnormalities & breakage [61, 176, 177]
Cell death & apoptosis	Induce apoptosis in hNPCs [178] Induce apoptosis during differentiation into neuron and glial cell Encode anti-apoptotic genes UL37 and UL38; [179, 180] Inhibit apoptosis in astrocyte [148]	Induce apoptosis in many cell types but not embryonic lineages Rubella capsid (C) is anti-apoptotic Inhibit chemical induced apoptosis in A549 [75] Does not induce apoptosis in fibroblast [66]

Cell cycle progression	Inhibit cell DNA synthesis in hNPCs, fibroblast [148, 178, 181]	Inhibit cell proliferation in primary fetal organ derived cell lines, selected fibroblast [61-63, 68]
Cytokine mediated damages	Yes	Not known yet
Altered fetal& embryonic gene expression	Premature differentiation of hNPCs [149]	Altered gene expression in human fetal fibroblast [182]
Impaired differentiation	Inhibit neuronal and glial differentiation [178, 181] (Controversial) premature differentiation	Altered differentiation seen in mesenchymal stem cells [64] (hMPro, our lab unpublished data)
Cell migration attachment	hNPC aberrant migration [183]	
Postsynaptic density	FYN	Citron kinase
Gene related	Schizophrenia susceptibility gene: Several genes may affect pathogen virulence, while the pathogens in turn may affect genes and processes relevant to the neurophysiology of schizophrenia. For such genes, the strength of association in genetic studies is likely to be conditioned by the presence of the pathogen, which varies in different populations at different times, a factor that may explain the heterogeneity that plagues such studies.[169]Me : in this study <u>CMV varies from RUBV in the genes related to schizophrenia, there are few overlaps in the associated genes between two viruses</u>	

Table 1.2 In vitro studies of RUBV infection in embryonic, fetal and neuronal cultures.

Lineage	Cell source/type	Virus strain	Result of RUBV infection	Reference
Embryo/ Fetal	Human fibroblast isolate from 2-4 month abortuses	West Point, Marshall, M-33, RW	Growth inhibition, stopped grow after several passages No morphological changes Differential responses from different organs from same embryo	[61, 63]
	Human embryonic lung cell		Found to carrying rubella virus	[62]
	Rubella carrier culture from infants		Virtually every cell in the carrier population was found to be producing virus	[49]
	Human diploid fibroblast (WI-38)		Produce a protein that slows mitosis	[68, 184]
	Human embryonic mesenchymal cells		Altered cell growth and differentiation Reduced collagen synthesis and alkaline phosphates content Decreased responsiveness to growth factor EGF	[64]
	Human embryonic cell		Support RUBV growth, no cytolytic effects observed	[67]
	Human fetus cells	Judith, HPV-77, RA27/3, Cenderhill	RUBV induce much less interferon than Sendai virus did Lung produce much higher interferon than other organ	[82]
	Human embryonic and fetal rat bones		Growth retardation No histological abnormalities observed Increased ³⁵ S uptake, indicating a disorder of mucopolysaccharide syntheses	[159]
	Mouse embryos		RUBV infect zona-free blastocysts resulted in a productive but non-cytolytic RUBV did not multiply in inner cell mass cells isolated from embryos at the blastocyst stage, although SFV did multiply in such cells.	[5]
	Human embryonal fibroblast		Chromosomal alternation	[158]
	Human embryonic fibroblast (HEF)	Gilchrist (GIL), Cordoba (COR)	RUBV induce apoptosis in normal-term placenta chorionic villi explants (CVE) and human monolayer of cytotrophoblasts (CTB) but not induce apoptosis in primary human embryo fibroblasts (HEF)	[66]
	Human primary fetal fibroblast	COR	Gene analysis showed an increased anti-apoptotic and decreased pro-apoptotic gene following RUBV infection to HEF Upregulation of interferon related genes was seen in both fetal and adult cells	[182]

Neuronal cell culture	Primary rat neural cell culture	Therien	RUBV multiplied to low titer and produced a partial cytopathic effect in rat glial cell cultures. A similar effect was produced following infection of myelinating neural cell culture but virus replication could not detect.	[107]
	Primary human fetal brain culture	Therien, 1B2 RA27/3, Cendehill	RUBV achieved high titer in the culture Astrocyte and microglial are highly susceptible to RUBV infection Only 5% oligodendrocyte were infected with RUBV Occasional neurons expressing viral antigen were seen	[108]
	Rat mixed glial culture	Therien; RA27/3	RUBV induces apoptosis in oligodendrocytes in rat glial cell cultures	[78]
	Rat glial cells	2872R	Restricted replication in immature glial (RG) but reactivated in replication in mature glial culture after treatment of dB-cAMP	[80, 185]
	Rat mixed neuron/glial culture	Therien	The virus causes disruption of cultures of pure glial cells, but there is no evidence of virus multiplication or cytopathic effect in pure neuron cultures. The cytopathic effect in mixed neuron/glial cell cultures is concluded to be glial cell mediated.	[79]

Table 1.3 Characteristics features of neurotropic viruses and their effects on the hNPCs

Name	Virus family	Genome	Effect on hNPCs	Long term neurological deficits	Reference
Cytomegalovirus (CMV)	Beta herpesviruses	DNA	Highly susceptible to virus infection Attenuate cell proliferation (controversial on apoptosis or not) Impede neuronal and glial differentiation by trigger apoptosis Both differentiated neuron and glial susceptible to infection Neuron is slightly refractory to the effect of virus (rare) induce premature and abnormal differentiation of hNPCs	Developmental brain defects, encephalitis, hearing loss, psychomotor deficits.	[148, 150, 178, 181, 186-190] Review in [147] [149]
Varicella-Zoster Virus (VZV)	Alpha herpesviruses	DNA	Support virus infection, support persistent infection for two month Low-level infectious VZV produced No CPE even in derived neurons (express viral transcripts and antigen) Replicate in sensory neurons derived from iPSCs	Meningoencephalitis, myelopathy, cascopathway and retinitis	[191-195]
Herpes simplex virus	Alpha herpesviruses	DNA	hNPCs were susceptible to virus infection Increased cell proliferation in SOX2 and Nestin + population at first 5 days after infection but decreased cell proliferation to overall population after 15 days after infection No CPE develop	Developmental brain defects, behavioral changes, hallucination, amnesia, hypomania	[196, 197]
HIV-1	Retrovirus	(+) RNA Single stranded	Support a restricted virus replication but can be maintained by addition of TNF- α HIV/gp120 attenuate cell proliferation by promote quiescence Transient activation of virus production of differentiation of HIV-infected progenitor cells to astrocyte HIV infected macrophage promote induce astrocytic differentiation of hNPCs Long –term HIV infection led to upregulation of GFAP and altered cell morphology	Developmental brain defects, learning and memory deficits, behavioral disturbance	[152, 154, 155, 198-201]
Coxsackie virus B3	Enterovirus	(+) RNA Single	Highly susceptible to virus infection Induce CPE and eventually cell death Virus replication reduced along differentiation	Meningitis, intellectual disability, Scholastic performance defi-	[153, 202-204]

		stranded	Altered progenitor cell differentiation Autophagy associated with cell-type specific susceptibility	cits, schizophrenia	
Japanese Encephalitis virus	Flavivirus	(+) RNA Single stranded	Support JEV replication (10^4 pfu/ml) Inhibit cell proliferation by arresting cell cycle but not triggering cell death Decreased virus load during differentiation into neuron Impair neuronal and astroglial differentiation by altering the expression of transcription factors involved in differentiation (JAK/STAT and AKT pathway) Developed immunogenicity following infection (MHC-1, IL-2 production)	Behavioral problem, learning deficits, speech problem	[205-208]
Borna Disease Virus	Bornavirus	(-) RNA Single stranded	Highly susceptible to virus infection Persist in hNPCs without altering undifferentiated phenotype and proliferation Impair neuronal differentiation by induce apoptosis of newly generated neuron Does not alter glial differentiation although virus actively replicated in cells Impair pERK1/2 pathway during neuronal differentiation	Learning deficits, schizophrenia, autism, mood disorders	[151, 209]
Sindbis virus	Alphavirus	(+) RNA Single stranded	Highly susceptible to virus infection Induce CPE and eventually cell death	Disorientation, ataxia, mental depression, convulsions	[161, 210] (also in this study)
JC virus	Polyomavirus	DNA	hNPCs can be nonproductively infected by virus, while human oligodendrocyte progenitors (hOPCs) support efficient replication of the virus Virus reactivate during differentiation into astrocyte	Progressive multifocal leukoencephalopathy (PML)	[211, 212]

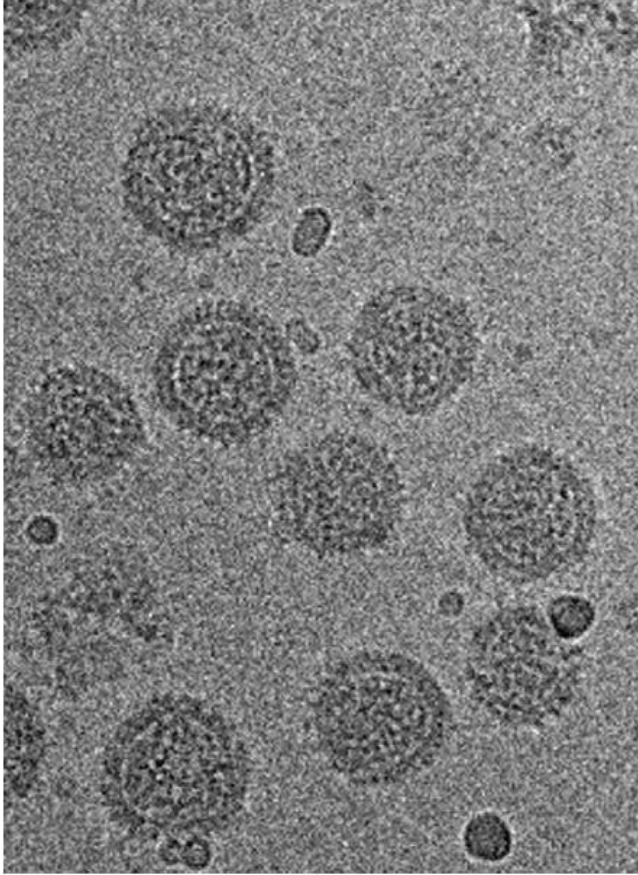


Figure 1.1 Cryo-electron micrograph of rubella virion.

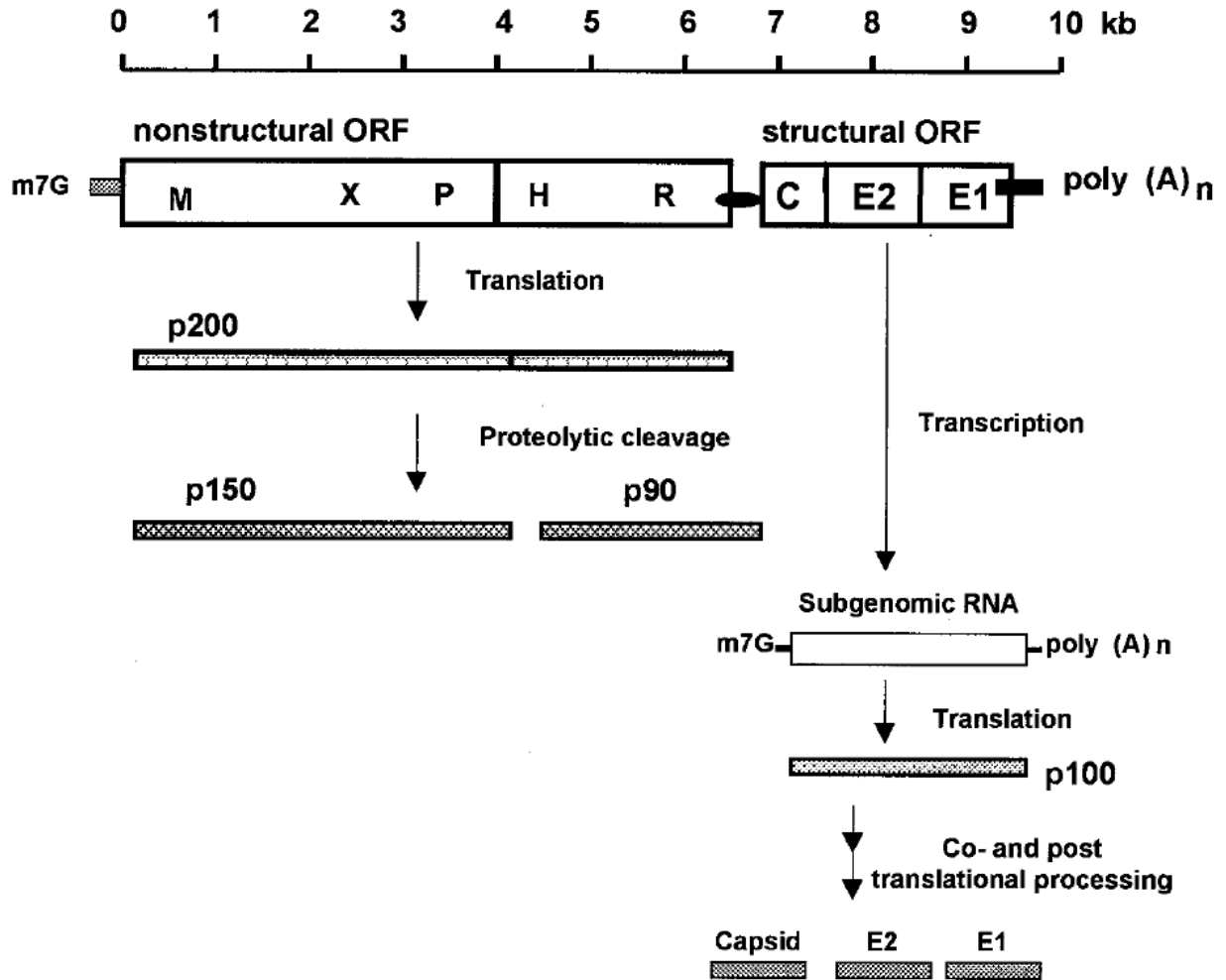


Figure 1.2 Schematic representation of the RUBV genome, translation and processing strategy of the RUBV nonstructural and structural proteins.

Reference [9].

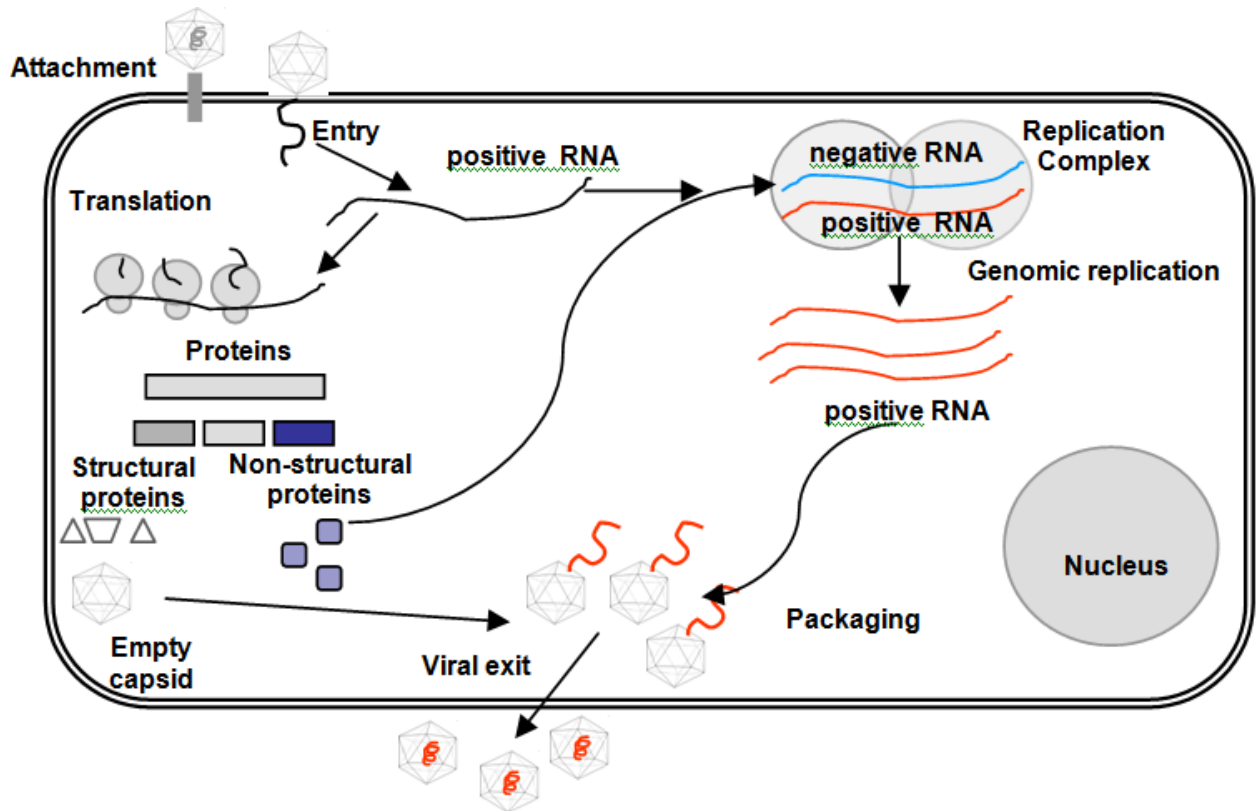


Figure 1.3 Schematic representation of the RUBV replication cycle.

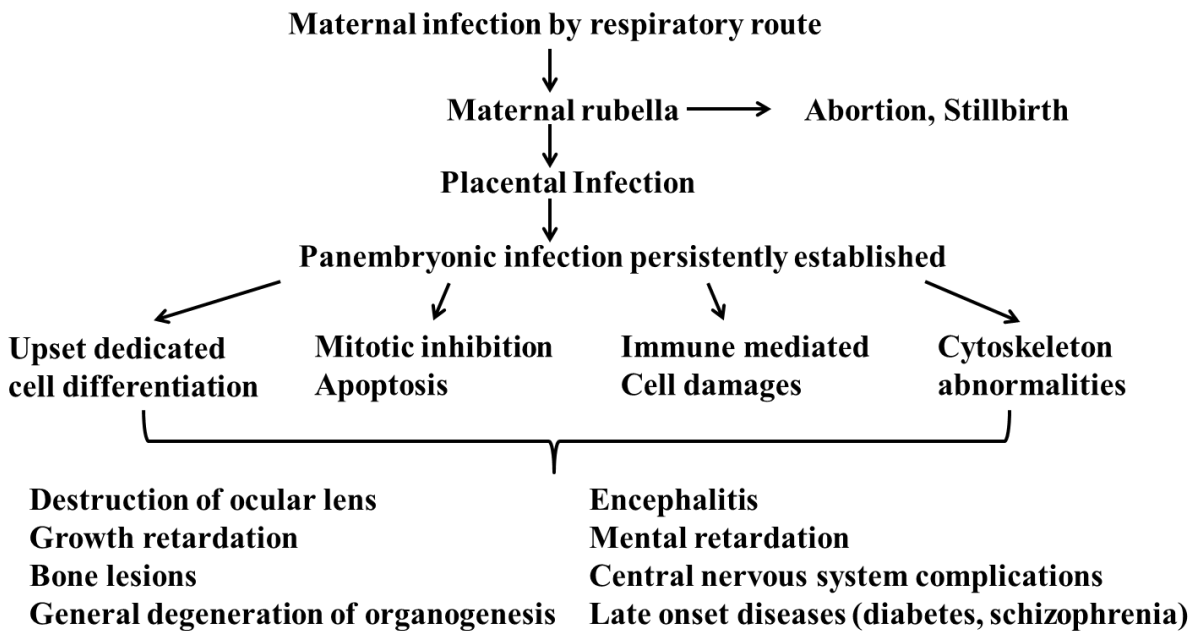


Figure 1.4 Proposed pathogenesis of congenital rubella.

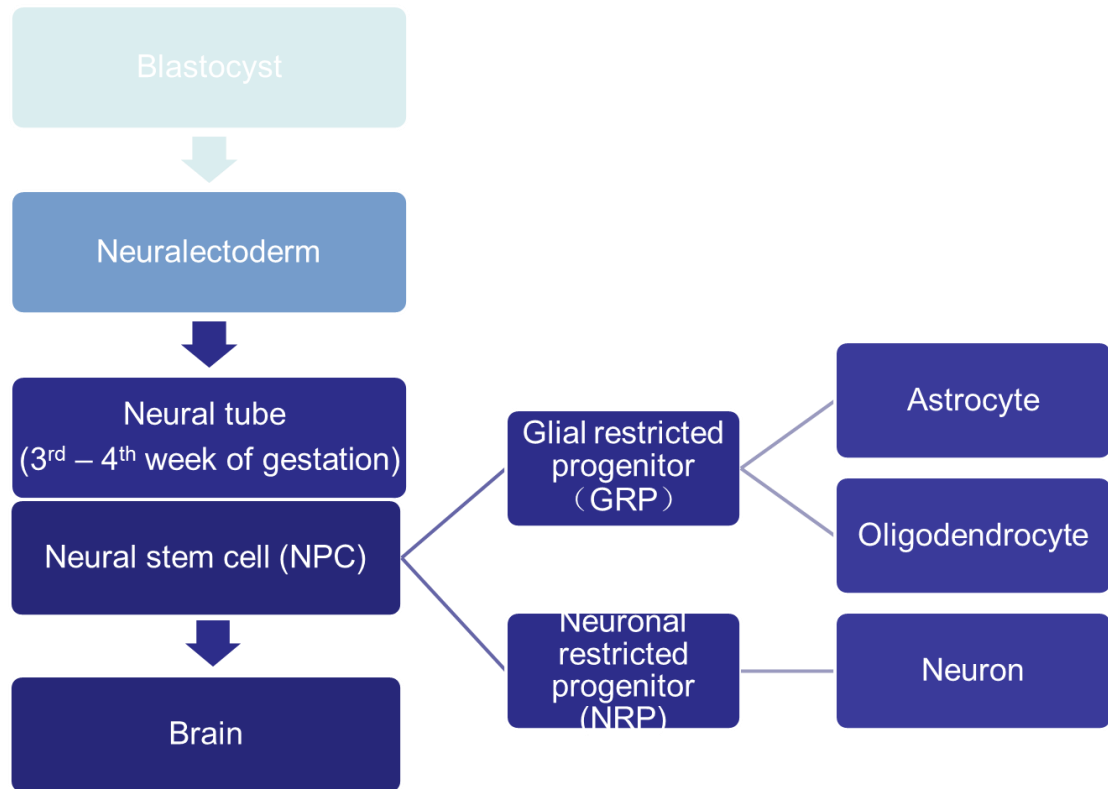


Figure 1.5 Embryonic neural development and the timing of NPC differentiation.

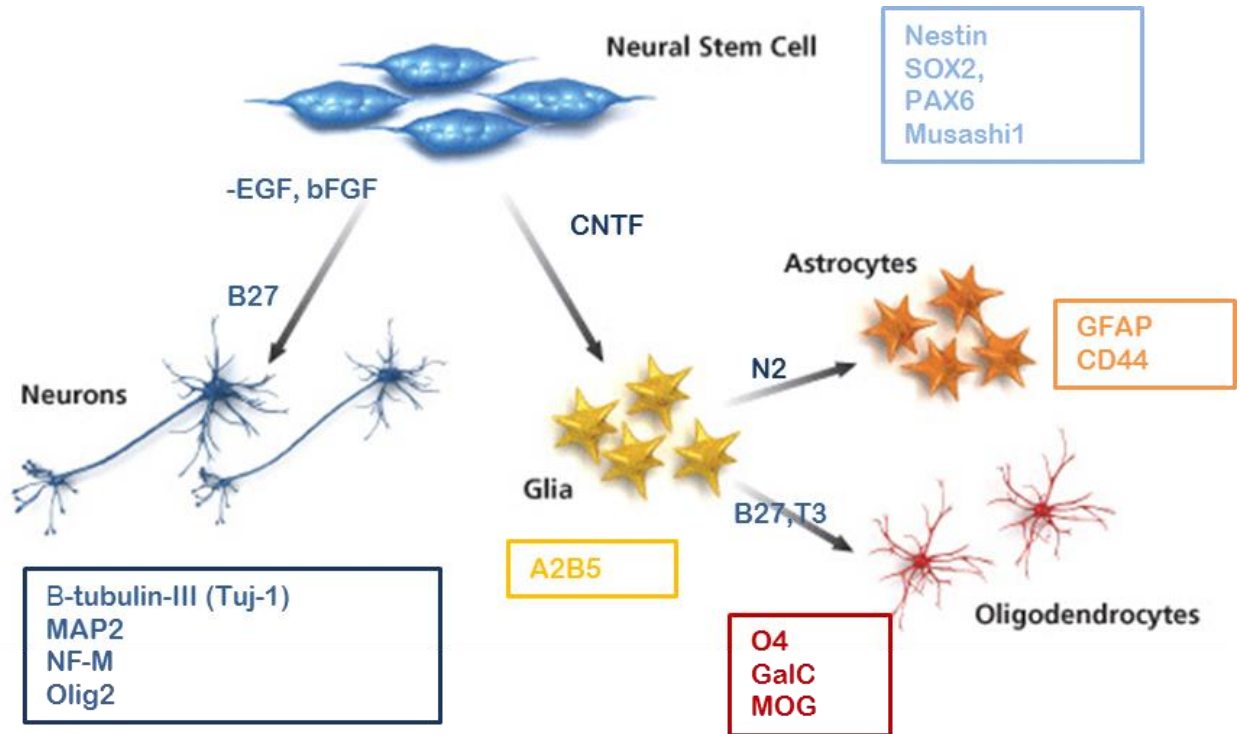


Figure 1.6 Embryonic neural stem cell (NSC and/or NPC) pathway in vitro and major markers for identification of each cell type before and after differentiation.

[Modified from Sigma-Aldrich website <http://www.sigmaaldrich.com/life-science/cell-biology/cell-biology>]

CHAPTER 2 : CHARACTERIZATION OF RUBV INFECTION OF HUMAN NEURAL PRO- GENITOR CELLS

2.1 INTRODUCTION

Several cell lines have been utilized to study RUBV replication as well as its pathogenesis *in vitro* including Vero, BHK21, RK13, human embryonic fibroblasts (HEF), and human lung epithelial carcinoma cells (A549). These *in vitro* models support robust RUBV replication and induce various types of cell responses. However, none of them accurately mimic the development of the fetus and therefore CRS pathogenesis remains a mystery. RUBV has a broad tropism for different types of tissues within the human body. The virus disseminates widely in the developing embryo and fetal tissue, establishing a chronic and generally nonlytic infection. Analyses of RUBV-infected specimens obtained during the first trimester showed that virus can be isolated from most organs of abortuses, including the central nervous system. Multiple studies have shown that RUBV causes CPE in oligodendrocytes, a subtype of neural cells [107, 213-215]. In addition, our preliminary data in which a similar WA09 derived progenitor cell line, human embryonic mesenchymal stem cells (hMPro) was found to be infectable by RUBV supports the notion of hNPC susceptibility to RUBV infection. In fact, hNPCs have been demonstrated as a reservoir for numerous neurotropic viruses *in vitro* and *in vivo*, with various outcomes after infection (see Table 1.3 for detail). Some of the viruses, such as HCMV and JEV, induce apoptosis in proliferating hNPCs, while others such as BDV persist in the cells without altering their morphology until cells are induced to differentiate. This study sought to determine the susceptibility of hNPCs to RUBV infection. We examined whether cells were capable of supporting the full viral cycle from entry into the cells to replication and propagation. We found that RUBV was able to enter ~10% of cells within the population and that hNPCs support a modest level of replication by the virus (10^3 - 10^4 pfu/ml) compared to that in cell lines in which the virus replicates efficiently, such as Vero (10^6 to 10^7 pfu/ml). In addition, RUBV and its replication have little impact on proliferating hNPCs, including their cell morphology and stemness marker expression, although the expression of proliferation marker Ki-67 was down-regulated at the transcrip-

tional level. Taken together, our results support the idea that hNPCs are susceptible to RUBV infection and that the percentage of infected cells closely mimics the pathology of CRS where few cells were found infected within affected tissue. This finding also sets the basis for the following studies in this dissertation in which virus impact on hNPC proliferation and differentiation will be analyzed.

2.2 MATERIAL AND METHODS

2.2.1 Cell culture

hNP1TM Neural Progenitor cells (hNPC's) (ArunA Biomedical) derived from WA09 hESCs were cultured in MatrigelTM (BD Bioscience) coated tissue culture dishes. Cells were maintained in complete neural expansion medium composed of AB2TM medium supplemented with 1x ANSTM (ArunA Biomedical Inc), 20 ng/ml Leukemia Inhibitory Factor (LIF, Millipore), 2 mM L- Glutamine, 0.5 U/ml penicillin, 0.5 U/ml streptomycin (both from Invitrogen), 20 ng/ml basal human fibroblast growth factor (bFGF, Millipore) at 37°C and 5% CO₂. Culture medium was changed every other day and hNP1 cells were passaged every 3–4 days using either a cell scraper or manual pipetting. For all the experiments described below, passage 6-10 cells were used. For Matrigel coating, the coating solution was made by diluting Matrigel 200-fold in ice-cold Dulbecco's modified Eagle medium (DMEM, Cellgro) and then applied to culture dishes in an amount according to the size of the dish (1 ml for a 35 mm² plate, 2 ml for a 60 mm² plate and 3 ml for a 100 mm² plate). Coated dishes were left at room temperature for 15minutes to 1 hour and coating medium was removed completely from plate prior to use. Pre-cooled tubes, pipettes and micropipette tips were required for manipulation of Matrigel. For cryo-preservation, cells were suspended at a concentration of 2×10^6 cell/ml in AB2 complete neural expansion medium and then the same amount of 20% DMSO (Sigma) in expansion medium was added to make a final 1×10^6 cell/ml in 10% DMSO AB2 complete neural expansion medium.

African green monkey kidney cells (Vero) used for preparing RUBV stock were maintained in DMEM containing 5% fetal bovine serum (FBS; Atlanta Biotech) and gentamycin (10 µg/ml; Gibco) at 35°C and 5% CO₂.

2.2.2 Virus stock preparation and infection

To prepare RUBV stock, 80% confluent Vero cells were infected with the RUBV laboratory adapted strain F-Therien at a multiplicity of infection (m.o.i) of 1. Culture medium was collected at 3 days post infection (d.p.i) when CPE was obvious in the culture. Cell-free (clarified) virus stock was prepared by collecting supernatant of such medium after high speed centrifugation. Each batch of virus stock was titered by plaque assay to calculate its infectivity. Medium for mock infection was similarly prepared from the non-infected Vero cells. hNPCs were infected as follows: after the removal of culture media, cells were washed once with phosphate buffered saline (PBS) with calcium and magnesium (KCl 2.68mM, KH₂PO₄ 1.47mM, NaCl 136.89 mM, Na₂HPO₄ 8.1mM, CaCl₂ 0.9mM, MgCl₂ 0.49mM) and infected with RUBV stock at the appropriate m.o.i. The plates were incubated at 37°C for one hour to allow adsorption. The inoculum was removed and replaced by complete neural expansion medium supplemented with growth factors. Culture medium was collected at appropriate times to test for the presence of virus by standard plaque assay on Vero cells.

2.2.3 RUBV growth curve characterization (infection strategy and plaque assay)

To characterize RUBV growth kinetics, hNP1 cells at 60-70% confluency were infected with RUBV at an m.o.i of either 0.1 or 10, and the medium was changed and collected on a daily basis for 10 days. For long-term characterization, mock and RUBV-infected cells were passaged every 7-10 days for 30 days. The amount of infectious RUBV in the medium collected from infected hNP1 cells was titered by plaque assay. For plaque assay, serial ten-fold dilutions of RUBV were inoculated onto semi-confluent Vero cell monolayers. After adsorption (1h, 35°C), the inoculum was removed and the cells were overlaid with MEM containing 0.7% plaque agarose (Miles) and incubated for 7 days at 35°C. Plaques were visu-

alized by staining the monolayer with crystal violet fixing solution (1% crystal violet, 3.7% formaldehyde, 1% Methanol in PBS) after removal of the agar overlay.

2.2.4 Virus genome detection by reverse-transcription PCR (RT-PCR) and quantitative reverse-transcription PCR (qRT-PCR)

Total RNA was extracted from mock and RUBV- infected hNPCs by using TRIzol reagent (Molecular Research Center, Inc) according to the manufacturer's instructions. Isolated RNA was quantified with a Nano Drop spectrophotometer (Thermo scientific) and 500 ng of RNA was reverse transcribed with Super-Script II reverse transcriptase (Invitrogen Life Technologies), using oligo dT (Invitrogen) as a primer to amplify all mRNAs or 3'-E1/808reverse primer (5'-TTTTTTTTTCTATACAGCAAC-3'; T₉ followed by the complement of nt 9751–9762 of the RUBV genome) to specifically amplify RUBV RNA. cDNA was used to perform real-time PCR with a Prism 7500 Fast Real-Time PCR System using SYBR green PCR master mix (Applied Bioscience) in a 20µl reaction mixture. For PCR, samples were held for 5 min at 95°C and then subjected to 30 amplification cycles consisting of incubation at 95°C for 30 sec, 56°C for 30 sec, and 72°C for 2min, with a final extension step at 72°C for 7 min. Primers used for viral genome detection were: Forward: F8812 (5'-CAACACGCCGCACGGACAAC-3') and Reverse: R9140 (5'-ACTCCACATACGCGCTGGAC-3'), this pair of primers amplified a region within the RUBV E1 gene. Primers for hNPC gene expression profiling are listed in Table 4.1.

2.2.5 Live-cell morphology changes

Cell morphology changes were monitored on an inverted Nikon TMS-F microscope (using a 20× objective). Non-infected and infected cells were monitored in parallel. Cell morphology and the presence or absence of CPE was compared.

2.2.6 Immunofluorescent assay (IFA)

Standard immunocyto-fluorescence was performed. hNPCs grown on coated glass-coverslips (80% confluence) were fixed with 4% paraformaldehyde (Electron Microscopy Sciences) in PBS for 10 minutes at room temperature, rinsed twice with PBS and then permeabilized with 0.2% TritonX-100 diluted in PBS for 5-7 min. Primary antibodies were incubated in 3% FBS diluted in PBS for 1.5-2 hours at room temperature, washed twice with PBS and incubated for 1 hr at room temperature with secondary antibodies in 0.1% FBS. After rinsing, cell nuclei were stained with 4,6-diamidino-2-phenylindole (DAPI; 0.1g/ml; Invitrogen).hNPCs have poor attachment properties on glass coverslips coated with Matrigel, therefore, all reagents mentioned above were pre-warmed to room temperature prior to usage. Primary antibodies used were directed against nestin (a neural stem marker; 1:450 dilution; Neuromics), E2 (a RUBV-envelope protein, 1:100 dilution, Epitomics) and β -tubulin (cytoskeleton marker, 1:200 dilution, Abcam). Secondary antibodies were anti-rabbit/mouse Alexa Fluor 488 and anti-rabbit/mouse Alexa Fluor 594 (1: 2000-4000 dilution; Molecular Probes-Invitrogen Life Technologies). Fluorescence images were acquired on a Zeiss Axioplan-epifluorescence wide-field microscope and processed with Axio-Vision software. For each condition within the same experiment, at least 3 fields of view were analyzed.

2.2.7 Flow cytometry

The percentage of cells expressing virus antigens or lineage specific markers was determined by flow cytometry. hNPCs were harvested and washed twice with 2%FBS/PBS (staining buffer) and then fixed with BD Cytofix/Cytoperm solution according to the manufacturer's instructions (BD Bioscience) in aliquots of 100,000 cells in replicate for each antigen. Each aliquot was stained with one or two of the selected cell marker antibodies for 1 hr on ice. Antibodies used were: anti-RUBV E2; anti-nestin, anti-SOX2 (either conjugated with appropriate fluorescent dye or in conjunction with a separate dye-conjugated secondary antibody), all obtained from BD Pharmingen. Cells were then washed twice with staining buffer and then labeled with secondary antibody for 45 min to 1.5hr, if appropriate. Cells stained

with isotype controls (mouse IgG APC, rat IgM PE, or mouse IgG FITC (BD Pharmingen) were used as controls. Flow cytometry was performed using a BD LSR Fortessa or FACS Canto, both from BD Bioscience and available in the Department of Biology Core Facility at Georgia State University. Forward and side-scatter plots were used to exclude dead cells and debris from the histogram analysis. Data analysis was performed using FACS Diva software (BD Bioscience). The percentage of cells expressing fluorescence intensity greater than the control cells was calculated using the FlowJo program (Tree Star, Inc., Ashland, Oregon).

2.2.8 Western Blot

Cells were lysed in 500 μ l lysis buffer (10 mM Tris (pH 8.0), 150 mM NaCl, 1% Triton X-100, 0.5% sodium deoxycholate, 0.1% SDS and 1 \times protease inhibitor cocktail (EDTA-free, Roche)) at appropriate time points. After clearing insoluble debris by high-speed centrifugation (10 min at 16000 g in an Eppendorf tabletop #5415D centrifuge), lysates were adjusted to 1 \times with the addition of 5X SDS-sample buffer (250 mM Tris-HCl pH 6.8, 20 mM DTT, 10% SDS, 0.2% bromophenol blue, 50% glycerol) and heat-denatured by boiling for 5min. Each lysate was loaded onto a 10% or 12% SDS-PAGE gel, resolved and transferred to nitrocellulose membrane (Whatman) using 1X transfer buffer (100 ml 10X transfer buffer (250 mM Tris, 192 M glycine), 200 ml methanol, and 700 ml deionized water) and a mini-Protean II apparatus (BioRad) at 100V for 1 hour. Blots were blocked in Tris-buffered saline (TBS: 25mM Tris, 150mM NaCl, 2mM KCl, pH7.4) containing 5% non-fat dry milk for 1 hour, washed once with TBS, followed by incubation with the primary antibody overnight at 4°C. After washing with TBS 3 times, the blots were incubated for 2 hours with alkaline phosphatase-conjugated anti-rabbit or anti-mouse antibody (1:5000 dilution; Promega). After 3 washes with TBS, the blot was reacted with NBT/BCIP (Roche) diluted in 10 ml alkaline phosphatase buffer (100 mM Tris, 100 mM NaCl, 50 mM MgCl₂-6H₂O, pH 9.8) for color development. Primary antibodies used in this assay were anti-GAPDH (1:5000 dilution; Abcam), anti-NF- κ B p65 (1:200 dilution; Santa Cruz); anti-phospho-STAT3 (1:200 dilution; Cell Signaling), anti-phospho-IRF3 (1:1000 dilution; Eptomics) and anti-cleaved-caspase 3 (1:1000; Cell Signaling).

2.3 RESULTS

2.3.1 hNPCs are permissive for RUBV infection

We assessed the ability of hNPCs to support the full RUBV viral life cycle, from entry at the cell surface to release of newly formed virions. First, to test the permissiveness of hNPCs for RUBV infection, we plated hNPCs onto Matrigel-coated plates and infected them at an m.o.i of 0.1 or 10 pfu/cell. The capacity of RUBV to enter, to replicate, and to disseminate in hNPCs were evaluated by immunofluorescence on days 1, 2, 4 and 6 following infection using an antibody directed towards the viral envelope protein E2. At an m.o.i of 0.1, E2 positive cells were minimally demonstrable throughout the infection time course (data not shown). However, at an m.o.i of 10, E2 positive cells were readily detectable, ranging from $5\% \pm 1.5\%$ to $11.5\% \pm 3.3\%$ during the infection time course (Figure.2.1A and C). E2 protein was distributed in perinuclear regions inside the cells, which is consistent with other cell lines infected by RUBV, but later spread to the whole cell. The infected hNPCs also expressed capsid protein, another marker of permissiveness for infection (Figure.2.1B). Presence of viral antigen inside cells, albeit a small number (~10%), confirmed that RUBV could gain access into hNPCs. The number of E2 positive cells increased significantly from day 1 to day 2 but not later, suggesting that RUBV replicated but was restricted in its dissemination (Figure.2.1C).

2.3.2 Infected hNPCs support a modest-level of replication of RUBV

To further evaluate the susceptibility of hNPCs to RUBV infection, we also examined the intracellular production of virus RNA and extracellular production of virus. First, intracellular viral RNA in hNPCs and its temporal changes post-infection were assessed by real-time qRT-PCR and RT-PCR at early and late times of infection. Control and RUBV infected (m.o.i of 10) cells were collected at days 1, 2, 4, and 6 after infection. Viral RNA levels, as tested by real-time qRT-PCR, increased moderately from day 1 to day 4 post infection, a good indication of RUBV replication in cell culture after infection. However, further accumulation of virus RNA was not demonstrated after 4 days of infection, which may be

concomitant with the inability of the virus to spread beyond 5-10% of the cells. (Figure.2.2.A). hNPCs failed to eliminate RUBV as viral genome was still detectable after 10 days of infection even by semi-quantitative RT-PCR (Figure 2.2.B). To evaluate extracellular virus yield, hNPCs were infected with either a high m.o.i. (10) or a low m.o.i. (0.1) and culture medium was changed daily so that amount of progeny virus produced each day could be determined. The extracellular virus titer obtained by plaque assay showed a similar trend as intracellular virus yield: although there was an increase in the virus titer from days 1 to day 4 post infection, daily virus production was not increased thereafter and a constant but modest level (10^3 - 10^4 pfu/ml) of progeny virus was released from the culture daily through 10 d.p.i (Figure.2.3). This pattern was not related to initial virus input as hNPCs infected with m.o.i of 0.1 of RUBV showed a similar virus growth curve as those infected with a m.o.i of 10. Taken together, this indicates that RUBV had a limited capacity to replicate, possibly related to the low percentage of infected cells, but was able to persistently infect hNPCs.

2.3.3 RUBV undergoes genetic modifications during infection in hNPCs

To characterize the mechanism of RUBV persistence in hNPCs, we compared the plaques of RUBV produced from infected hNPCs to RUBV produced from the standard cell line, Vero, since the shape and size of a virus plaque often indicates if there were significant mutations within a persistent population compared to original stock and mutations often contribute to virus persistence in culture [216]. Although both samples of virus were able to form plaques with smooth edges, a smaller plaque size was observed by the RUBV produced from infected hNPCs compared to those propagated from Vero cells (Figure.2.4.A and B), suggesting extensive genetic modification and selection events occurred during infection of the hNPCs. The smaller plaque size of RUBV also suggested replication-limited mutants were selected in the hNPCs, which possibly explained the ability of the virus to persist without adversely affecting the infected cells. RUBV infected

2.3.4 RUBV infected hNPCs did not develop CPE

We also monitored morphological changes using light-microscopy to assess the development of cytopathic effect (CPE) in RUBV infected hNPCs (data not shown). Vero and hNPCs were infected in parallel. CPE developed in infected Vero cells at 3-4 days post infection evidenced by detachment of cells from the monolayers (so called : "floaters") , while RUBV infected hNPC cultures and uninfected cells both appeared healthy 10 days post infection. Four weeks after infection, more than 90% cells still stained positive with anti-Nestin and SOX2 antibody (Figure. 2.6 D). Since Nestin and SOX2 are two important markers for multipotency, this result indicated that RUBV did not alter the stemness.

2.3.5 RUBV infected cells exhibit hNPC stemness marker

Finally, considering the nonhomogeneous nature of hNP1 cells [137], we wanted to verify that RUBV infected cells in hNPC cultures were authentic neural progenitors instead of other lineages. Double staining of the infected culture at an early time points (4 and 6 d.p.i) showed that viral antigen E2 colocalized with the stemness marker Nestin which is present in neural progenitor populations (Figure 2.5A). Among E2 negative cells, ~90% were found to be Nestin positive, while among E2 staining positive cells, ~100% were found to be Nestin positive, indicating that RUBV preferentially infects the neural progenitor population (Figure 2.5B). Therefore, we demonstrated that RUBV infected cells within the hNPC culture were authentic progenitors and not other lineages. Also, RUBV infection did not alter the expression of cellular stemness markers in the hNPCs during early infection.

2.3.6 Influence of long-term RUBV infection on biological features of hNPCs

To investigate whether RUBV persistence in hNPCs has the potential to cause biological changes in the neural progenitor cell population, RUBV virus production, cell morphology, lineage specific marker expression and CPE were compared in long term RUBV-infected and uninfected hNPCs.

Intracellular and extracellular virus yield

hNPCs were infected at either a high m.o.i (10) or a low m.o.i (0.1) as described above and further subcultured, with an average of one passage a week for up to one month. Culture medium was collected every other day to determine the amount of virus shedding from the culture. Infectious virus was present in culture fluid for up to one month, especially in the cells infected with a high m.o.i., demonstrating that RUBV established a persistent infection in hNPCs (Figure.2.6.A). The decrease in virus titer during time course was likely due to either the loss of infected cells during passaging or to the cells becoming too old and no longer able to support virus replication. Although extracellular virus production was not detectable after 27 days following an infection at an m.o.i. of 0.1, intracellular viral RNA was still readily detectable by more sensitive techniques, such as RT-PCR (Figure.2.6.B). Taking this into consideration, RUBV indeed was able to persist in hNPCs long term.

Cell morphology changes

Previous studies have shown that RUBV alters cell morphology in persistently infected cultures [93]. We next examined if this is the case in hNPCs. After 2 to 3 subcultures following RUBV infection (m.o.i of 10), hNPCs were double stained with anti-E2 antibody to detect RUBV infected cells and anti-Tubulin antibody to highlight the hNPC's cytoskeleton system. Cell morphology was first compared between infected cells (E2 positive) and neighboring cells (E2 negative) within infected culture, with no detectable difference seen between these two groups (Figure.2.6.C). We then wondered if the entire infected culture underwent morphological changes compared to uninfected cultures. Therefore, we compared the cell morphology between individual cells within uninfected and RUBV-infected cultures. Random cells were selected and no significant alteration of cell morphology was observed between the two cultures (Figure 2.6.D). At later passages, it was not unusual to observe cells with a different morphology. However, this was observed in both infected and uninfected cultures, and therefore was not due to RUBV infection but rather to natural differentiation occurring in hNPCs grown on matrigel-coated plates. Quantification of morphological properties showed that the median cell body area and cell process /dimensions of long-term RUBV infected progenitor populations (21 days after infection) did not differ significantly

from cells in uninfected populations (data not shown). Therefore, although RUBV persisted in hNPCs long-term, the virus did not induce morphological changes to individual infected cells as well the whole population.

Stemness and lineage specific marker expression

To determine whether RUBV infection altered expression of cellular markers in the hNPCs, the expression of stemness as well as lineage specific markers was examined at both the protein and RNA level. At 27 days post-infection, expression of two stemness markers, Nestin and SOX2 (markers that are constantly expressed by proliferating hNPCs; literature from ArunA Biomedical), between RUBV infected and uninfected hNPC cultures was examined. As expected, RUBV infection did not alter the percentage of cells expressing Nestin or SOX2. Quantification of the number of cells displaying these markers by flow cytometry showed that expression did not vary in response to RUBV infection either at a high m.o.i (10) or a low m.o.i. (0.1). These data showed that $87\% \pm 1.2\%$ of uninfected hNPCs were Nestin positive versus $84\% \pm 1.5\%$ Nestin positive following RUBV infection. Similar results were obtained when the expression of the SOX2 marker was examined (84.3% of the uninfected hNPCs vs. 83% positive following viral infection Figure 2.6.E). Mean fluorescence intensity for these markers also remained unaltered during infection. The percentage of Nestin and SOX2 positive hNPCs after long-term culture was generally lower than those hNPCs at early passages (85% of hNPCs cultured for long term vs. >90% of hNPCs at passage 6-8), confirming the morphological observations. Thus, the immature state of hNPCs was affected by serial passaging on matrigel-coated plates, but no alteration of the undifferentiated phenotype, based on morphology or expression of Nestin level, was observed in relation to RUBV infection.

At the end of the infection time course, 30 d.p.i, real-time qRT-PCR was used to investigate the changes in hNPCs multipotency (stemness) as well as lineage specific marker mRNA levels after RUBV infection (Figure.2.6.F). A wide spectrum of cellular markers were tested, including one pluripotency marker (Oct3/4), four classical multipotency markers (Nestin, SOX2, Pax6 and Musashi-1), one early

neuron/glia specific marker (Olig2), two neuronal specific markers (Map2 and Tuj-1 (β -tubulin-III)), one astrocyte specific marker (Gfap) and a proliferation marker Ki-67. Compared to uninfected hNPCs that had been cultured for same period of time, RUBV-infected hNPCs did not have significant up-regulation or down-regulation in the expression of either multipotency as well as lineage specific genes. However, the mRNA level of Ki-67 was down-regulated ~ 7 fold in RUBV infected cultures compared to the uninfected cultures, indicating that proliferation of hNPCs may be attenuated upon virus infection. This was further verified at protein level by flow cytometry quantitation (shown in Chapter 4). Together, this data suggested that RUBV did not alter hNPCs multipotency as well as lineage specific marker expression upon infection, and instead, may impact cell proliferation in the long-term.

Cytopathic effect

CPE was examined at every passage during the long-term infection course using light-microscopy. RUBV infection induced no cytopathic effect to hNPCs cultures, either at early or late passage (data not shown)

2.4 DISCUSSION

As summarized in the Introduction, RUBV remains the most efficient infectious agent with respect to induction of fetal neurodevelopmental defects, including microcephaly, mental retardation, encephalitis, cerebral palsy, autism, schizophrenia, and sensorineural deafness [94]. The mechanisms underlying such congenital disorders are still unclear. Since the primary time in gestation when RUBV exhibits profound teratogenicity, i.e. the first trimester coincides with organogenesis in the developing fetus, it was proposed that RUBV interferes with the maturation of fetus by upsetting the delicate balance of the proliferation as well as the differentiation of embryonic and progenitor cells during early stages of gestation [101]. Such a notion is further supported by the observations that RUBV successfully infects selective neuronal cell cultures *in vitro* [5], but the underlying mechanism is unclear, especially considering the lack of suitable human cell culture models. In this study, we took advantage of the availability of human

embryonic stem cell derived neural progenitor cells to investigate the effect of RUBV on the fetal nervous system development processes to gain insight into the mechanisms of teratogenicity. Furthermore, we wanted to test RUBV infection of hESC's and hESC-derived precursor cells to determine its utility as such a model system.

To this end, we first investigated the susceptibility of hNPCs to RUBV infection, which means ability of hNPCs to support the full RUBV viral life cycle, from entry at the cell surface to release of newly formed virion. The ability of RUBV to infect hNPC's was demonstrated by a roughly 1-log increase in virus titer, which represents extracellular virus production, over the infection time course, albeit at 1-2 log lower levels than produced in permissive Vero cells. Additionally, qRT-PCR analysis of intracellular viral genome has shown a similar increase over the time course. We found that only 10~20% of the cells in infected cultures exhibited RUBV-E2 antigen and the percentage of antigen positive cells did not significantly increase over time, indicating RUBV had limited access to the progenitor cells. Infectious virion production as well as viral nucleic acid was readily detectable in hNPCs even through 30 days after infection, suggested hNPCs did not clear RUBV and the virus was able to persist in the culture for at least one month. Together, hNPCs were susceptible to but supported a restricted replication and dissemination of RUBV.

Nevertheless, the limited nature of RUBV infection in hNPCs shown here correlated well with the situation in CRS : RUBV can be readily isolated from most organs of aborted CRS fetuses, including the CNS, however only very low numbers of cells were actually infected (in the range of 1 in 10^3 to 1 in 10^5 cells) [49, 63]. Also, RUBV produced a similar titer in primary human fetal fibroblasts as in hNPCs [61, 182]. Persistent viral infection, similarly, is also a hallmark of CRS: cell cultures derived from organs from abortuses are persistently infected with RUBV and most CRS infants excrete viruses for up to 6 months after birth [52, 62]. Thus, we believe RUBV infection of hNPCs well mimics the real situation in CRS and therefore it was worthwhile to look at how RUBV further impacts properties of hNPCs including cell morphology, cell attachment, proliferation and differentiation.

RUBV has limited access to hNPCs. In this regard, it is important to note that RUBV infection of even permissive cell lines is asynchronous for unknown reasons. In Vero cells, 90% of the cells are infected, but not until 48 hpi [12]; in the recently characterized infection of A549 cells, roughly 50% of the cells are eventually infected (Y. Zhou, personal communication). The first possible explanation for this is lack of RUBV-receptors on hNPCs' cell surface to support robust viral entry. RUBV, like most enveloped mammalian viruses, utilizes receptor-mediated endocytosis to enter targeted cells [217]. The only known RUBV receptor, MOG, was not expressed in the hNPC cultures in our study (data not shown) [10]. MOG is a marker for mature oligodendrocytes and therefore we would expect no expression in undifferentiated hNPCs [218]. It is thus likely that RUBV enters cells through interaction with other receptors that not yet been identified and that are not uniformly expressed on cells in hNPC cultures. Second, it has been postulated that embryonic stem/progenitor cells have intrinsic restrictive factors or lack cellular factors required for virus replication [219]. A good example of such intrinsic factors is cell surface charge. In our study, we tried using polybrene, a small chemical that neutralizes the charge repulsion between virions and sialic acid on the cell surface. Briefly, we use a mixture of viruses (m.o.i. of 10) and increasing amounts of polybrene for infection and quantified the number of viral antigen positive cells two days after infection. However, adding polybrene did not succeed in increasing the numbers of infected cells [220] (data not shown). In addition, since adding polybrene is considered to be a manipulation of cell culture, we did not use this chemical in our following studies that requires the cells in their natural status.

Restricted virus replication in hESCs and their derived cell lines has been shown with other viruses. Varicella-Zoster Virus (VZV) and human herpesvirus 8 (HHV-8 or KSHV), both Herpes viruses, are unable to infect hESCs cultured on mitotically inhibited feeder cells. This restriction remains even after bypassing of viral entry by transfection of the viral DNA into cells [219]. Epstein - Barr virus (EBV), a Herpes virus, demonstrated a limited expression of viral genes in B Cells derived from murine ESCs and this was attributed to aberrant splicing and premature termination of EBNA mRNAs within the infected cells. Similarly, HCMV establishes a latent or latent-like infection in hESCs as the virus enters hESCs but does

not initiate a lytic infection as usual [221]. RNA viruses, for example influenza A virus, were able to enter mouse ESCs and express some viral proteins, but the replication cycle was incomplete and no infectious virus was produced [128]. Moreover, induced pluripotent stem cells (iPS) derived from human fibroblasts were shown not to be susceptible to HCMV infection, which usually exhibit efficient infection in hNPCs [222]. Thus, the hESCs and its derived embryonic progenitors appear to have some intrinsic resistance to virus infection.

On the other hand, the apparent inability of RUBV to establish a robust productive infection in hNPCs is in striking contrast to some of the other teratogenic and/or neurovirulent viruses where a fully permissive of hNPCs to infection was seen. Viruses that produce a robust infection in hNPCs *in vitro* range from the positive strand RNA virus West Nile virus to DNA viruses such as HCMV and HSV [4, 119, 124, 148] (for a full list of virus see Table 1.3). We also showed that our hNPC cultures were fully susceptible to SINV. One possible explanation to this difference is the sources of cells utilized in the study. Most other studies used hNPCs derived from aborted fetuses or immortalized hNPC cell lines. Alternatively, considering its slow progression in neurological disease, RUBV simply does not develop a typical pathology in hNPCs as other teratogenic viruses do. In fact, RUBV, together with measles virus, JC virus, HIV and HTLV, were categorized as slow viruses as they have a long period of incubation time before the onset of neurological disease symptoms. [112]. Conversely, there is a great difference in hNPCs cell susceptibility between RUBV and HCMV, which also teratogenic and induces similar congenital neurological deficits. All of this suggests a distinct response from the host to RUBV infection during the early stages of embryonic development in comparison with other viruses.

Interestingly, although RUBV did not efficiently infect hNPCs, it showed a potential to establish a persistent infection in hNPCs. Virus nucleic acid was still readily evident in cultures that initially infected with either a high or low m.o.i after 30 days of infection, indicating the failure of hNPCs to eliminate RUBV in the long term. This type of persistence (minimum virus production) has been previously demonstrated in our lab study using permissive Vero cells, either infected with virus [87] or stably trans-

ected with a RUBV replicon (a construct lacking the structural proteins)[163]. In the former case, the virus persisted even in the presence of antiviral antibody that inhibited cell to cell virus spread. In the latter case, in presence of high doses IFN, the replicon still persisted despite suppression of gene expression. It is possible that RUBV persistence in hNPCs plays a role in progression of neurological disorders associated with CRS. In fact, our observation of a limited number of cells being infected with RUBV in hNPC culture coincides with the “clonal expansion” hypothesis which postulated that viral persistence contributes to the self-limited chronic infection seen in CRS [223]. Meanwhile, we should also take into account the possibility of reactivation of RUBV replication at later stages of development or after birth, since this has been demonstrated in HIV-1 infection to hNPCs: the virus production was undetectable after 10 days but could be stimulated by the addition of tumor necrosis factor alpha (TNF- α)[198]. A transient instead of persistent infection mechanism was postulated recently to provide a plausible alternative mechanism that could explain many of the inconsistencies in MS and PRP research, where evidence of the presence of RUBV in PRP and MS brains are debatable[98, 104, 110, 111, 113-115, 224, 225]. However, this model cannot provide information on the factors initiating the disease, and both the triggering and relapse phase it proposes requires long-term viral residency. It should be noted that result of viral persistence on CNS development seems to be host dependent. Although it is known from CRS that RUBV can persist in human tissue and has an affinity to the CNS both in CRS and following acute infection, no unique neuropathological features are known which would explain the development of a progressive neurological disorder. It seems that once a virus which has a tendency to persistence enters the CNS, a disease process may start which in its clinical/pathological features is more host than virus dependent [226].

For the mechanism underlying establishment of persistence in hNPCs, it is possible that RUBV undergoes genetic modifications during replication as we observed a reduced virus plaque size in RUBV produced in hNPCs compared to stock RUBV. A similar plaque-size mutant was observed in a the study of RUBV persistence in human breast cells (MCF-7)[86].It is also possible that defective interfering (DI)

RNAs were generated as was shown in persistently infected Vero cells[87], however, this needs to be confirmed. Our lab previously demonstrated that DI particles appeared to play no role in the slow, non-cytopathic replication of the virus [12]Alternatively, viral proteins possibly play a role in persistence instead of genetic modification. It has been suggested that RUBV capsid protein plays a role in stabilizing viral RNA therefore supported a long-term residence of RUBV genome in host cytoplasm[163] (Heather Mousa, unpublished data). The capsid protein is also anti-apoptotic [75], which would preserve infected cells.

RUBV did not alter the cell morphology or induce CPE in infected hNPCs. This is consistent previous studies with RUBV in which human and murine embryonic cells infected with RUBV showed no apparent abnormalities [53, 61, 62, 66]. The non-cytopathic effect nature of RUBV is also seen in vivo in brain autopsies of PRP patients [36]. Although disintegration of actin-filament has been demonstrated in BHK-21 cells and an elongated cell shape was observed in A549 cells after RUBV infection, however, neither of these cells were embryonic and therefore do not represent the authentic situations congenital infection[89].

RUBV also did not alter the expression of stemness and lineage marker of proliferating hNPCs, indicating that RUBV did not change the multipotency of such cells upon infection. This is in contrast with the hMPro studies, where the virus down-regulated the expression CD73 in the cells (Y. Zhou, unpublished data). Therefore, the result of RUBV infection to the stemness of progenitor cells seems to be lineage specific. The lack of apparent change in cell marker and cell morphology in hNPC upon RUBV infection could possibly due to low percentile of virus being infected in hNPC culture. However, this could also be attributed to the non-cytolytic nature of the virus regardless of the permissiveness of the cell culture used in the study. In a recent study, human fetal endothelial cells (HUVEC) were shown highly permissive to RUBV infection (90%~100% of cells were infected), but there was no changes in cell morphology as well as global protein synthesis [221]. Not limited to RUBV, BDV infection proceeds without

an overt pathogenic effect in hNPCs, impairing neither their cell morphology nor their undifferentiated phenotype [151, 209].

Thus, in this section we showed that RUBV infected hNPCs and confirmed our plans to explore this model system. However, there is a recently developing caveat. The RUBV strain F-Therein was employed throughout this study. F-Therein is a derivative of a wild type (wt) clinical strain, Therein, which was selected for large plaques and high virus yield and plaque purified in Vero cells [227]. The virus strain was chosen in our study because of its robust replication rate in Vero and other cell lines routinely used in RUBV *in vitro* studies as well as because it is our standard lab strain. However, in a recent study in HUVECs, capillary endothelial cells which are thought to be a target organ during RUBV infection, it was shown that fresh clinical isolates induced a much higher rate of infection (90-100%) than did lab adapted strains, such as F-Therien (similar results have been obtained with HCMV)[228, 229]. This publication came out after our study was completed and the authors refused to share their clinical viruses with us until after their study appeared and an MTA executed. Considering their findings, it would be of great interest to infect hNPCs with fresh clinical isolates to see if characteristics of the infection, in particular the percentage of infected cells, would be affected.

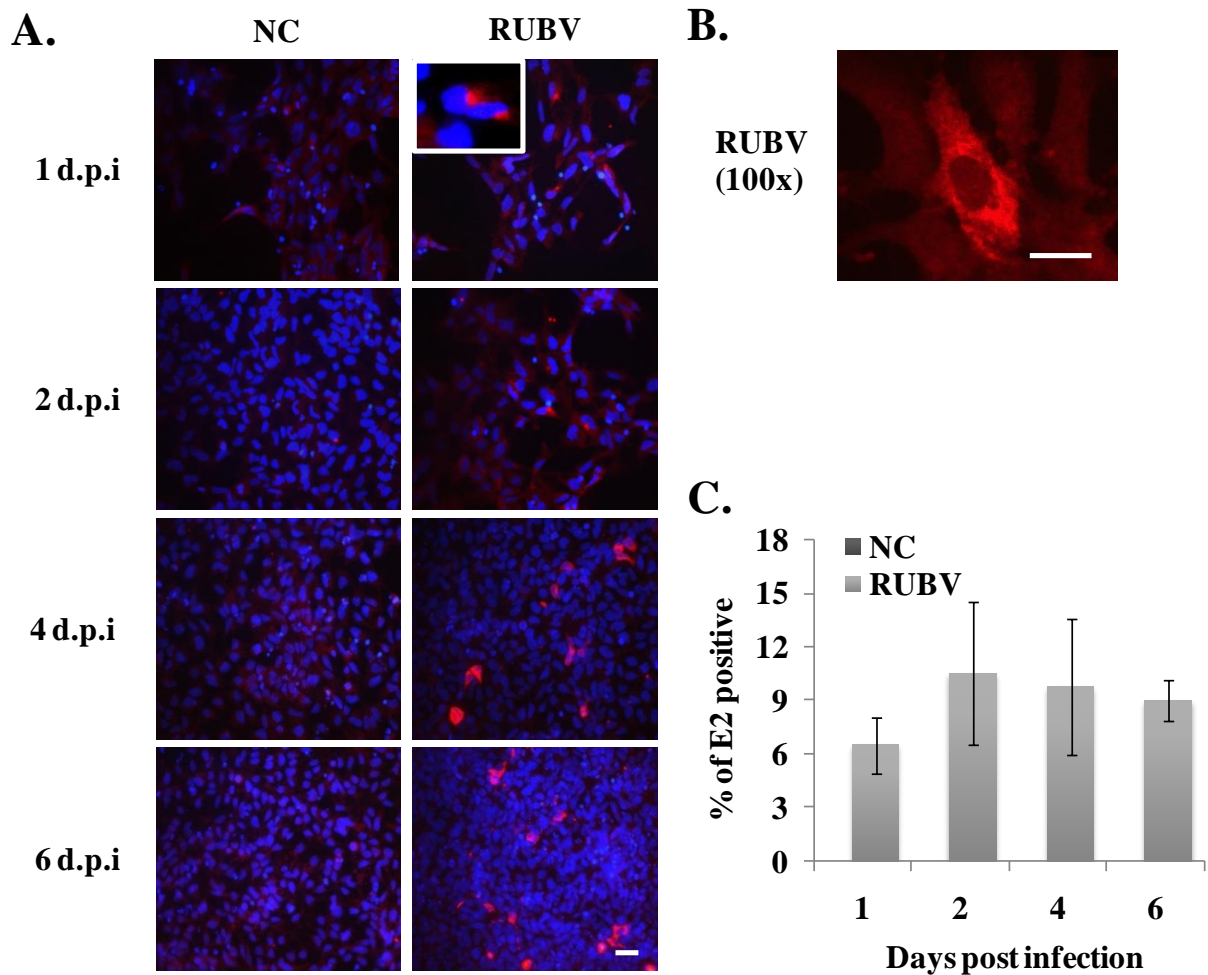


Figure 2.1 Viral antigen detection and percentage of infected cell determination by indirect immunofluorescent assay.

(A) The susceptibility of hNPCs to RUBV infection was analyzed with an antibody directed toward the viral envelope protein E2. At day 1, 2, 4, and 6 days post infection (d.p.i) (m.o.i.=10), cells were fixed, permeabilized, and analyzed by fluorescence microscopy. Perinuclear distribution of viral antigen was shown in higher magnification (upper left panel in RUBV 1d.p.i). Anti-E2 antibody (red) detected RUBV antigen and Hoechst stain (blue) detected nuclei. Bars, 10 μ m. (B) Immunofluorescence staining of infected cells with anti-RUBV-Capsid at 100x magnification. Hoechst stain (blue) was used to detect nuclei. Bars, 10 μ m. (C) Based on E2 immunostaining, the percentage of infected hNPCs was determined. At least 200 cells from three different fields were counted at each time point. Each time point was repeated at least twice. Error bars represent SDs.

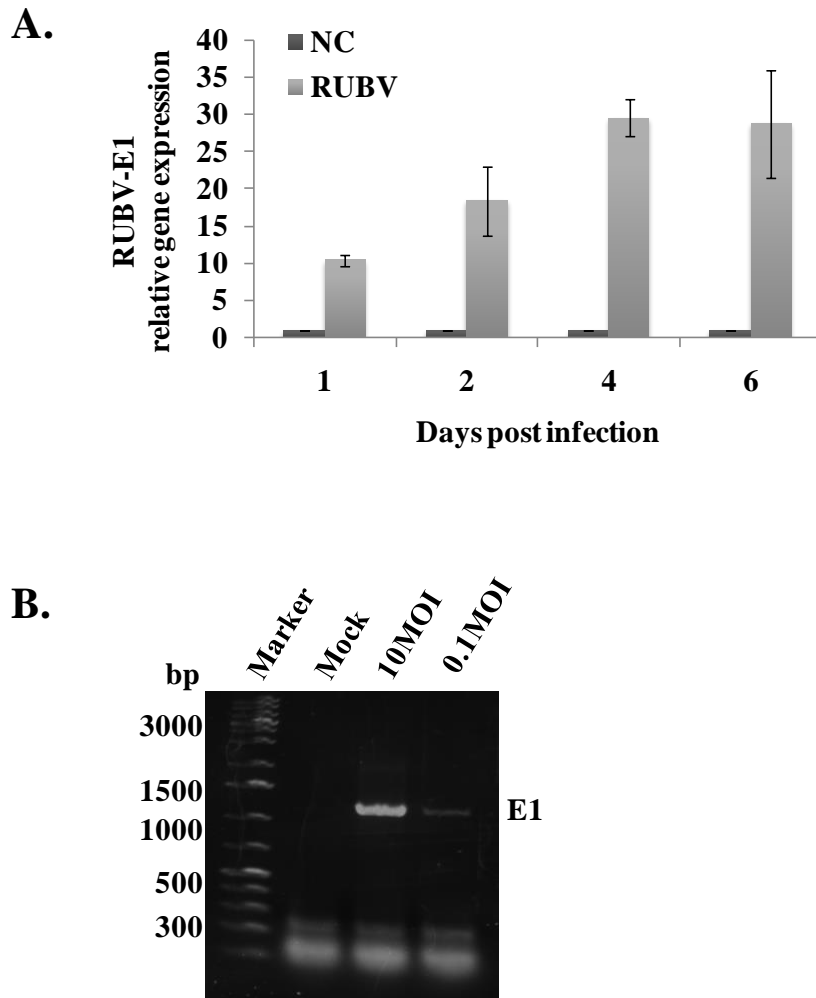


Figure 2.2 Viral RNA detection at early and late times of infection.

(A) hNPCs were infected with RUBV at an m.o.i of 10, and intracellular RNA was extracted at days 1,2,4, and 6 post infection. Intracellular viral RNA levels were assessed by real-time qRT-PCR. Each experiment was done in triplicate and repeated at least twice. Representative data from one experiment are shown. The viral RNA levels were normalized to GAPDH mRNA in the same sample and are shown as fold change over the amount of viral RNA in non-infected control (NC). (B) RT-PCR against RUBV E1 gene (1110bp) after 10days of infection (cells from the growth curve experiment), showing positive amplification of viral nucleic acid at infection of m.o.i.'s of both 10 .and 0.1. This experiment was repeated three times and a representative gel is shown.

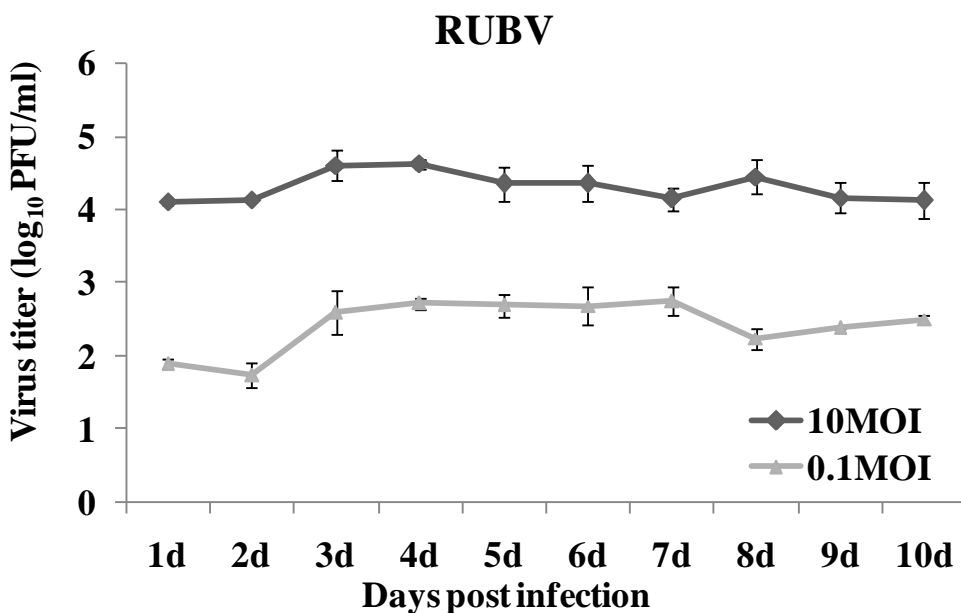


Figure 2.3 RUBV growth curve in proliferating hNPCs.

Undifferentiated hNPCs (passage 6-10) were seeded in plates and infected with RUBV at an m.o.i. of either 10 or 0.1 on the next day. For 10 days, the medium was changed and collected daily for titrating the amount of virus produced daily. Each data point is the average of duplicate titration from three experiments. Error bars represent SDs.

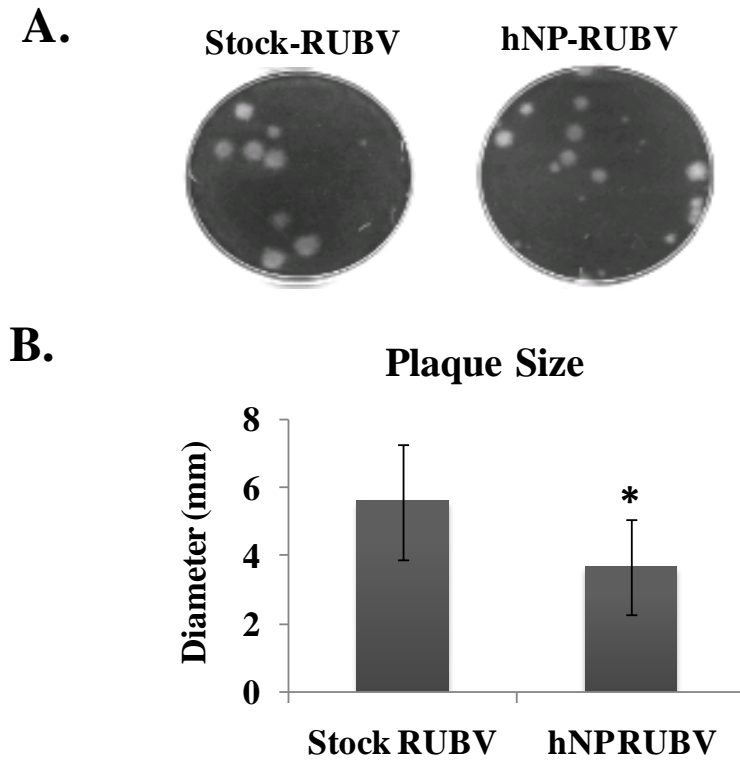
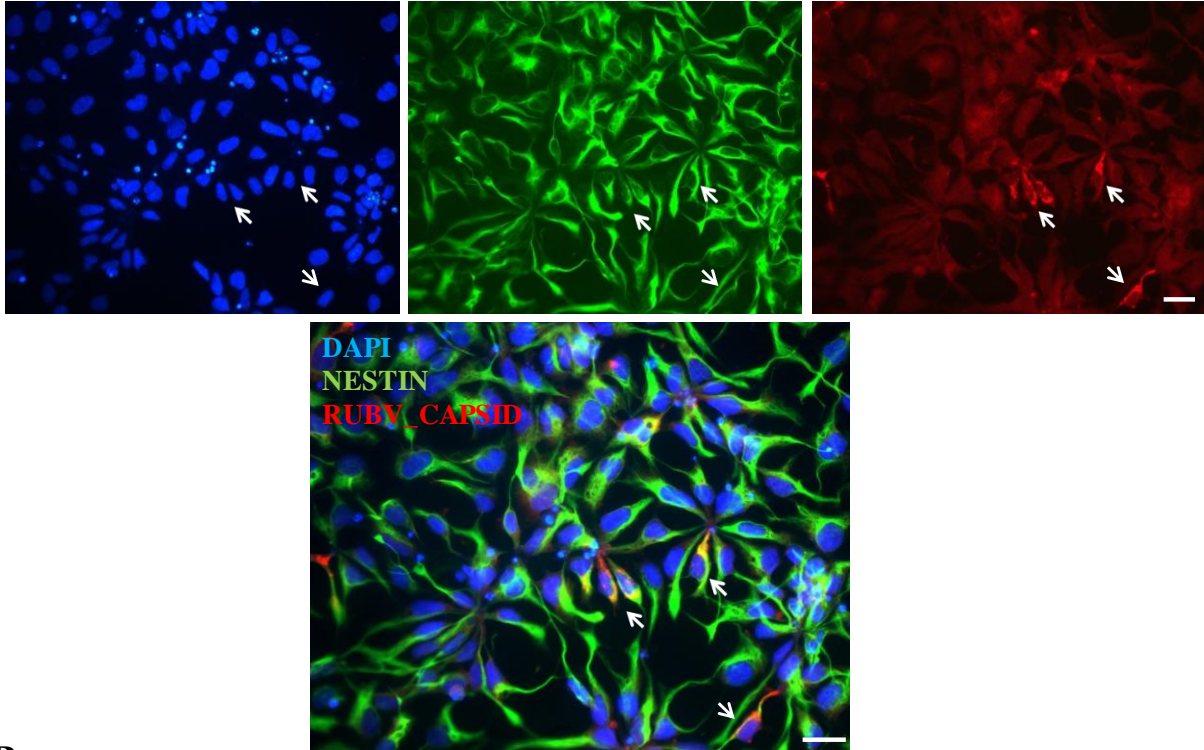


Figure 2.4 Plaque size comparison between stock RUBV and hNPCs produced RUBV.

hNPCs were infected with RUBV at an m.o.i of 1, which is the moi used to produce stock RUBV in Vero cells. Virus was collected at day 3 post infection and then titered by standard plaque assay together with original stock RUBV. (A) Image of plaques produced by stock RUBV and virus grown in hNPCs (B) Quantification of plaque size. This experiment was repeated 3 times and the error bars represent SDs. *, statistical significance compared to the stock control was determined at a 95% confidence interval ($P < 0.05$).

A.



B.

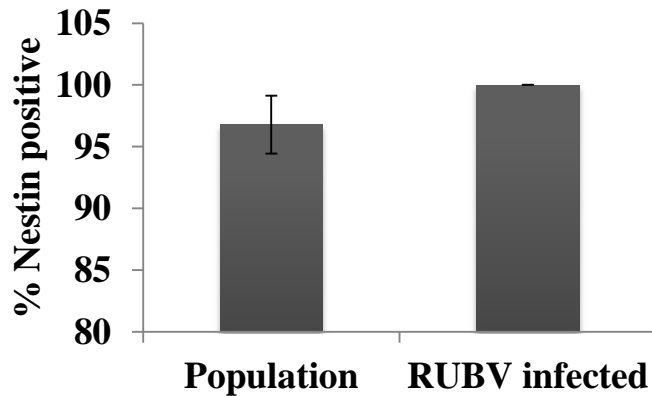


Figure 2.5 Infected cells display the hNPC stemness marker Nestin.

(A)hNPCs (passage 6-10) were infected with RUBV at an m.o.i of 10. At day 3 post infection, cells were fixed, permeabilized, and analyzed by immunofluorescence microscopy. Anti-E2 antibody (red) detected RUBV E2 antigen, anti-Nestin (green) detected Nestin protein, and Hoechst stain (blue) detected nuclei. Arrows denote colocalization of E2 viral antigen and stemness markers Nestin present on hNPCs. Bars, 10 μ m. (B) Enumeration of Nestin positive cells by immunofluorescence staining. The percentage of Nestin positive cells within the whole population and within the RUBV infected (E2 positive) population was determined. Error bars indicate SDs .

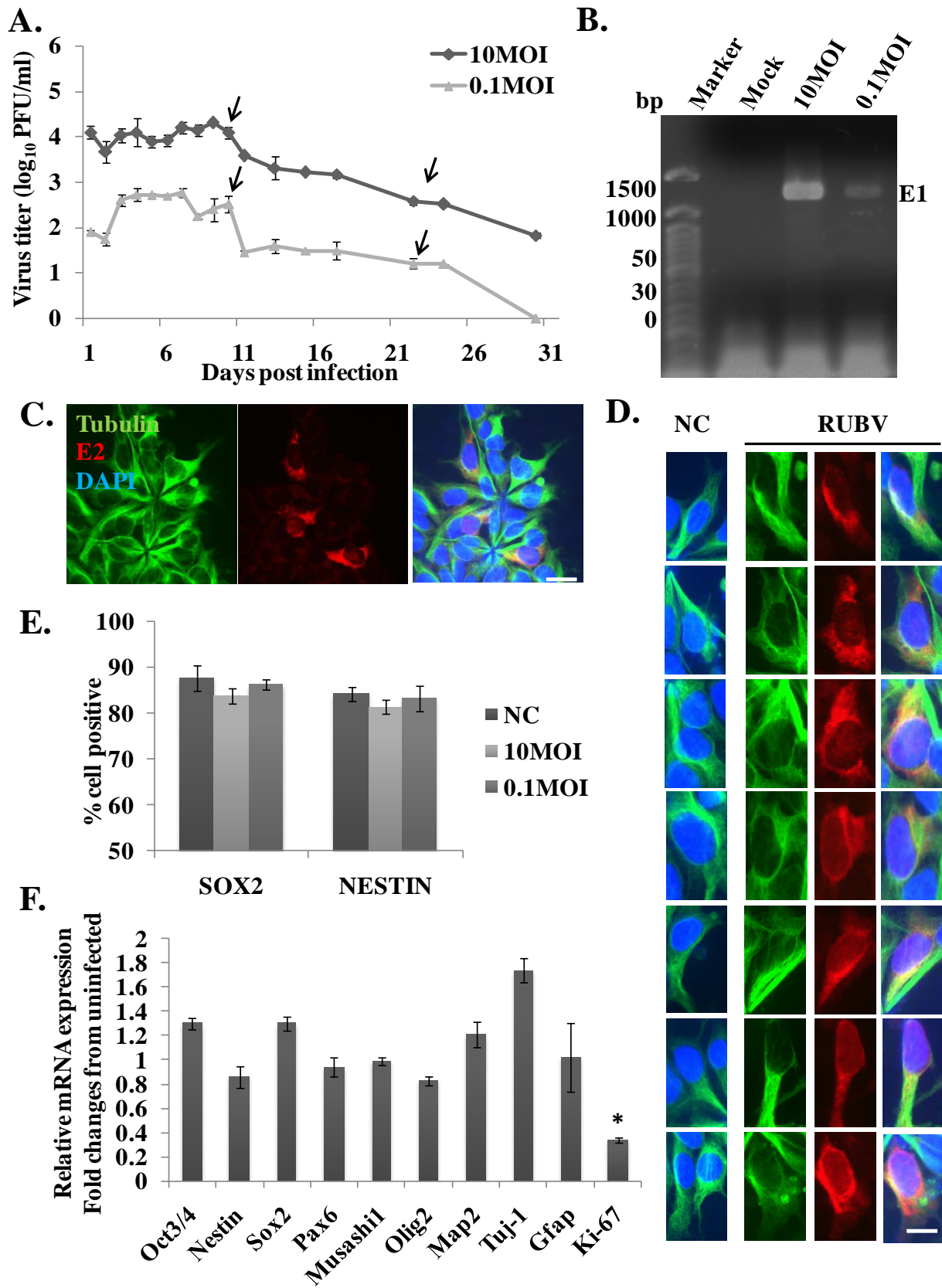


Figure 2.6 RUBV persists in hNPCs without altering their morphology and undifferentiated phenotype.

(A) hNPCs (passage 6-10) were infected with RUBV at an moi of 10 or 0.1 and subcultured as denoted by the arrows. Extracellular virus yield was determined by plaque assay on Vero cells. Each data point is the average of duplicate titration from at least two experiments. Error bar represent SDs. (B) RT-PCR against RUBV E1 gene (1110bp) after 27days of infection (cells from the growth curve exp), showing positive amplification of viral nucleic acid after infection with both m.o.i.'s. This experiment was repeated three times. (C,D) At day 21 post infection, cells were fixed, permeabilized, and then cell morphology was analyzed by immunostaining with anti-tubulin antibody (green) together with anti-E2 antibody (red) to detect infected cells and Hoechst stain (blue) to visualize nuclei. Cell morphologies were compared between infected cells and neighboring uninfected cell within the infected culture (C), or individual cells in the uninfected culture with those in the infected culture (D). Bars, 10 μ m. (E) Expression of stemness marker Nestin and SOX2 were examined at day 27 post infection by flow cytometry. Error bars represent SD from at least two independent experiments. (F) RNA isolated from control and RUBV infected hNPCs at day 30 post infection were used to perform real-time qRT-PCR of various stemness and differentiation genes. Each experiment were done in triplicate and repeated at least twice, and representative data from one experiment are shown. The gene expression level was normalized to GAPDH mRNA in the same sample and was shown as fold change over the amount in the uninfected control at same time point. Error bars represent SDs. *, statistical significance compared to the control (P<0.05).

CHAPTER 3 : RUBV ATTENUATES HUMAN NEURAL PROGENITOR CELL GROWTH BY MITOTIC INHIBITION INSTEAD OF TRIGGERING CELL DEATH

3.1 INTRODUCTION

RUBV-induced fetal damage is hypothesized to be multi-factorial, resulting from a combination of virus-induced effects [22]. A constant feature of CRS is fetal growth retardation, which has been speculated to be due to reduced or slower cell division [36]. Microscopic analyses of aborted infected fetuses revealed cellular damage in multiple sites, with noninflammatory characteristics being common in the structures of the eyes, heart, brain, and ears [40]. Additionally, as previously stated, RUBV replication did result in cytopathic effect on neural lineage cells and was reported to induce apoptosis in those cells [78]. *In vitro* studies are similarly controversial: RUBV was reported to induce apoptosis in Vero, BHK, human normal-term placenta chorionic villi explants (CVE) and in monolayers of cytotrophoblasts (CTB), but does not induce apoptosis in primary human embryo fibroblast (HEF) cultures. Hobman et.,al reported recently that RUBV infection caused resistance to staurosporine (ST) induced apoptosis in A549 cells [75]. RUBV nonstructural protein P90 was also reported to bind to the cell division regulators RB and Citron-Kinase [69], adding difficulties in finding reasons behind retarded growth of CRS infants.

Therefore, in this part of the study, the effect of RUBV infection on hNPC cell proliferation and division was analyzed, first on a population level by cell counting and EdU incorporation assay. We found a modest effect on hNPC proliferation, but cell death (the presence of floaters) was not induced upon virus infection. Since few cells were infected in the hNPC population, we then investigated how virus impacts hNPCs proliferation at a single cell level mostly by double-immunofluorescence staining of virus antigen and desired cell markers. We showed that RUBV attenuated cell growth by introducing cell mitotic inhibition instead of apoptosis, a mechanism suggested previously by others [61, 64, 66-69, 159,

230]. Finally, a cellular inflammatory response in the form of inflammatory cytokines was not induced by RUBV infection, possibly explaining in part the lack of an apoptotic response.

3.2 MATERIAL AND METHODS

3.2.1 Cell culture

hNPCs were maintained as previously described in Chapter 2 and for all experiments passage 6-10 cells were used. Human adenocarcinomic alveolar basal epithelial cells (A549) were used as a control and were maintained in Ham's F-12, Kaign's modification (Cellgro), 10% Fetal Bovine Serum (Atlanta Bio-Tech), and 100 unit/ml Pen-Strep (Invitrogen) at 37°C and 5% CO₂.

3.2.2 Cell growth curve characterization

To obtain a cell growth curve in the absence or presence of RUBV infection, a standard cell counting experiment was performed in which 50,000-100,000 hNPCs were plated onto each well of a 24 well plate, infected with RUBV at m.o.i of 10 pfu/cell the next day, and the medium was changed every day for 10 days. Every day, one well of the mock infected and RUBV infected cells were counted for total cell number present in well (including floating cells present in medium). To do so, the cells were scraped from the well and counted manually using a hemocytometer under a light microscope.

3.2.3 EdU incorporation assay

A Click it™ Alexa Fluor-547 EdU incorporation kit (Invitrogen) was used to assess the cell proliferation rate according to the instructions of the manufacturer. EdU (5-ethynyl-2'-deoxyuridine) is a novel alternative for the standard BrdU (5-bromo-2'-deoxyuridine) assay to directly measure active DNA synthesis or S-phase synthesis of the cell cycle. EdU is a nucleoside analog of thymidine and is incorporated into DNA during active DNA synthesis. Detection of EdU is based on a click reaction, which is a copper (I) catalyzed reaction between an azide and an alkyne. Briefly, cells in monolayers were first pulsed with 10 μM EdU for 2 hours. Cells (1×10^6 per 50 μL) were fixed with BD Fix/Perm buffer (BD Bioscience) and

washed twice with PBS-1% FBS and then permeabilized with BD Perm/Wash buffer (1:10 diluted in de-ionized water). After the fixation/permeabilization process, cells were treated with Click it™ reaction mixture for 30-45 minutes to expose incorporated EdU for detection. Samples were washed twice with Perm/Wash buffer before analysis using flow cytometry as described in Chapter 2.

3.2.4 Apoptosis assays

Multiple assays were used to detect apoptotic events in hNPC cultures. (a) For the assessment of viral induced cell apoptosis, active-caspase-3/RUBV-E2 double staining was performed according to standard immunofluorescence assay (IFA) protocol (see Chapter 2). A monolayer of hNPC was seeded onto a coverslip and infected with RUBV at a m.o.i of 10 the next day. Cells were fixed and analyzed at days 1, 2, 4 and 6 post infection. Primary antibodies used in this assay were anti-active-caspase-3 (1:500; Cell Signaling) and anti-RUBV-E2 (1:100; Eptomics). For image analysis, the number of active caspase-3 positive cells, number of E2 positive cells, and number of active-caspase-3 and E2 positive (double positive) cells over number of total cells in same field was compared between mock-infected and RUBV-infected cells. (b) A terminal deoxynucleotidyltransferase-dUTP nick end labeling (TUNEL) assay carried out using the Click-it™ TUNEL Alexa Fluor Imaging Assay kit (Molecular Probes, Inc), in accordance with the manufacturer's instructions. (c) To assess number of apoptotic cells in a whole cell population, cells were scraped and resuspended at a concentration of 1×10^6 cells/100 μ l, followed by standard flow cytometry analysis as described in Chapter 2. Antibody used in this part of study was BD Horizon^s V450 anti- active Caspase 3 antibody (5 μ l/aliquot).

3.2.5 Cell death assay by propidium iodide staining

For assessment of total cell death in uninfected and infected cultures, uninfected control and RUBV infected hNPCs at different d.p.i (2, 4, 6, 8, and 10 d.p.i) were detached and collected in 1% FBS/PBS. Then 500 μ l of each sample (1×10^6 cells) was incubated with 1 μ l of propidium iodide (PI) (1mg/mL; Invitrogen) in the dark for 30 min at room temperature. After a wash with 1% FBS/PBS, the samples

were analyzed by cell sorting using a BD LSR Fortessa. Data analysis was performed using FACS Diva software (BD Bioscience).

3.2.6 Proliferation assays

Ki-67 and RUBV-capsid double staining was performed to assess the effect of RUBV infection on the hNPC cell cycle. Briefly, hNPCs were seeded onto coverslips and were infected at an m.o.i of 10pfu/cell with RUBV the next day. Cells were fixed at day 2, 6, and 8 post infection. Standard immunofluorescence assay (see Chapter 2) was performed to detect proliferating cells as well as viral antigen positive cells. Antibodies used in this study were anti-Ki-67 (1:150; BD Bioscience) and anti-RUBV-capsid (1:100; Eptomics). For image analysis, the number of Ki-67 positive cells, the number of capsid positive cells, and the number of Ki-67 and capsid positive (double positive) cells over number of total number of cells in same field was compared between the mock infected and RUBV infected cultures. Ki-67 gene expression was also assessed by qPCR as described in Chapter 2.

3.2.7 Image processing by Cell Profiler

Image quantification was performed using the Cell Profiler (<http://www.cellprofiler.org/>) software (Broad Institute). Pipeline was used to identify the number of objects per image (primary object) and then number of positive cells under each fluorescent color (secondary object). The percentage of positive cells was calculated by overlaying identified secondary objects with the primary object. More specifically, CellProfiler allows for the automatic calculation of cell number via nuclei extraction and quantification. An optimized cell outline is then generated for each nucleus based on the intensity and distribution of peri-nuclear-immunostaining. Individual frame wise thresholds for overall immunostain intensity and immunostain intensity/cell area were then established on the basis of a consensus selection of representative cells considered to be either immune-positive or negative. Application of these thresholds across the entire frame then allowed for the automatic quantification of positive and negative cells.

3.3 RESULTS

3.3.1 RUBV slightly decreases hNPC proliferation

One signature of the CRS fetus is reduced organ size and total cell number[101]. *In vitro* studies have also had shown RUBV attenuates cell proliferation in various cell models (see Table 1.2 for detail). Therefore, we investigated if RUBV infection could affect proliferation in our hNPC model. First, total cell number in the absence or presence of RUBV was counted and compared from day 1 to day 10 post infection. Virus infected hNPC cultures exhibited attenuated cell growth from day 7 post infection and a 5-7% reduction of total cell number was observed at 10 days post infection (Figure.3.1). However, this difference was not statistically significant. EdU incorporation assays of cells helped to further determine the proliferative potential of hNPCs; an exact quantification of the number of proliferating cells was determined by calculating EdU incorporation using flow cytometry. After a single pulse of EdU, the hNPCs were collected and EdU positive cells were detected by FACS. Consistent with the cell counting results, upon RUBV infection there was a detectable, but not significant, reduction in EdU positive cells compared to uninfected control(Figure.3.2. A, B and C).To further illustrate this marginal effect and to serve as a control for overall technique, we also infected A549 cells, for which RUBV is known to significantly disturb cell proliferation (Yumei Zhou, et.al., unpublished data) (Figure.3.2.A.B and D). The percentage of EdU positive cells in infected A549 cultures were significantly reduced by almost 2-fold compared to that of the uninfected control.

Therefore, we concluded that the effect of RUBV infection on the undifferentiated hNPC proliferation was slight at best. The detectable, but statistically insignificant, effect of RUBV on cell proliferation could be due to the low percentage of infected cells present in the culture. Thus, it was still worth it to investigate the mechanisms behind this attenuation effect, especially at the single infected cell level. The reduction in the total cell number observed in infected the culture, in comparison to uninfected cultures,

could be a consequence of inhibition of cell cycle progress and/or induction of cell death and/or other nonclassicalcytopathic effect.

3.3.2 RUBV did not induce apoptosis and other cell death events in infected hNPCs

We first investigated whether the diminished propagation of RUBV-infected hNPCs was due to RUBV induced cell death. Apoptosis, a typical cell death event that can be induced by virus infections, including RUBV [76], was detected by the expression of activated-caspase 3. At early infection time points (from day 1 to day 6), cells were double stained with anti-RUBV-E2 antibody and anti-active-caspase 3 antibody so that not only apoptotic cells within whole hNPC pool, but apoptotic cells within infected population could be identified (Figure 3.3.A). RUBV infection did not increase the percentage of active-caspase 3 positive cells at the total population level or within RUB V infected cell population. The lack of overlapping signal between E2 and active-caspase 3 in infected hNPCs, together with the observation that the percentage of apoptotic cells within the RUBV infected (E2 positive) population is lower than what is seen in the overall hNPC pool, indicates that RUBV may actually block apoptosis, as has been shown by other investigators in other cell lines [66, 75] (Figure. 3.3 A and B). Expression of active caspase 3 was likewise not elevated at later times of infection (10 d.p.i), as examined by Western Blot (Figure.3.3.C). This is also virus load independent as cultures infected with moi's of both 10 and 0.1 did not exhibit elevated caspase 3 expression. When we also performed TUNEL and active-caspase 3 flow cytometry to test the whole population for programmed cell death events, no differences were seen as well (data not shown). To rule out that other cell death events which could possibly induced by RUBV infection, such as necrosis, we conducted live cell PI staining on uninfected as well as RUBV infected hNPCs (m.o.i = 10). The number of PI staining positive cells in RUBV infected hNPCs was comparable to uninfected hNPCs at day 7 post infection (Figure.3.3 D). The results clearly suggest that RUBV induced cell death in hNPCs is not the factor in the reduction in the hNPC proliferation rate following infection.

3.3.3 RUBV induces mitotic inhibition (cell senescence) in hNPCs

To address whether RUBV mediated cell proliferation inhibition in hNPCs resulted from attenuated proliferative ability or impaired cell cycle progression, we examined expression of the signature proliferation marker Ki-67 in RUBV infected and uninfected hNPCs. Ki-67 was identified recently as a cellular marker that is strictly associated with proliferating mammalian cells, including human neural progenitors [231]. During interphase, the Ki-67 antigen can be exclusively detected within the cell nucleus, whereas in mitosis most of the protein is relocated to the surface of the chromosomes. Ki-67 protein is present during all active phases of the cell cycle (G1, S, G2, and mitosis), but is absent from resting cells (G0). To investigate whether Ki-67 is actively expressed in RUBV infected cells, hNPCs were double stained with anti-RUBV-capsid antibody and anti-Ki-67 antibody so that not only proliferating cells within the whole hNPC population, but also within infected cell population, could be identified (Figure 3.4.B). At 2 d.p.i, no significant change in percentage of Ki-67 positive cells was noticed. However, at 6 d.p.i, the percentage of Ki-67 positive cells was reduced considerably from 70% in uninfected hNPCs to 55% in RUBV infected cultures and further to 41% (almost 2-fold reduction) within capsid positive RUBV infected hNPCs. This decrease in Ki-67 positive cells upon infection was seen at 10 d.p.i as well (Figure.3.4.A). The reduction in Ki67 positive cells correlates with the significantly lower level of Ki67 gene expression in RUBV-infected hNPC's, as shown in the previous Chapter (Figure 2.6F)

Thus, reduced cumulative Ki-67 labeling in RUBV infected hNPCs clearly indicates that RUBV inhibits proliferation potential in hNPCs. In addition, Ki-67 was recently defined as a marker for cell senescence; therefore, it is possible that RUBV inhibits hNPC proliferation by inducing those cells into cell senescence.

3.3.4 The ability of RUBV to alter cell adhesion may contribute to the reduction of hNPC proliferation

A fetal alcohol syndrome study that used this same hNPC model found an increased number of floating but live cells observed following ethanol treatment (Rodney Nash, personal communication), in-

dicating that ethanol-treated hNPCs had altered cell adhesion properties. To test whether RUBV infection altered hNPC cell adhesion, the number of floating as well as adherent cells was counted separately in the presence or absence of virus. Despite a decrease in total cells following RUBV infection of moi of 10, a slight increase in the number of floating cells was observed (Figure.3.5). This suggested that the effect of RUBV infection on cell growth may be partially due to an increase in floating cells in the culture. As the medium needs to be changed every two days during maintenance, this effect cannot be ignored. To further investigate, we compared the cellular distribution of pFAK between RUBV infected cells and uninfected cells. pFAK plays an important role in the control of several biological processes, including cell spreading, migration, and survival. It has been shown that pFAK also plays a role in regulating hNPC cell adhesion [232]. However, no difference was seen upon virus infection (data not shown). Thus, other cell adhesion molecules, such as integrin, need to be studied.

3.3.5 RUBV did not induce inflammatory cytokine responses in hNPCs cultures

Virus infection is a powerful inducer of type I interferons and other inflammatory cytokines [228, 233], as many virus components are recognized by pattern recognition receptors. Massive cell death upon virus infection can be due to strong innate/ inflammatory cytokine responses (bystander effect)[229, 234]. We therefore wanted to investigate if this is the case in RUBV infected hNPCs. In other words, we wished to determine whether the insignificant cell loss in RUBV infected hNPCs was due to a deficient cytokine response. To determine the cytokine expression in hNPCs upon RUBV infection, we examined the expression at the protein level as well as the RNA level of IL-6 and IFN-beta. During the first four days of infection, none of those cytokines had an elevated expression on the RNA level, even in presence of robust RUBV replication (Figure.3.6.A). Similar results were seen on the protein level, as confirmed by ELISA (data not shown, personal communication with Yumei Zhou). To further prove those observations, we examined key regulators and signaling molecules (NF-kB p65, pSTAT3 and RIG-I) that regulate the expression of these cytokines, and no detectable difference was seen between RUBV infected and uninfected cultures during the infection time course (Figure.3.6.B). This was as we expected, as proteins

such as pSTAT3 also play an important role in regulating hNPCs neuronal differentiation. Abnormal expression of such proteins would have a drastic effect to the multipotency of hNPCs. Thus, the absence of cytokine responses could partially explain why there was no massive reduction of hNPCs population upon RUBV infection.

In summary, herein we showed that RUBV moderately attenuates hNPC proliferation, through cell cycle interruption instead of cell death or apoptosis. The level on the population level was moderate probably due to low percentage of cells infected. No inflammatory cytokine response, which could affect cell viability and proliferation, was seen as well.

3.4 DISCUSSION

In the second part of our study, we sought to determine whether and how RUBV affect proliferation of hNPCs. The first step is to characterize hNPC cell growth in presence of RUBV, as this is the foremost and most decisive reflection of cell proliferation. Indeed, less hNPCs cells were present in RUBV infected culture compared to the control (~10-20% reduction) after 10 days of infection. However, this difference was not statistically significant after a t-test examination. We further addressed this question by closely investigated our calculation methodology. It was suggested that in a case of nonsignificance, the sample size is very important [235]. Since we only repeated the experiment for three-times, it is highly possible that the experimental repeats were not sufficient to generate statistical significance. Therefore, a hypothetical fourth experiment using same experimental data as the third repeat was added to the data pools. This time we indeed observed a statistical difference ($p=0.01$ and 0.05 for day 9 and 11 respectively). Therefore, the non-significance of our result from cell growth is due to lack of experimental repeats but not necessarily a lack of biological significance. Also, considering that only 10% of cells in the culture are infected, it is highly possible that infected cells had altered proliferation but just because there were so few of them, the effect of RUBV infection on hNPC growth was not reflected in a popula-

tion view. Thus, RUBV attenuation effect to the growth of hNPC is slight at the most from a population view and a single-cell-based investigation of infected cells was required for further characterization.

The reduction in the number of cells present in our infected cultures is in agreement with previous findings[61, 62, 65, 67], and can be due to RUBV induced cell death, inhibition of cell cycle progression and anoikis which is a specific response to be studied considering the embryonic source of hNPCs[236, 237]. Therefore, in our next step, we conducted experiments on individual cells to investigate if RUBV induces each or any of these cellular responses.

Cell death

Two types of cell death were previously reported in the brains of CRS abortuses and patients who died from PRP, namely apoptosis and necrosis [106, 238]. A common feature of these two types of cell death is chromosomal breakage which can be picked up by PI staining[239]. However, our living cell PI analysis over the total population of hNPCs showed no increase upon RUBV infection, indicating RUBV did not trigger massive cell death to the hNPCs.

Studies of RUBV infection to in vitro cell models suggested RUBV induce apoptosis in a caspase-dependent pathway [239]. We therefore use active-caspase 3 in combination of RUBV-E2 antibody to pick up individual infected cells that undergoing apoptosis. A significant reduction in active-caspase 3 positive populations was seen among RUBV-infected cells compared to the non-infected control, indicating that RUBV does not induce but instead blocks induction of apoptosis. The immunofluorescence imaging techniques we used to directly pick up single infected cells and apoptotic cells in the population gives a more accurate picture of the relationship between virus and cell death responses. We did not stain cells with additional necrosis marker to further investigate this cell death event. This is because during apoptotic studies, we did not observe swollen cell bodies and chromosomal breakage, which are two hallmarks of necrotic cells, in infected cells picked up by RUBV-E2 antibody.

In previous studies in our lab, it was shown that while RUBV infection induced apoptosis in adult human fibroblasts, it did not do so in fetal human fibroblasts [66, 182]. Frank inhibition of apoptosis during RUBV infection was previously reported by another group in a study in which it was shown that the RUBV capsid protein (C) alone could inhibit chemical staurosporine (ST) induced apoptosis [75], in line with the results of our study. In addition, in studies on selected non-human cell lines, although viral replication is required to induce apoptosis, it is the non-infected neighboring cells that undergo this effect [240]. Other viruses also inhibited induction of apoptosis upon infection in hNPCs. HCMV, which is also teratogenic, blocks apoptosis in primary human fibroblast and in hNPCs derived from abortuses [148, 179, 180]. Highly neurovirulent flaviviruses similarly did not induce cell death in hNPCs: the percentage of cells undergoing both apoptotic and necrotic death was not significantly higher in JEV/ WNV infected hNPCs after 7 days post infection than in uninfected ones [124, 207]. Expression of HIV gp120 also results in few apoptotic TUNEL positive cells in murine NPCs [199]. Since NPCs are equipped with certain anti-apoptotic factors, like IAP family members (c-IAP1), it has been postulated that it is a factor in the resistance to virus induced cell death [146, 241]. In addition, it has been shown that the pattern of c-oncogenes expression during embryonic development promotes proliferation and inhibits apoptosis in a cell-specific and time-specific manner [242, 243]. In studies from our lab, resistance to RUBV-induced apoptosis by fetal cells was attributed to the pattern of gene expression in the fetal cells which was anti-apoptotic [182]. Though some of the anti-apoptotic mechanisms has been elucidated in NPCs that make them resilient to apoptotic signals, however, direct evidence of how they evade virus induced cell death is still not established.

Clearly, our results showed RUBV did not induce cell death in hNPCs, either to the population or in single-infected cells. Actually, we would expect this result: if cells in the hierarchy of CNS development, such as hNPCs, were dead after infection, we would not expect birth defects but rather fetal death. As for the mechanism: there is likely a natural resilience of hNPC's to virus induced cell death, however our results indicate a specific anti-apoptotic response on the part of the virus.

Cell cycle arrest

A key marker identified for proper isolation of proliferating NPCs is Ki-67, which is only expressed in NPCs undergoing active cell cycling [244]. In single-cell-based examination of Ki-67 expression in RUBV infected cells, we found a significant (over 50%) decrease in the percentage of Ki-67 positive cells in E2-positive cells in infected cultures in comparison with uninfected cells (either in the control or RUBV-infected cultures). This was further confirmed on the mRNA level by qRT-PCR (see Chapter 2). Our EdU incorporation analysis, which reflects level of DNA synthesis by proliferating cells, showed slight, but not significant, reduction in EdU incorporation in RUBV infected compared to uninfected cultures (this assay was not done by counting E2-positive cells). However, we do not rule out the possibility of sample size problems in calculating a statistical significance. In addition, the virus induced cell decrease in Ki67 was exaggerated most at day 10 post infection when the effect of RUBV on the hNPC growth curve was most pronounced. Therefore, these data implied that RUBV induced cell cycle quiescence was the primary factor to the inhibition in cell growth seen in RUBV infected hNPCs.

Sustained proliferation is a key feature of NPCs and it was recently shown that a number of viruses can induce quiescence in these cells by impairing their proliferative ability (see Table 1.3 for a complete summary). The proliferation arrest in hNPCs upon HCMV infection is indicative of a switch from cellular DNA synthesis to viral DNA synthesis[245]. Evidence from several labs corroborated that JEV infection leads to cell cycle arrest at G1—S phase [207]. Quiescence in adult hNPCs following HIV-1 infection was attributed to the chemokine receptors, CCR3 and CXCR4, which are used by the cells to maintain their ability to proliferate [246-248]. Reduced Ki-67 expression has been demonstrated in slow growing tumors associated with ocular surface squamous neoplasia (OSSN) in presence of HIV infection[249]. The proportion of Ki67-positive cells also correlated with tumor stage of progression associated with Epstein-Barr virus-encoded latent membrane protein (LMP1) in nasopharyngeal carcinoma [250].

As for RUBV, numerous previous studies suggested that the virus affects cell proliferation by inducing cell cycle arrest (reviewed in [7, 65]). Growth inhibition is particularly notable in RUBV infected primary diploid cells derived from human fetal organs, providing an explanation for underdevelopment of organs in congenitally infected children that results in microcephaly as well as autocrine and bone abnormalities [61, 67, 251, 252]. The mechanism of such inhibition is attributed to a) virus association with certain cytokinesis regulatory proteins such as retinoblastoma (RB) and cyclin-dependent kinase (CK)[69, 253], b) virus induced production of a growth inhibitory factor[64, 68], and/or c) virus disruption of microfilaments which play a crucial role in mitosis [89]. The results of our study has suggested a new mechanism by which RUBV infection attenuates cell proliferation, namely by directly altering expression of cell cycle regulatory protein. Whether this mechanism is unique to neural precursors or can be generalized to other embryonic/fetal cells remains to be tested.

Anoikis

Considering hNP1TM cells we used in this study are loosely adherent, we also investigated a non-typical cytopathic effect that could associate with virus-infection called anoikis. Anoikis is defined as a form of programmed cell death which is induced by anchorage-dependent cells detaching from the surrounding extracellular matrix (ECM)[237]. This cytopathic event plays an important role in cancer metastasis and recently has been shown to be associated with tumorigenic viruses such as Epstein-Barr virus, KHSV and Hepatitis B virus (HBV) [254-256]. In our study, starting from day 5 post infection, there were fewer adherent cells in RUBV infected hNPCs compared to uninfected ones. However, the percentage of viable cells remained the same as shown by previous PI staining result. Thus, RUBV induces detachment of a subpopulation of hNPCs while not killing most of the cells. This type of viral induced cell detachment, although counter to the anoikis hypothesis, was previously demonstrated in SINV infection to PBMCs [161]. The day post infection on which we observed reduced adherent cells in infected cultures coincident with the reduction of total cell number, suggesting that RUBV induced hNPC detachment may partially contribute to attenuated cell growth upon infection. However, we did not observe an alteration in

the expression as well as intracellular distribution of focal adhesion kinase (FAK) upon virus infection. It is possible that virus directly affects the integrity of integrin or other adhesion molecules. Thus, further studies will determine whether the detached cells were infected by RUBV and whether crucial cellular adhesion molecule such as integrin was affected upon infection.

Cytokine profiling

Previous studies suggested that CRS is partially due to immune damage mediated through a bystander effect [234]. However, our result showed no up-regulation of classical RUBV induced cytokines IL-6 and IFN β . This indicated that RUBV did not directly trigger inflammatory or innate immune responses in hNPCs. The observation was in line with the lack of inflammatory reactions seen in brains of CRS infants [106]. The vascular lesions present in these brains may be triggered by immune responses within endothelial cells as we observed dramatic elevation of IL-6 expression in hMPro even after 3 days post infection. Impaired cytokine production and moderate immunosuppression was reported in school-girls who received a rubella vaccination [257], suggesting RUBV can suppress cytokine responses. A posttranscriptional suppression of IL-6 production in human fibroblasts upon HCMV infection has also been reported [258]. Whether the lack of IL6 and IFN induction in hNPCs is virus-specific or cell specific thus needs further investigation.

Induction of inflammatory cytokines by RUBV has been previously demonstrated *in vitro* in various other models: A549 cells infected with RUBV produced enormous amount of IL-6 and IFN- β with 24 h.p.i; similarly, a drastic elevation of IL-6 expression in hMPro cells was observed after 3 days post RUBV infection (Yumei Zhou, et.,al, unpublished data). In addition, RUBV infected human fetal fibroblast showed a burst of IFN and chemokine expression within 24 h.p.i [182]. These findings are in striking contrast to the obvious non-inflammatory characteristics of RUBV showed in the hNPCs model. However, giving recent mechanistic studies in our lab using other cell models; it is not difficult to explain why inflammatory cytokines such as IL-6 and IFN- β were not induced by RUBV. First, using a RUBV harbor-

ing Vero cell line 925-IN, we found that although exogenous IFN α suppressed replicon RNA and protein synthesis, but did not cure the cells[163]. Then, surprisingly, the replicon reappeared within one week of suspension of IFN α treatment. Besides, we observed cells that are negative in viral protein synthesis but positive for the residence of viral replicon RNA in 925-IN cultures. Those results in together suggested that RUBV infection in cell culture is refractory to IFN treatment, the virus can persistent in culture with minimum expression / transcription of its genes. In this context, RUBV is able to avoid from being detected by host intracellular pathogen recognition machinery which initiate cytokine responses. Second, in characterizing host innate immune responses to RUBV infection in A549 cells, we found that the signaling transduction induced by the virus was postponed and peaked at 48hrs post-infection, indicating that RUBV has a degree of intrinsic resistance to cellular IFN response, possibly at the stage of interference with the signaling transduction (e.g. IRF3) downstream of RIG-I/MDA5. Such intrinsic resistance may also partially explain the non-inflammatory characteristics seen in hNPCs upon RUBV infection.

In summary, a combination of cell death and mitotic inhibition is reflected in the pathology of CRS, which exhibits features of both destruction within specific tissues and growth retardation. In our study, we demonstrated that hNPCs are not susceptible to the cytopathogenic effect of RUBV and that a cell cycle inhibition may more predominant in these embryonic cells in the early fetus development. A tissue-specific apoptosis may thus account for the myriad of dysfunctions observed in CRS patients.

It has been suggest that virus infection early in development adversely affects undifferentiated precursor cells by inducing apoptosis, leading to underdevelopment[76]. Our results argue against this idea in neural precursor cells, which can be infected without undergoing apoptosis. As for the fate of such infected cells in subsequent developmental stages, additional characterization utilizing advanced techniques such as laser capture or live-cell antibody labeling is needed so as to track the infected cells in infected hNPC cultures also under differentiation. Additionally, chromosomal breakage may need to investigated since this has been demonstrated in infected human embryo cells [67].

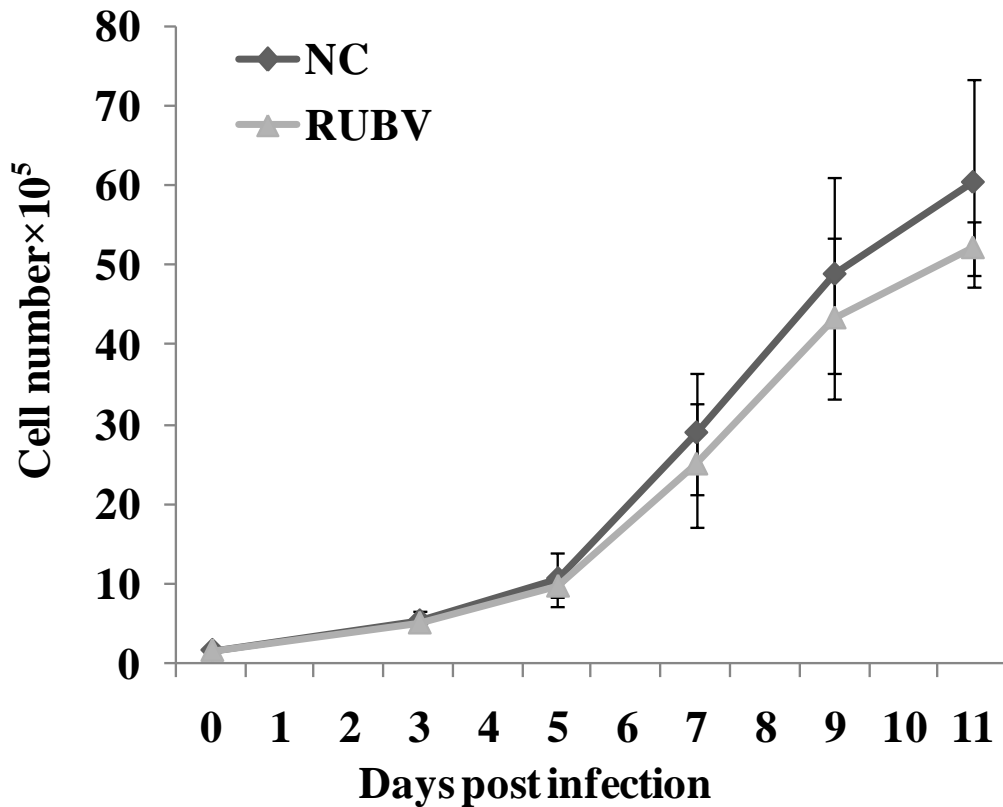


Figure 3.1 hNPC growing kinetics in presence and absence of RUBV.

Equal numbers (5×10^5) of hNPCs (passage 7-10) were seeded in each well of a 24 well plate and mock infected or infected with RUBV the next day (m.o.i=10). The culture medium was changed daily. Total cell number in the infected and uninfected cultures was determined at indicated time points through 11 days post infection. This experiment was repeated three times and the error bars indicate SDs. Despite the apparent differences in cell numbers at the later time points, these were not statistically significant at a 95% confidence interval ($P < 0.05$).

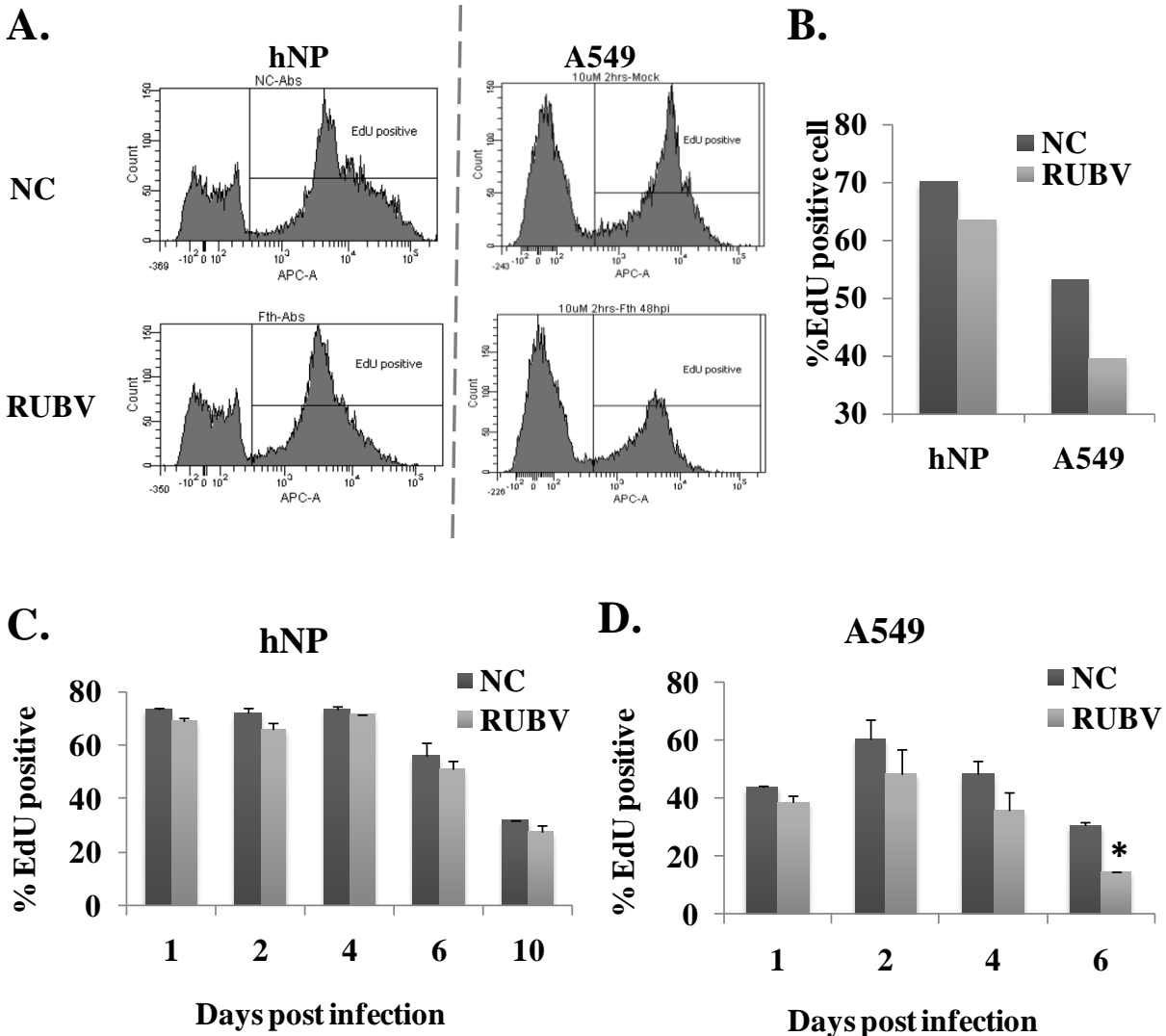


Figure 3.2 Proliferation of hNPC vs A549 after RUBV infection as measured by EdU incorporation assay.

hNPCs and A549 cells were seeded at similar densities and either left uninfected or infected with RUBV (moi = 10) the next day. Cell proliferation and DNA synthesis were analyzed by a non-radioactive EdU incorporation assay; the percentage of proliferating, EdU positive cells was quantified by flow cytometry. (A) FACS analysis using an Alexa Fluor® 647 Click-iT® EdU Flow Cytometry Assay Kit. At 6 days post infection, both hNPCs and A549 cells were treated with EdU for 2 hours and then processed for EdU incorporation according to the manufacturer's recommended protocol. The figures show a clear separation of proliferating cells (which have incorporated EdU) and non-proliferating cells (which have not). (B) Quantification of results shown in (A). (C) Proliferation of hNPCs during an infection time course; EdU incorporation was assayed on days 1, 2, 4, 6, and 10 postinfection. (D) Proliferation of A549 cells during an infection time course; EdU incorporation was assayed on days 1, 2, 4, and 6 postinfection. Both experiments were repeated at least twice. Error bars represent SDs. *, statistical significance compared to the uninfected control at the same time point determined at a 95% confidence interval ($P < 0.05$).

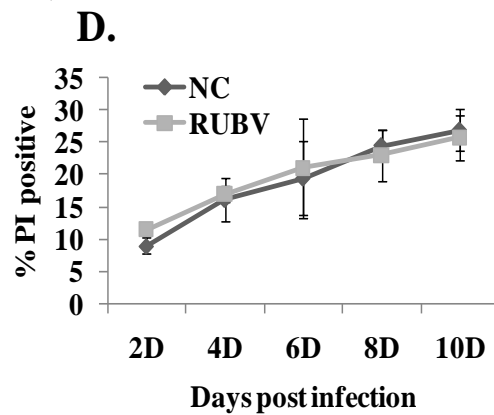
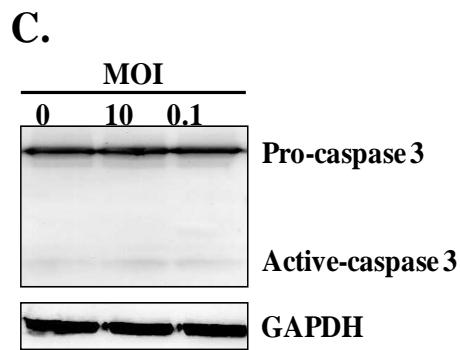
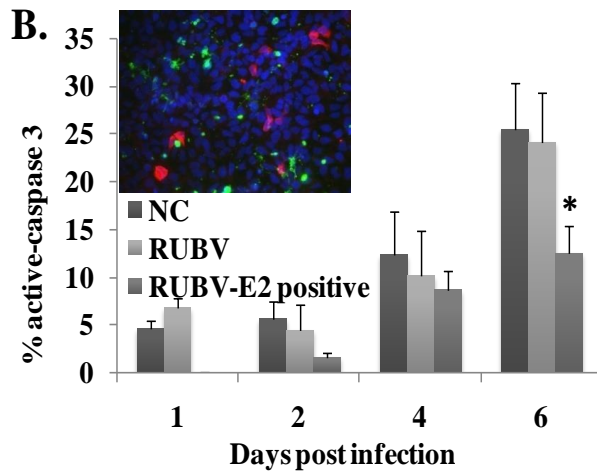
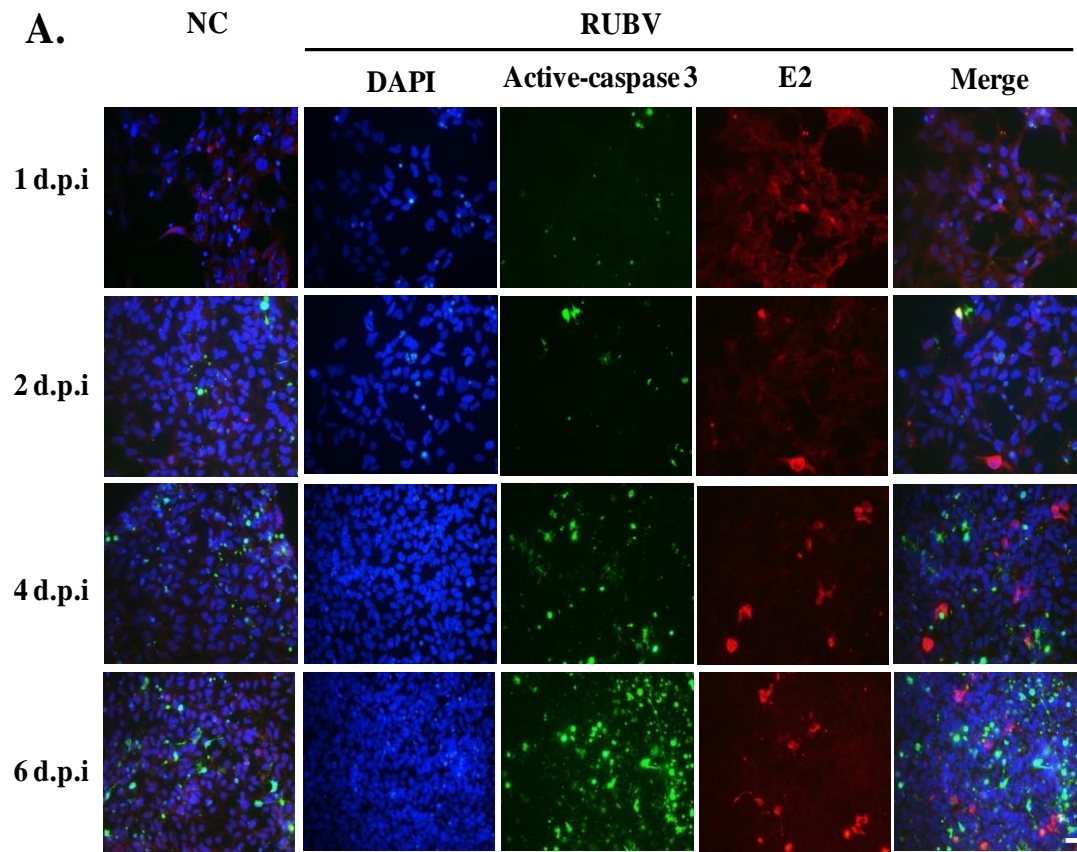


Figure 3.3 RUBV did not induce apoptosis in infected hNPCs.

Mock infected and RUBV-infected hNPCs were examined for the expression of active caspase 3, a marker for apoptosis, by immunofluorescence staining. **(A)** hNPCs were mock infected (NC) or infected with RUBV at an m.o.i of 10 (RUBV), fixed at 1, 2, 4, and 6 days post-infection, and analyzed by fluorescence microscopy. Apoptotic cells were detected with anti-active caspase 3 antibodies (green), RUBV-infected cells with anti-E2 antibody (red), and nuclei were visualized with Hoechst dye (blue). Individual stains are shown for the RUBV infected cells while merged images are shown for the NC. **(B)** The percentage of active caspase 3 positive cells in the mock infected culture, the RUBV-infected culture and among E2 positive cells in the RUBV-infected culture was determined. To make these determinations, the experiment was repeated 3 times and at least three fields of view were counted in each experiment. Error bars indicated SDs; *, - significance compared to the uninfected control ($p < .05$), **(C)** Western Blot analysis to detect active caspase 3 at 10 dpi in hNPCs following mock infection or RUBV infection at MOIs of 10 and 0.1. The experiment was repeated 3 times and a representative blot is shown. **(D)** Live cell PI staining measuring total cell death events in mock-infected and RUBV infected (moi=10) hNPCs at 2, 4, 6, 8 and 10 days post infection. Quantification of the percentage of positive cells present in population was done by flow cytometry. The experiment was repeated 3 times and error bars represent SDs.

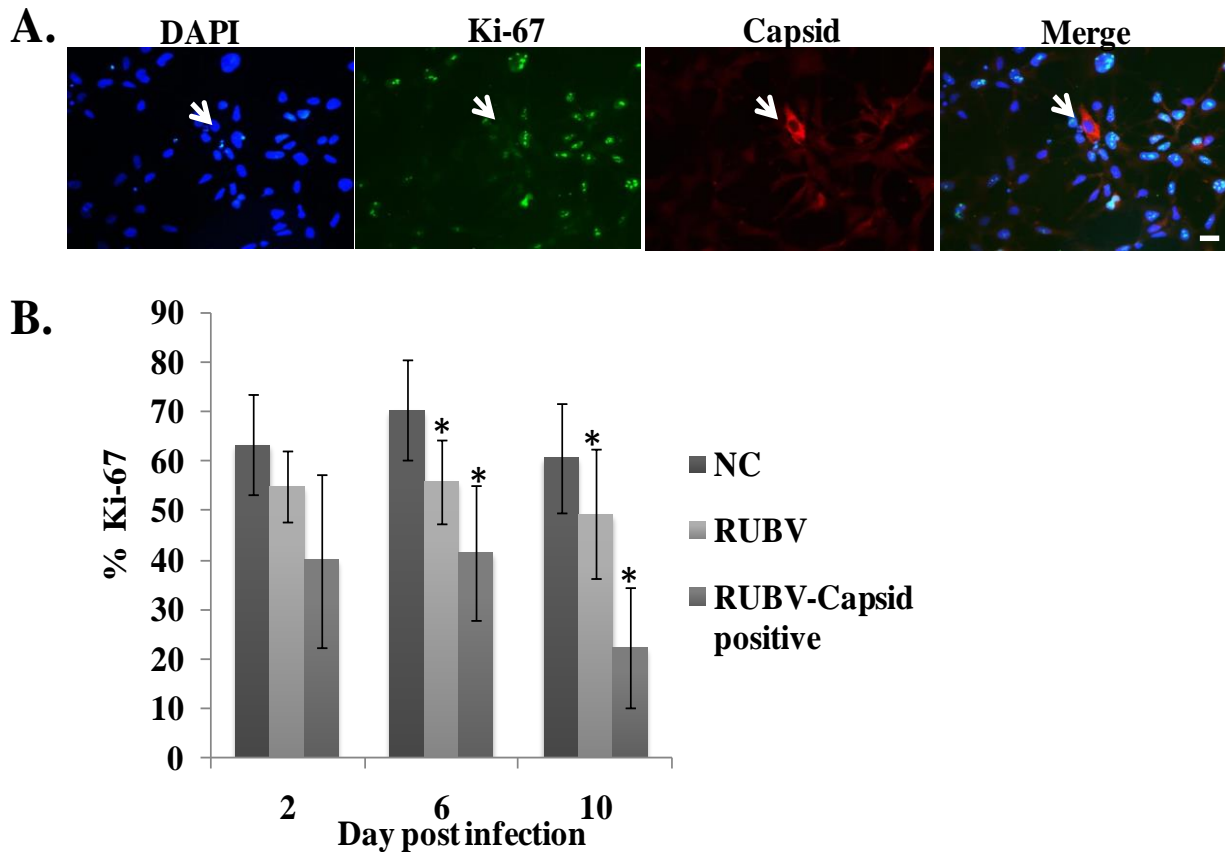


Figure 3.4 RUBV induce cell senescence to hNPCs.

Mock-infected and RUBV-infected hNPCs were examined for the expression of Ki-67, a marker for proliferating hNPC by immunofluorescence staining. The absence of Ki-67 is also an indicator of senescence. (A) hNPCs were mock infected (NC) or infected with RUBV (m.o.i = 10) (RUBV) were fixed at 2, 6, and 10 days post infection and analyzed by fluorescence microscopy for Ki-67 (green) and RUBV E2 (red); nuclei were visualized with Hoechst dye (blue). A representative image of RUBV-infected cells captured on day 6 post infection is shown. The arrow denotes a cell positive for E2 but negative for Ki67. (B) The percentage of Ki-67 positive cells in the mock-infected and RUBV-infected cultures and among E2 positive cells in the RUBV culture was determined. The experiment was repeated 3 times and in each experiment at least 3 fields of view were counted. Error bars indicate SDs. *, -statistical significance compared to the uninfected control ($P < 0.05$).

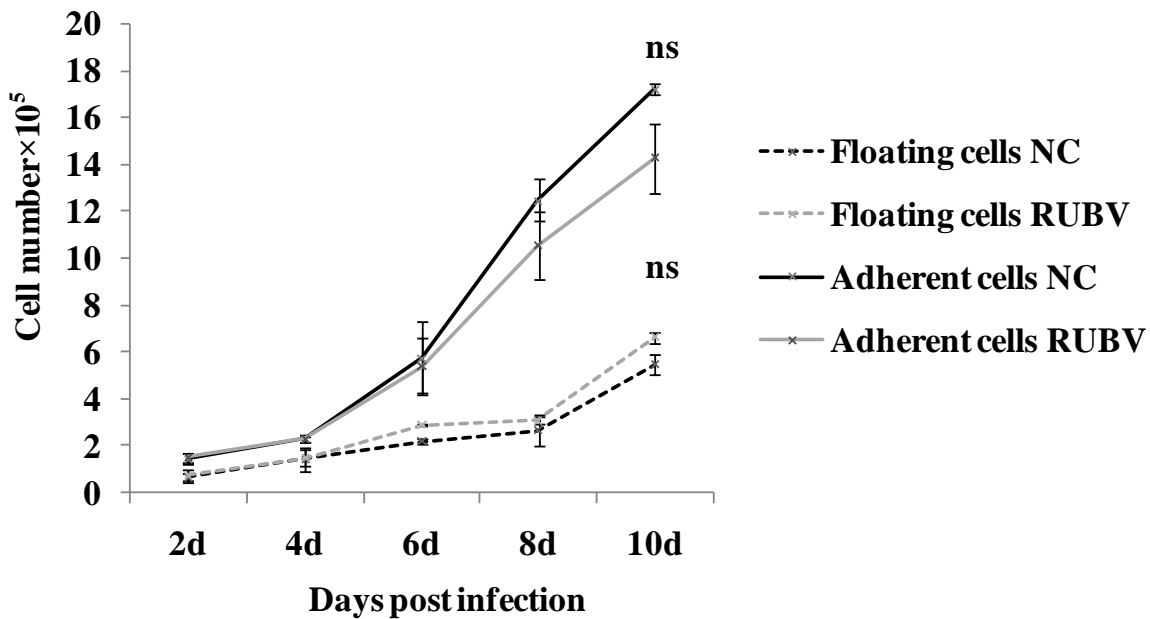


Figure 3.5 RUBV infection of hNPCs did not increase the number of "Floaters".

Equal numbers (5×10^5 cells) of hNPCs (passage 7-10) were seeded in each well of a 24 well plate and either mock infected (NC) or infected with RUBV (m.o.i=10) the next day. The culture medium was changed daily. On days 2, 4, 6, 8, and 10 post-infection, the adherent and floating cells in one well of each culture were collected and counted. The experiment was repeated three times and the error bar indicates (SDs).ns, no statistical significance compared to the mock infected control at a 95% confidence interval ($P < 0.05$).

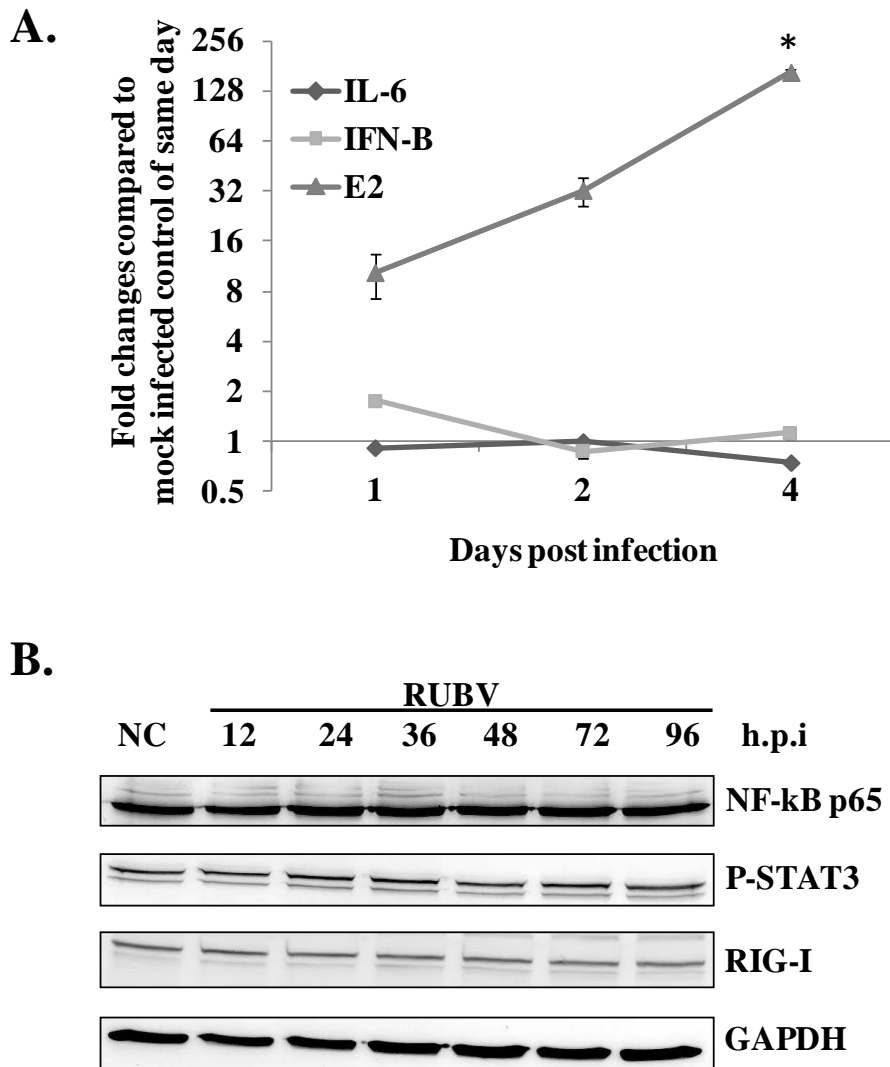


Figure 3.6 RUBV did not induce inflammatory responses in hNPCs.

(A) RNA isolated from mock-infected and RUBV infected (moi=10) hNPCs at days 1, 2, and 4 post infection was used to perform real-time qRT-PCR to detect the viral E2 gene and mRNAs for the inflammatory cytokines IL-6 and IFN-beta. Each experiment was done in triplicate and repeated at least twice, and representative data from one experiment are shown. The gene expression levels were normalized to GAPDH mRNA in the same sample and are shown as fold change over the amount of RNA in the mock-infected control at same time point. Error bars indicate SDs. *, statistical significance compared to the control ($P < 0.05$). (B) Western Blot analysis of expression of three inflammatory signaling proteins during early infection. Each experiment was performed at least twice. A representative blot is shown. GAPDH: loading control.

CHAPTER 4 : CHARACTERIZATION OF THE EFFECT OF RUBV INFECTION ON HUMAN NEURAL PROGENITOR CELL DIFFERENTIATION INTO NEURONS AND GLIAL CELLS

4.1 INTRODUCTION

Multi-sensory impairment (MPI) is a typical clinical feature of CRS [259]. Hearing loss is often accompanied by eye defects, indicating sensory neurons that are shared by both systems can be affected by RUBV infection. In rare cases, CRS infants can develop severe CNS degenerative disease such as mental retardation and progressive rubella panencephalitis (PRP), suggesting that RUBV has the capacity to impact the development of the host neural system. In addition, other viral teratogens (e.g. HCMV, CVB, JEV) that cause similar congenital defects as RUBV were shown to disrupt hNPC differentiation *in vitro*, further supporting the possibility of RUBV induced abnormalities in hNPCs, including its differentiation [260].

The human CNS is mainly composed of two types of cells: neurons and glial cells. Neurons are the cells that establish communications transmit signals and administrate various actions throughout the body; while glial cells provide support and nutrition, maintain homeostasis, form myelin, and participate in pathogen clearance in the nervous system. The total number of neurons and glial cells are almost the same within in brain areas and glial cells play important roles in maintaining CNS integrity. Therefore, it is worthwhile to investigate whether and how RUBV infection impacts the differentiation of hNPCs into both cell lineages. Additionally, this is the first time that RUBV infection has been studied for its effect on the differentiation of a human cell line.

To test whether RUBV affects the differentiation of hNPCs into neurons and/or glial cells, hNPCs undergoing neuronal and glial differentiation were analyzed for their response to virus infection, which was introduced at different points of the differentiation process, including both the induction and committed phases. Cell morphology and expression of selected stemness markers were analyzed by immunofluo-

rescence microscopy. Genome expression profiling analysis was carried out on RUBV infected hNPCs at the end of the differentiation process to further investigate detailed cell markers or pathways that could be impacted by the virus. Interestingly, the virus had a marginal effect to the induction of cell differentiation into both cell types. To explain that observation, we investigated the susceptibility of differentiated cells to RUBV infection and we found that extracellular production of RUBV was significantly reduced upon the initiation of differentiation and that differentiated cells no longer expressed virus antigen. Therefore, the effect of RUBV infection on hNPCs differentiation was marginal at most and that this is mostly due to lack of infectivity of RUBV in those differentiated cells.

4.2 MATERIAL AND METHODS

4.2.1 Cell culture and differentiation

Proliferating hNPCs were cultured and passaged as described in Chapter 2, passage 6-10 cells were used in following studies. For hNPC differentiation:

(1) For spontaneous differentiation, which yields mostly neurons, hNPCs were grown for 14-21 days in neural expansion medium lacking bFGF to promote random differentiation. Briefly, mid-passage hNPCs were seeded in 60 mm plates coated with Matrigel at a density of 1×10^6 cells/plate. Differentiation was initiated after the cell reached 70%-80% confluency by replacing the AB2 complete neural expansion medium with differentiation medium (AB2 complete neural expansion medium without bFGF). Differentiation conditions were maintained for 3 weeks, during which the medium was changed every 2-3 days. For study of the effect of RUBV on hNPC differentiation, cells were similarly seeded onto 60mm plates, infected with an m.o.i of 10 with RUBV the next day and then recovered in AB2 complete neural expansion medium for 2 days before differentiation was initiated. Cells were passaged every 7 days or as needed (when cells reached 100% confluency) during differentiation.

(2) For astroglial differentiation that yield mostly astrocytes and oligodendrocytes, hNPCs were grown for 14 days in neurobasal medium supplemented with 1x B27 (define), 1x Pen-Strep, 2mM L-glutamine, (all from Gibco, Invitrogen), 20mg/ml bFGF and 10ng/ml ciliary neurotrophic factor (CNTF, Millipore), as previously described[137]. Briefly, mid-passage hNPCs were seeded in 60mm poly-L-ornithine (20µg/ml, Sigma) and laminin (5 µg/ml, Sigma) coated plates at a density of 1×10^6 cell/plate. Differentiation was initiated after cells reaching 70%-80% confluency by replacing the neural expansion medium with differentiation medium (as described above). Differentiation conditions were maintained for 2 weeks, during which medium was changed every 2-3 days. For study of the effect of RUBV infection on hNPC differentiation, cells were similarly seeded onto 60mm plates, infected with RUBV at a an m.o.i. of 10 the next day and then recovered in AB2 complete neural expansion medium for 2 days before differentiation was initiated. Cells were passaged every 7 days or as needed (when cells reached 100% confluency) during differentiation.

For optimal astroglial differentiation, hNPCs were grown on poly-L-ornithine and laminin coated plates. For poly-L-ornithine/laminin coating: The growth substrates poly-l-lysine and laminin were purchased from Sigma–Aldrich. The culture dish was first coated with a solution of 50 µg/ml poly-l-lysine in sterile water for 1 hr (37 °C), rinsed once with sterile water, air dried and coated with a solution of 20 µg/ml laminin in sterile phosphate-buffered saline (PBS) for 1 hr(37 °C) or overnight (4°C), rinsed twice with PBS before use or directly put into 4°C for storage

For RUBV infection at later stage, briefly, hNPCs that have been cultured in differentiation medium for 14 days were infected with RUBV at moi of 10. After 1 hr, the virus inoculum was removed and cells were refeed with differentiation medium. The infected cultures were analyzed two day post infection by immunofluorescence staining for virus antigen and culture medium was used to titer extracellular virus production.

4.2.2 Monitoring the stage of differentiation and the loss of multipotency by flow cytometry

Flow cytometry was performed during hNPC differentiation to monitor multipotency changes. For spontaneous differentiation, cells were collected for analysis each week during the three week differentiation process. For astroglial differentiation, cells at the end of the differentiation (week 2) were subjected to flow cytometry analysis. Flow cytometry was carried out as described in Chapter 2. For this experiment the following antibodies were used: anti-Nestin (conjugated with PE); anti-SOX2 (conjugated with FITC); anti-Ki-67 (conjugated with V450), all from BD Bioscience, 5 μ l for each sample.

4.2.3 Cell differentiation marker expression profiling by qRT-PCR

RNA was isolated from cells at either 21 days of differentiation (spontaneous) or 14 days of differentiation (astroglial) followed by quantification and cDNA synthesis following protocols described in Chapter 2. In order to acquire the hNPCs differentiation status as well as multipotency changes, several genes were probed (see Table 4.1 and 4.2 for target gene list and primers). Those target genes covered markers of hNPC multipotency and all three lineages of terminally differentiated neuronal cells, namely neurons, astrocytes and oligodendrocytes. PCR was performed in ABI Prism 7500 system and data was acquired using SDS 2.2.1 software (Applied Biosystems). Gene expression data (done in triplicate) were acquired and ABI Prism 7500 software and ABI data assist (both from Applied Biosystems) were used to estimate relative fold change values using the $\Delta\Delta C_t$ quantitation method. We compared gene expression in differentiated cells (both mock and RUBV infected) and normalized this to gene expression levels in undifferentiated hNPCs. Endogenous GAPDH was used for normalization and calibrated gene expression for each sample against undifferentiated hNPCs. Statistical analysis was performed as previously described [135] and briefly discussed under data procurement and statistical analysis below. Means were compared and grouped using Student test at 5% level of significance.

4.2.4 Immunofluorescence staining of differentiated hNPCs

Cells were grown on coverslips, fixed in 4% paraformaldehyde and stained with anti-Nestin (1:450; Neuromics), anti-neuron specific β -tubulin III (Tuj1) (1:1000; Abcam); anti-A2B5 (1:100; Abcam); anti-GFAP (1:300; Abcam); anti-MOG (1:100; Abcam); anti-RUBV E2 (1:100; Eptomics) and anti-RUBV capsid (1:100; Eptomics). Immunofluorescence staining and image acquisition were carried out as described in Chapter 2.

Cell Profiler software was used for image processing and quantification. Pipeline set up was conducted as described in Chapter 3. For morphology/cell phenotype analysis of differentiated neurons, at least three random fields of view (each with more than 20 cells) from two different experiments of Tuj-1 immunostained cells were used. Briefly, the DAPI stained images were used for identification of nuclei before identification of differentiated neurons using Tuj1 stained images. “Measurement-Neuron” pipeline was utilized to acquire both the number of differentiated neurons as well as their average shape parameters (trunks and branches). After recovery of the image, that parameter was obtained and results were compared between differentiated cells in presence or absence of RUBV. For quantifications of differentiated astroglial, A2B5 was used as the phenotype marker. Positive stained cells were quantified as described in Chapter 3. The percentage of A2B5 positive cells were compared between astroglial differentiated cells in the presence or absence of RUBV. Each experiment was repeated at least twice for statistical analysis.

4.2.5 Viral susceptibility studies

For assessment of susceptibility of hNPCs to RUBV infection during the differentiation, (1) To test extracellular production of virus during differentiation course compared to the undifferentiated control: culture medium of undifferentiated and differentiated hNPCs infected with RUBV were collected at indicated day post infection. Extracellular production of virus during the differentiation time course was tested by standard plaque assay (see chapter 2). (2) To examine the expression of virus antigen in differenti-

ated cells: at 14 days after initiation of differentiation, infected cultures were stained with lineage specific markers (Tuj-1 for neurons and A2B5 for astroglia) together with antibodies for virus antigen (E2 or Cap-sid) by standard immunofluorescence assay (described in chapter 2). (3) To examine susceptibility of differentiated cells to RUBV infection: Uninfected hNPC cultures differentiated for 14 days were infected with RUBV at a m.o.i of 10, expression of virus antigen was tested 2 days later. Culture medium was also collected and tested for extracellular production of the virus by plaque assay. Control undifferentiated hNPCs were similarly infected and tested for the production of the virus at same d.p.i.

4.3 RESULT

To investigate whether RUBV infection impairs the differentiation of hNPCs, hNPCs were infected with RUBV at the initiation of cell differentiation (to test whether RUBV impairs the induction of differentiation), or at a later stage of cell differentiation (to test whether RUBV impairs the function of hNPCs that already committed to differentiation). Two differentiation pathways were examined in this study: hNPCs differentiated into neurons (neuronal differentiation or neurogenesis) and hNPCs differentiated into astroglial cells (glial differentiation or gliogenesis).

4.3.1 Effect of RUBV infection on hNPCs neurogenesis

hNPCs are capable of differentiating into neurons

To mimic the neurogenesis process, we utilized the “spontaneous differentiation strategy” according to the company's (ArunA Biomedical) protocol which indicated would yield mostly neurons (Figure. 4.1.A). Immunofluorescence demonstrated that more than 90% of cells in the undifferentiated cultures expressed the neuroepithelial stem cell marker Nestin (Figure.4.1.B left). Upon growth factor bFGF withdrawal, the cells stopped proliferating and differentiation was initiated. During differentiation, cells were passaged as necessary, usually every 7 days. The cells that had lost differentiation potential or were unable to further differentiate would be gradually selected out from the culture plate by cell detaching (most-

ly progenitor cells). Cells grown on Matrigel-coated plates would eventually become neurons and exhibit distinguishing phenotype that contrasts with undifferentiated hNPCs on the basis of morphology and cell marker expression. By the end of the differentiation process, around 40% of cells were differentiated, as determined by elongated neurite outgrowth as well as Tuj-1 (β -tubulin III) positive immunostaining (Figure.4.1.B). Expression of stemness markers, such as Nestin and SOX2, decreased during differentiation as cells gradually lose their multipotency (cells positive for Nestin expression decreased from $92.9\% \pm 3.31\%$ to $54\% \pm 3.54\%$; cells positive for SOX2 expression decreased from $87.6\% \pm 4.21\%$ to $50.9\% \pm 5\%$, Figure.4.1.C). Using this differentiation strategy, very few cells had the morphology typical of oligodendrocytes and astrocytes, and expressions of astroglial lineage marker (Gfap, Mbp, etc.) genes were not detectable by quantitative real-time PCR (data not shown).

RUBV infection did not significantly impair the induction of hNPCs' neuronal differentiation

To investigate whether and how RUBV infection impacts the induction of hNPC neuronal differentiation, proliferating hNPC cultures were infected with RUBV (moi = 10) two days prior to the initiation of spontaneous differentiation. Cells were maintained for 3 weeks following differentiation and passaged as necessary (Figure.4.1.A). As a control, hNPCs were similarly infected and passaged, but not subjected to differentiation.

To evaluate the effect of RUBV infection on neurogenesis, hNPCs that had undergone differentiation for 21 days (at the end of differentiation) were fixed and immunostained with an antibody directed against the neuronal marker Tuj-1 (Figure.4.2.A and B). Gross examination did not reveal major morphological differences between the uninfected and RUBV infected cultures. Tuj-1 positive cells were heterogeneous, occasionally exhibiting no neurites or short neurites, but most exhibited long neurites. The extensive neurite outgrowth indicated that neurons had acquired a more mature morphology. Alteration in neurite length or branching was not detectable when comparing the uninfected to virus-infected cells at this time point, indicating that RUBV infection did not interfere with the induction of neurogenesis. The enu-

meration of Tuj-1 positive cells showed an average of 44 ± 1.2 neurons per field in non-infected culture, whereas 51 ± 2.1 neurons were present in RUBV infected cultures (Figure.4.2.C). Thus, numerous neurons had been generated in both non-infected and RUBV infected cultures and a ~7% increase occurred in infected culture, which was not statistically significant. This increase in neuron numbers could be due to loss of proliferating hNPCs upon RUBV infection, which was demonstrated in Chapter 3. As hNPCs naturally require sufficient room for robust generation of neurons, the loss of hNPCs during differentiation due to infection could yield more room, therefore supporting outgrowth and production of more neurons at the local site of infection. No difference was observed between the entire population of hNPCs in the presence or absence of RUBV at the protein level of Tuj-1, NF-M (another neuronal lineage marker) and key regulators of cell differentiation such as NF- κ B and pERK (Figure.4.2.D). Therefore, RUBV infection at the induction of spontaneous differentiation had a marginal effect on the overall generation of neurons.

We then investigated if RUBV infection caused any changes during the differentiation process. First, the expression of neural stem markers, Nestin and Sox-2 as well as the proliferation marker Ki-67 was examined and quantified at every passage by flow cytometry to determine if there was any changes of cell multipotency during differentiation in all four experimental groups (undifferentiated, undifferentiated infected with RUBV, differentiated, differentiated infected with RUBV) (Figure.4.3.A). As expected, all three markers were down regulated during differentiation, Nestin by 40%, Sox-2 by 50% and Ki-67 by 40%, indication of loss of cell stemness. Compared to controls, RUBV infected hNPCs exhibited growth attenuation as a further reduction in Ki-67 expression was seen in both undifferentiated as well as differentiated cells. This was consistent with what was previously observed in the proliferation study in Chapter 3. Despite that, a similar percentage of reduction in Nestin and Sox-2 expression was observed in both RUBV-infected and uninfected cultures, revealing that virus infection does not alter hNPCs in their capacity to lose their multipotency and commence a differentiation program.

To further evaluate the temporal profile of expression of lineage-specific genes and transcription factors involved in neuronal differentiation, real-time qPCR was performed using RNA isolated from cell cultures 4 days to 21 days post initiation of differentiation (Figure. 4.3 B and C). At 21 days post infection, which corresponds to the end of the experiment, a significant increase in the mRNA levels of neuronal lineage marker Tuj-1 (beta-Tubulin-III), NF-M and Olig2 were observed when comparing differentiated groups to the undifferentiated control (20 fold for Tuj-1, 45 fold for NF-M and 12 fold for Olig2. respectively). However, no alteration was found between uninfected and RUBV-infected cells that had undergone differentiation, which was also supported by the immunofluorescence results. There were no detectable changes in the mRNA levels of others markers that represent astroglial lineages, including MOG, MBP, Gfap, NG2 (for a detailed description of each marker, see Table 4.2), further confirming that no astroglial lineage cells were present in the differentiated culture at this time (Figure. 4.3.B). On the other hand, RUBV affected lineage marker expression at the mRNA level at an early time point of differentiation. Olig2 and NF-M mRNA showed increased expression at 4 days of differentiation in control hNPCs and was significantly ($p=0.021$ and 0.043 respectively) decreased in case of differentiated RUBV infected hNPCs at the same time point. (Figure.4.3.C)

RUBV infection did not impair hNPCs that had already committed to neuronal differentiation

We next investigated if RUBV could impact hNPCs that had already committed to neuronal differentiation. hNPCs at 14 days after spontaneous differentiation were infected with RUBV at a m.o.i of 10. Cells were collected 2-3 days after infection and evaluated for morphology changes, cell marker expression, as well as CPE that would possibly be induced upon virus infection. At this time point, RUBV infection did not induce any morphology changes, cell marker alterations, or CPE events to the differentiated culture compared to the uninfected control that had been differentiated for same number of days (data not shown). Therefore, hNPCs already committed to neuronal differentiation were not sensitive or responsive to RUBV infection in terms of the differentiation program.

hNPCs under spontaneous differentiation are less susceptible to RUBV infection

Clearly, RUBV infection did not significantly alter hNPC neuronal differentiation. Whether this could be explained by a lack of permissiveness to the RUBV infection of cells differentiated into neurons was thus evaluated (refer to Figure. 4.4 A for experimental design). The evidence that extracellular virus yield, as assessed by the viral titer, was decreased by 10 fold during the differentiation process supported this hypothesis (Figure.4.4.B). Virus replication, as determined by quantification of genomic RNA, was significantly decreased during the differentiation process, further supporting our hypothesis that hNPCs differentiating into neuronal lineage did not support RUBV replication (Figure.4.4.C). More importantly, we found that during differentiation, progenitor cells were infected, as shown by E2 immunostaining, but not those that showed more mature neuron morphology, 14 days after the induction of differentiation (Figure.4.4.D, left panel). In addition, the non permissivity of neurons to RUBV infection was confirmed by directly infecting a “neuron enriched” culture where hNPCs had already differentiated for 14 days. Cells susceptible to RUBV infection were evaluated by double staining the culture for E2 and Tuj-1 two days after infection. Again, only progenitor cells instead of differentiated neurons exhibited E2 positive staining, demonstrating that the virus could only replicate in hNPCs but not differentiated cells (Figure.4.4.D, right panel). Finally, a 10 fold decrease in virus titer was seen in the differentiated cultures compared to undifferentiated hNPCs infected for the same period of time (Figure.4.4.E).

4.3.2 Effect of RUBV infection on hNPC gliogenesis

hNPCs are capable of differentiating into astroglial lineages

To determine whether RUBV infection could influence hNPC glial differentiation, we first optimized the differentiation protocol to yield astrocytes and oligodendrocytes in addition to neurons. When we initiated this study, there were no established protocols for hNPC astro-glial differentiation. Protocols used in most other studies yielded a very low percentage of glial lineages (<10%). The current protocol we utilized in this part of study is illustrated in Figure. 4.5.A: Astroglial differentiation was carried out as

an optimization of a previously suggested method, adding both CNTF and bFGF to promote the propagation of astroglial cells during the regular expansion of the hNPCs[137]. During differentiation, cells grown on poly-L-ornithine and laminin coated plates were passaged as necessary, usually every 5-6 days. Under this protocol, ~10% of the cells would eventually become astroglial lineage cells, showing a distinguishing phenotype from undifferentiated hNPCs on the basis of morphology and cell marker expression. The differentiated cells have a signature spongy nucleus as well as an obviously different morphology (eg. Star/branched shape) than its neighboring progenitor cells, as demonstrated by tubulin/Hoechst staining (Figure.4.5.C). Immunostaining of those cells showed that they were positive for the astroglial marker A2B5 while negative for progenitor marker Nestin, confirming that they represented an authentic astroglial lineage and not undifferentiated progenitor cells (Figure.4.5.B). Expression of stemness markers such as Nestin and SOX2 did not decrease significantly (Nestin from $92\% \pm 3.2\%$ to $89\% \pm 2\%$ of the cells; SOX2 from $84\% \pm 1.2\%$ to $79.7\% \pm 3.2\%$ of the cells, data not shown), as only a low percentage of cells were terminally differentiated. Under this differentiation protocol, very few cells had the typical morphology of neurons and the neuronal lineage marker (Tuj-1) gene was not detectable by quantitative real-time PCR (data not shown).

RUBV does not impair the induction of hNPC astroglial differentiation, but limits the differentiation of neurons under these conditions

Previous studies showed that RUBV infection of oligodendrocytes triggered demyelization[108]. We wondered if this would be the case in hNPC induced to become astroglial cells as these cells undergo extensive myelination during differentiation. To investigate whether and how RUBV infection impacts the induction of hNPC astroglial differentiation, proliferating hNPCs were infected with RUBV (MOI = 10) two days prior to the initiation of their differentiation. The cells were allowed to differentiate for 2 weeks and passaged as necessary (Figure.4.5.A). As a control, hNPCs were similarly infected and passaged but left undifferentiated.

Immunostaining revealed that a number of astroglial lineage cells were formed 14 days after the onset of differentiation in both uninfected and RUBV infected cultures. The size of astroglial cells in RUBV infected cultures were generally larger than that in uninfected cultures, probably due to the additional room available on the plate in RUBV infected culture due to the decreased cell number. Besides the size of astroglial cells, no morphological differences were observed between the two cultures (Figure.4.6.A). This suggested that astroglial differentiation occurred normally in the infected culture. This idea was further confirmed by the enumeration of cells, which showed that a similar number of astroglial cells was generated in infected (4.6 ± 0.2 per field) and uninfected cultures (3.9 ± 0.5 per field) (Figure.4.6.B). We also noticed a number of neurons formed during astroglial differentiation, which was identified by a strong signal of Tubulin staining (Figure.4.6.A). To our surprise, under this differentiation protocol, it seemed that RUBV infection significantly impaired the propagation of such cells. No neurons were found in RUBV infected cultures after 14 days of differentiation. Enumeration of cells demonstrated that numbers of neurons in RUBV infected cultures (0.3 ± 0.2 per field) was significantly lower than in uninfected cultures (2.3 ± 0.3 per field) (data not shown).

In addition, we evaluated the changes of hNPC multipotency and proliferation marker expression upon RUBV infection (Figure.4.7.A). As a low percentage of cells were terminally differentiated, it was not surprising to see few changes in the global expression of multipotency/stemness markers. Similar percentages of Nestin and SOX2 positive cells were obtained before and after 14 days of differentiation (Nestin from $92\% \pm 3.2\%$ to $89\% \pm 2\%$ of the cells; SOX2 from $84\% \pm 1.2\%$ to $79.7\% \pm 3.2\%$ of the cells). Thus RUBV infection did not alter the multipotency of the overall hNPC population, as no detectable changes were observed in the expression of Nestin and SOX2 between uninfected and RUBV infected cells in either undifferentiated or differentiated groups. The percentage of Ki-67 positive cells, a marker for cell proliferation, was down-regulated by RUBV in undifferentiated and differentiated groups as seen previously. However, the difference was not as pronounced as seen in proliferating hNPCs or during neu-

ronal differentiation. Therefore, the effect of RUBV on hNPCs multipotency during astroglial differentiation conditions was marginal at most.

Finally, to further evaluate the temporal profile of the expression of lineage specific genes and transcription factors involved in astroglial differentiation, real-time qPCR was performed using RNA isolated from cell cultures 14 days after the initiation of differentiation (Figure. 4.7.B). The profiling provided ample information for the differentiated population. A drastic increase in the mRNA expression of astroglial lineage marker NG2 (Neuron Glial Antigen 2, a marker for early astroglial lineage cells) and Olig2 (a marker for early neurons and type 2 oligodendrocytes) was observed in differentiated cells compared to the undifferentiated control, indicating successful generation of astroglial lineages. A moderate increase in NF-M indicated presence of neurons in differentiated culture. Expression of mature oligodendrocytes marker, MBP, was modestly up-regulated, indicating differentiated cells at this time point were at a less mature stage. RUBV infection, on the other hand, up-regulated the expression of two astroglial lineage markers, NG2 and Olig2, compared to the uninfected control that had undergone the same differentiation protocol. This was possibly due to an enlargement of the cell body instead of increased cell number of differentiated cells (as seen in Figure.4.6.A). Expression of NF-M was down-regulated by RUBV infection, which further confirmed our immunostaining observations.

hNPCs under astroglial differentiation are less susceptible to RUBV infection

Apparently, RUBV infection exhibits least influence on hNPC astroglial differentiation. We evaluated whether this could be explained by an increase in the permissiveness to RUBV infection in cells differentiated into astroglial lineage (refer Figure 4.4 A for experiment design and annotation). The evidence that extracellular virus yield, as assessed by the viral titer, was decreased by 10 fold during the differentiation process did not support this hypothesis (Figure.4.8.B). Virus replication, as determined by quantification of genomic RNA, is significantly decreased during the differentiation process, further demonstrating the loss of RUBV permissiveness during astroglial differentiation (Figure.4.8.C). More important-

ly, we found that during differentiation progenitor cells were themselves infected, but not those showing astroglial lineage morphology, as shown by E2 immunostaining 14 days after the induction of differentiation (Figure.4.8.D). Finally, the lack of permissivity of astroglial differentiated cells to RUBV infection was confirmed by directly infecting an enriched culture where hNPCs had already differentiated for 14 days. Cells susceptible to RUBV infection were evaluated by double staining the culture for E2 and A2B5 two days after infection. Again, only progenitor cells instead of differentiated glial cells stained positive for E2, demonstrating that the virus could replicate in hNPCs but not differentiated cells. A ~10 fold decrease in virus titer was seen compared differentiated cultures two days after infection compared to undifferentiated hNPCs infected for some period of time (Figure.4.8.E). However, how RUBV affected differentiating hNPCs under astroglial differentiation conditions remain to be elucidated.

Therefore, RUBV did not severely impact hNPCs neurogenesis and gliogenesis. Besides that, RUBV seems to exhibit an effect only on undifferentiated or progenitor cells in cultures but those undergoing differentiation, indicating that the major type of cells impacted by were the progenitors. The observation of enhanced differentiation after virus infection, if there was any, could possibly be achieved by depletion of precursor cells. This was plausible because in both types of differentiation, cells required additional space to achieve optimal differentiation such as neurite outgrowth and demyelination. The evidence of lack permissiveness of differentiated cells to RUBV infection further supports this idea.

4.4 DISCUSSION

NPCs are multipotent cells, which can give rise to both neuronal and glial lineages upon commitment induced by specific intrinsic and extrinsic cues. The process of neurogenesis and gliogenesis are intricately orchestrated and a number of viruses affect the differentiation into the proper lineages (see Table 1.3 for detail). As for RUBV, it has long been proposed that the virus inhibits differentiation of cells involved in organogenesis [168]. Taking advantage of the infectability and differentiability of hNPCs,

we investigated if RUBV infected affect nervous system development by upsetting the delicate process of hNPC differentiation.

Neuronal differentiation

We first sought to determine if RUBV affects hNPC differentiation into neuronal lineages. Our results demonstrated that RUBV did not block the overall differentiation of hNPCs, as a similar decrease in the expression of neural stem cell markers, Nestin and Sox-2 was observed in uninfected and RUBV infected cultures. This is also confirmed by the lack of alterations in the expression of lineage specific markers Tuj-1, NF-M and Olig2 that was seen at both the protein level and the RNA level between RUBV infected and un-infected cultures after 3 weeks of spontaneous differentiation. Indeed, we observed an impaired/delayed neuronal differentiation at an early time point of differentiation (4 days after initiation of differentiation) evident by decreased expression of Olig2 and NF-M, however, these differences were diminished during the differentiation process. One possible explanation is that hNPCs were blocked in undifferentiated stage; cells engaged along the neuronal pathway were not affected by the presence of the virus. Thus, infected hNPCs were selected out before their differentiation, the room that depleted hNPCs provided in the infected culture thus allowed additional differentiation of hNPCs into neuronal cells which catch up the delay seen at 4 days after the induction of differentiation. This notion is further supported by the non-permissiveness of differentiated cells to RUBV infection and the lack of gross differences in the number and morphology of neuronal cells between the uninfected and infected cultures. Furthermore, proliferation of infected cells (as illustrated by Ki-67 expression) was not as attenuated during differentiation than among undifferentiated cells, indicating that RUBV infection primarily impacts precursor cells.

In fact, it has been repeatedly shown in previous studies that fully differentiated neurons in culture were not affected by RUBV infection (see Table 1.2 for detail). In both rat and human cultures, neuronal cells were rarely infected by RUBV. Although cytopathic effect was reported in one *in vitro* study, it was

concluded that it resulted from toxic factors released from damaged glial cells [79]. *In vivo*, a complete loss of Purkinje cells (GABAergic) was reported in PRP patients [261]. This observation is similarly explained by glial cell triggered immune-mediated damage. Taking these results together with ours, it is indicated that the effect of RUBV on neurons, if there is any, is restricted to precursor cells instead of developing or developed neurons.

Comparatively, most teratogenic viruses impair neurogenesis of hNPCs, but using quite diverse mechanisms (see Table 1.3 for detail). BDV does not cause any damages to undifferentiated hNPCs, but induces high-level apoptosis to cells undergoing neurogenesis. Coxsackie virus B3 (CVB3) induces massive cell death in hNPCs and therefore prevents further differentiation of the cells [204]. HCMV impacts undifferentiated hNPCs directly by causing a premature differentiation of the cells [149]. Although the ability of HCMV to induce neuron formation declines after 3-4 days of differentiation [150], this is not because lack of permissiveness of virus in differentiated cells as virus antigen is present in fully differentiated neurons. Therefore, this observation is caused by neurons becoming refractory to the effect of the virus instead of changes of tropism. However, it must be noted that most of these teratogenic viruses do not induce slow progressive diseases as RUBV does in the case of PRP. Therefore, our finding that RUBV does not have a direct effect on the neuronal population may also contribute to the explanation of why PRP patients appear healthy and normal during the long-incubation period.

Astroglial differentiation

We also investigated if RUBV infection affects gliogenesis of hNPCs by inducing such differentiation in presence of RUBV. The positive staining for glial specific marker A2B5 and obviously different cell morphology of the differentiated cells confirmed that hNPCs were undergoing gliogenesis. At the end of the differentiation process, significant up-regulation in the expression of glial markers NG2 and Olig2 was observed in infected cultures compared to the uninfected ones, and this was accompanied by a cytoplasmic swelling of a few astroglial cells. These observations suggested that RUBV infection has the po-

tential to trigger gliosis of the differentiating hNPCs. Since NG2 and Olig2 are both oligodendrocytes precursor markers, specific up regulation of those two genes in infected culture indicating that RUBV infection preferentially impacted oligodendrocyte lineages. Whether this preference is related to the differentiation protocol we utilized needs to be further investigated. Also, one unsettled point is that RUBV does not alter the expression of Nestin and SOX2, markers that essentially represent the stage prior to differentiation. One explanation is that RUBV, although causing changes in morphology of glial cells did not necessarily alter the composition of cell population, as evident by enumeration of cells (undiff/ diff cell ratio). Thus, RUBV does not necessarily change the expression of these stemness markers in most of the cells but instead induces overexpression of glial specific proteins within individual cell. Alternatively, there were very few swollen cells (1/100 cells) present in the population, any changes caused by RUBV therefore are on a minimal number of cells.

Several previous studies suggested that RUBV infection causes damage to astroglial lineages in brain and in *in vitro* cell cultures [36, 65, 101] (Table 1.3). However, in our culture, we did not observe increased cell death nor demyelination but swelling of a few differentiated cells. Cytoplasmic swelling of glial cells following virus infection was previously reported for HIV-1 and canine distemper virus (CDV) [262, 263] and suggested a mechanism for virus persistence and sustained replication in the CNS. Cell swelling has also been associated with hypoxia and cell-cell fusion during Sendai virus infection [264]. Thus, it is possible that RUBV triggers a similar type of cell damage. Since virus antigen could not be detected in differentiated cells, how RUBV infection triggered this abnormal phenotype of cells remains unknown. However, it must be noted that in our experimental settings, astroglial lineages do not reach a fully mature stage, as shown by morphological immaturity as well as lack of expression of fully mature glial cell markers such as GFAP and MBP. Therefore, future studies should focus on whether those astroglial lineage cells can regain their permissiveness to RUBV (or a reactivation of RUBV replication) after they acquired a mature phenotype and also whether the abnormalities of those glial cells could further lead to demyelination as well as cell death during their maturation. Also, we observed a specific

depletion of “neuron-like cells” in RUBV infected culture undergoing gliogenesis and further characterization of the lineage of such cell types is needed.

Multiple factors can contribute to brain damages and demyelination is seen in CRS and PRP brains. As reviewed by Stohlman and Hinton, "demyelination induced by virus infection can result from 1): a direct viral infection of oligodendrocytes resulting in cell death; 2) a persistent viral infection, resulting in the loss of normal cellular homeostasis and subsequent oligodendroglial death; 3) a cytokine storm mediated by virus infection of cells other than oligodendrocytes; or 4) infection initiating activation of immune responses specific for either oligodendroglia or their myelin component" [265]. RUBV infection of mature rat oligodendrocytes, triggering cell death, has been demonstrated previously, along with the observation of subsequent myelin removal [78]. A molecular mimicry between a RUBV antigen and MOG has also been proposed to explain the relevance of virus-specific oligoclonal IgG detected in CRS and PRP patients and its role in demyelination [266]. In this proposed mechanism, antibodies are confused between MOG and RUBV antigen, thus, the virus infection of CNS can sensitize to subsequent autoimmune demyelination. However, a general point to remember is that the ways in which the CNS can respond to virus infections are limited: the neurons themselves may undergo lysis, demyelination, or spongiform degeneration and the inflammatory response is mainly expressed by the appearance of lymphocytes and activation of microglia, the macrophages of the CNS. Thus, in absence of microglial cells (which are derived from other hematopoietic stem cells) in our culture, it is hard to verify the molecular mimicry idea. But still, we were able to detect abnormalities in differentiating glial lineages which may serve as a preliminary to demyelination events and we did not rule out that a persistent infection of RUBV in hNPCs may contribute to demyelination at a later time in infected individuals.

Throughout the differentiation study (both neuronal and glial), we found that RUBV infection affected the expression of Olig2 in both neuronal and glial differentiation processes. Oligodendrocyte transcription factor 2 (Olig2) is a bHLH transcription factor essential for the selection of both the motor neuron and oligodendrocyte pathways and directing the choice of neural progenitors to either proliferate or

differentiate during early development. Olig2 also plays an important role in reactive gliosis and neuronal repair *in vivo*. SNPs in the Olig2 gene have been associated with schizophrenia [267-270]. The activity of Olig2 in cell fate determination as well as in sustained hNPC proliferation is regulated by phosphorylation state of this protein: phosphorylation at S147 directs the formation of Olig2 homodimers that promote the expression of motor neuron-specific genes and silence others while dephosphorylation at same site enables Olig2 to form heterodimers with bHLH proteins such as Ngn2 and induce oligodendrocyte progenitor specific genes. In hNPCs, the phosphorylation of a triple serine motif at the N terminus is necessary for Olig2 enhancement of proliferation [267]. In our study, expression of Olig2 mRNA was significantly altered in both neuronal and glial differentiation, suggesting Olig2 is a critical cellular target for RUBV in differentiating hNPCs. This impact was not seen in undifferentiated hNPCs, indicating RUBV primarily affects Olig2's expression in cell fate determination. Our finding of RUBV impact on a key transcription factor for early embryonic development is in congruence with the idea that the virus is most teratogenic during first trimester of pregnancy. And we foresee a possible mechanism by which RUBV affecting Olig2 expression contributes to the progression of CRS associated neurological abnormalities.

Permissiveness changes during differentiation

One important factor that affects the outcome of cell differentiation during infection is the cell's permissiveness or susceptibility to the virus during the process. In our study, both differentiated neuronal and astroglial cells lost their permissiveness to RUBV infection. In both types of cell culture, a decrease in extracellular virus production as well as in intracellular viral genomes was noticed compared to undifferentiated hNPCs that were similarly infected. The loss of virus load was further attributed to loss of virus replication in the differentiated cells in the culture as we did not detect any virus antigen in those cells, even after direct infection of cultures enriched in differentiated cells. It is possible that differentiated cells have intrinsic factors (receptor shifts, defensive machinery) that prevent infection or restricted the virus to an inactive/silenced form with minimum virus genome present in the cytoplasm. Therefore, further investigation is needed to detect the presence of viral RNA or transcripts in single cells undergoing differentia-

tion. Finally, viral RNA was still readily detectable at the end of differentiation process, indicating failure of the culture in toto to clear RUBV during differentiation. Thus, in current experimental setting, we showed that 1), RUBV loses its replication in hNPCs undergoing differentiation; 2) hNPCs failed to eliminate viruses under a differentiation culture environment.

Our permissiveness study result correlates well with the situation in CRS: during fetal development CNS cells become fully differentiated and lose their permissiveness for RUBV infection; this correlates with the decreased incidence of fetal infections with the progress of pregnancy. The lack of permissiveness for RUBV infection of neuron cells seen in our study was consistent with most of the *in vitro* studies using mixed neuronal/glial cell culture for RUBV infection. However, the lack of permissiveness in astroglial lineage does not agree with several of these studies (Table 1.2). Both rat and human brain cell cultures demonstrate permissiveness of glial cells for RUBV infection. Even in the only available studies using human brain cells, astrocyte and microglia were the two type of cells that supported robust RUBV replication, instead of neuron and oligodendrocytes [108]. This could possibly be explained by a lack of mature astroglial lineages in our current differentiation protocols. Immature cells may also gain permissiveness to RUBV at later stages of differentiation after the derivation of specific astrocyte and oligodendrocyte lineages, however, an optimized differentiation protocol is required to achieve the terminal differentiation. Otherwise, differences in observations could simply be strain specific as the viruses used in the two studies were different.

Reduced virus replication in hNPCs undergoing differentiation was seen in studies using other viruses: JEV viral load was significantly higher in undifferentiated NPCs than in those upon differentiation, although the virus infection altered migration and differentiation of the neurospheres [207]. VZV, on the other hand, established a nonproductive replication in pure populations of terminally differentiated human neurons [192]. As noted before, it is possible that RUBV may persist in differentiated hNPCs in an inactive form. “Silenced” viral genome expression was previously reported by our lab in a study of RUBV resistance to IFN using cell lines stably transfected with RUBV replicon[163]. Also, reactivation of virus

replication has previously seen in HIV-1 and JC virus (JCV) during differentiation of NPCs into astrocytes[200, 212]. In both cases, the virus exerts prominent impact to the terminal differentiation into astrocytes. Therefore, we do not rule out the possibility of a reactivation of RUBV replication in terminally differentiated astroglial cells. However, such studies require the detection of the presence of virus genome in individual hNPCs undergoing differentiation and also the ability to produce a terminally differentiated glial cell culture to verify our reactivation hypothesis, which we could not achieve using our currently available protocols,

In summary, the failure of RUBV to replicate in differentiated hNPCs as seen in our study correlated well with the time period for fetal infections with congenital manifestations, which is first trimester of pregnancy. After this period of time, the brain structure is established, most cells are differentiated and therefore fetuses are less susceptible to RUBV infection[132]. In addition, the permissiveness study also established that the major population being impacted by RUBV is progenitor/precursor cells. Further studies will be needed to determine the intrinsic cell programs that eliminate permissiveness to virus infection in differentiated cells.

A comparison with another classical teratogen—HCMV

HCMV is the most significant infectious cause of congenital anomalies in the CNS caused by intrauterine infection in humans nowadays; it is therefore a model virus to study congenital virus infection on CNS development. As reviewed by Tsutsui, numerous studies have engaged in the study of susceptibility of embryonic and fetal cells to HCMV and the effect of the infection on brain development of fetuses[147]. We therefore contrast our result in this study with those summarized from HCMV studies to give a more comprehensive understanding of teratogenesis of RUBV infection. (See Table 1.1 for other references).

1) RUBV and HCMV share similar cell tropisms. Both HCMV and RUBV demonstrated more robust replication in glial cells than in neurons in *in vitro* cell models, indicating that both viruses may di-

rectly hijack astroglial lineages that balance nervous system homeostasis. In addition, both viruses infect hNPCs as their teratogenic nature. HCMV efficiently infect hNPCs while RUBV only establishes a non-productive replication in those cells, possibly explaining the results of congenital infections by both viruses to CNS: HCMV cause malformations of brain while RUBV does not.

2) RUBV and HCMV affect CNS cell proliferation, but by different mechanisms. HCMV infection is primarily cytolytic, as evident in both hNPCs and those differentiated into glial lineages. The non-cytolytic effect of the virus on neuronal lineages was attributed to intrinsic factor C/EBP β , which suppresses CMV promoter activity [188]. RUBV, on the other hand, induces cell cycle arrest in hNPCs. But obviously both viruses deplete the neural precursor pool so as to achieve its long term effect to brain development.

3) HCMV has a profound impact on hNPC differentiation. In HCMV the virus inhibited glial differentiation of hNPCs by lytic infection, presumably causing brain malformations, while neuronal cells tended to be infected persistently, presumably causing brain dysfunctions. Meanwhile, hNPCs population's underwent severe depletions, making brain repair impossible. This is obviously not the case for RUBV: the virus tends to establish a persistent infection in hNPCs, even in those cells under differentiation. Any lytic/ necrotic effect to glial lineages may happen at a later stage of differentiation but obviously not at the initiation process. The effect of virus infection to the brain development depends more on vascular damages.

Therefore, although HCMV and RUBV are teratogenic, they affect the development of CNS probably by quite different mechanisms.

Table 4.1 List of target genes and primers used in gene expression profiling study

Gene name	Primer Sequence	Size(bp)
Oct3/4	Sense:5'-GACAGGGGGAGGGGAGGAGCTAGG-3' Antisense:5'-CTTCCCTCCAACCAGTTGCCCAAAC-3'	144
Nestin	Sense: 5'- CAGCTGGCGCACCTCAAGATG-3' Antisense: 5'-AGGGAAGTTGGGCTCAGGACTGG-3'	209
SOX2	Sense:5'-AGTCTCCAAGCG ACGAAA AA-3 Antisense: 5'-GCA AGA AGC CTC TCC TTG AA-3'	141
Pax-6	Sense: 5'-AACAGACACAGCCCTCACAAACA-3' Antisense: 5'-CGGGAACTTGAAGTGGAACTGAC-3'	275
Musashi-1	Sense: 5'-GGCTTCGTCACTTTCATGGACCAGGCG-3' Antisense 5'-GGGAACTGGTAGGTGTAAC-3'	542
Olig2	Sense: 5'- CAGAAGCGCTGATGGTCATA-3' Antisense: 5'- TCGGCAGTTTTGGGTATTTC-3'	208
MAP2	Sense: 5'- TGCCATCTTGGTGCCGA-3' Antisense:5'- CTTGACATTACCACCTCCAGGT-3'	367/460
Tuj-1	Sense: 5'-ACTTTATCTTCGGTCAGAGTG-3' Antisense: 5'- CTCACGACATCCAGGACTGA-3	97
GFAP	Sense: 5'-ACATCGAGATCGCCACCTAC-3' Antisense: 5'-ACATCACATCCTTGTGCTCC-3'	219
Ki-67	Sense: 5'-ACGAGACGCCTGGTTACTATC- 3' Antisense: 5'-GTCATCAATAACAGACCCATTAC-3'	226
MOG	Sense: 5'-CAT ATC TCC TGG GAA GAA CGC-3' Antisense: 5'-GTA GCT CTT CAA GGA ATT GCC-3'	500
MBP	Sense: 5'-CTGGGCAGCTGTTAGAGTCC-3' Antisense: 5'- CTGTGGTTTTGGAAACGAGGT-3'	275
Tuj-1	Sense: 5'-CAACAGCACGGCCATCCAGG-3' Antisense: 5'-CTTGGGGCCCTGGGCCTCCGA-3'	244
NG2	Sense: 5'- ACTGGCTAGGGGTGTCAATG-3' Antisense: 5'-TCCTCAAGGTCCTGCTGAGT-3'	271
NF-M	Sense: 5'- AAGCCAATCAGACCAGAATA-3' Antisense: 5'-GCAGCGATTTCTATATCCAG-3'	366
RUBV-E1	Sense: 5'- CAACACGCCGCACGGACAAC -3' Antisense: 5'-CAGGTCGCGCATACACCTCA-3'	328

Table 4.2 Description of markers used in this study

Name	Lineage specification	Brief summary	Reference
Oct3/4	Totipotent ES cells	Transcription factor that is expressed in embryonic stem (ES) cells and germ cells, and its expression is required to sustain cell self-renewal and pluripotency.	[271]
Nestin	Neural stem/progenitor cells	Intermediate filament structural protein expressed in primitive neural tissue	[272]
Sox2	Pluripotent to multipotent stem cells	Transcription factors with diverse roles in development. Functions in specifying the first three lineages present at implantation and in regulating proliferation and differentiation in the developing nervous system.	[271]
Pax6	Neural stem/progenitor cells	Transcription factor expressed as ES cell differentiates into neuroepithelium	[273]
Musashi-1	Neural stem/progenitor cells	Musashi1, a neural RNA-binding protein, plays an important role in regulating cell differentiation in precursor cells. Human neuralepithelial cells (NEP) derived from neural rosettes isolated from fetus and from ESCs are positive for both Nestin and Musashi-1	[271, 274]
Olig2	Motor neuron and Oligodendrocyte	Oligodendrocyte transcription factor 2 (Olig2) are bHLH transcription factors expressed in the progenitor domain of the spinal cord. Olig2 is required for oligodendrocyte and motor neuron specification in the spinal cord. It is also well known for its role in sustaining replication in early development. SNPs in Olig2 have been associated with schizophrenia. Olig2 also plays a role in reactive gliosis and neuronal repair.	[267-270]
Map2	Neuron	Microtubule-associated protein-2 (Map2) Dendrite-specific MAP; protein found specifically in dendritic branching of neuron	[275]
Tuj-1	Neuron	Class III β -tubulin (Tuj-1) is a microtubule element expressed exclusively in neurons, and is a popular identifier specific for neurons in nervous tissue.	[276]
NF-M	Neuron	Neurofilaments medium subunit (NF-M) is intermediate filament that are major components of the neuronal cytoskeleton. The level of neurofilament gene expression seems to directly control axonal diameter, which in turn controls how fast electrical signals travel down the axon. Mutant mice with neurofilament abnormalities have phenotypes resembling amyotrophic lateral sclerosis	[277, 278]
A2B5	Glial progenitors	A2B5 is a surface antigen expressed on several gangliosides that remain as yet uncharacterized. It has been used as a glia progenitor marker. Expression of A2B5 is down-regulated as the cell differentiates into the mature oligodendrocytes.	[136, 218]
NG2	Oligodendrocyte progenitors	Neuron/glia-type 2 antigen (NG2) is a type I integral membrane proteoglycan found on oligodendrocyte precursor cells, macrophages and melanoma cells. It binds multiple components of the ECM. NG2 glia are homogeneously present in the grey and white matter. In white matter, they are found along unmyelinated axons as well as myelinated axons, engulfing nodes of	[279-281]

		Ranvier.	
MOG	Mature oligodendrocyte	Myelin Oligodendrocyte Glycoprotein (MOG) is an Ig superfamily member found exclusively in myelinating oligodendrocytes in the central nervous system. Multiple isoforms of human MOG exist. Though its molecular function is not elucidated yet, MOG seem play an role in demyelinating disease, such as MS and Rubella induced mental retardation. MOG is the only known receptor for Rubella.	[10, 282]
MBP	Mature oligodendrocyte	Myelin basic protein (MBP) is one of the major proteins of CNS myelin and constituent of myelin sheath of oligodendrocytes and Schwann cells in nervous system. Knockout mice deficient in MBP showed a progressive disorder characterized by tremors, seizures and early death. Interest in MBP has centered on its role in multiple sclerosis (MS). A "molecular mimicry" hypothesis of MS has been suggested in which T cells are essentially confusing MBP with human herpesvirus-6 (HHV-6).	[283, 284]
Ki-67	Proliferating cells	Ki-67 is a nuclear protein that belongs to a molecular group comprised of mitotic chromosome-associated proteins. It is contextually expressed in all cells that are not in the Go phase of the cell cycle. Thus, Ki-67 qualifies as a cell proliferation marker. Functionally, Ki-67 is known to interact with Hk1p2, a protein that promotes centrosome separation and spindle bipolarity. It also directly interacts with NIFK, and apparently binds to UBF, thus playing a role in rRNA synthesis.	[231, 285]

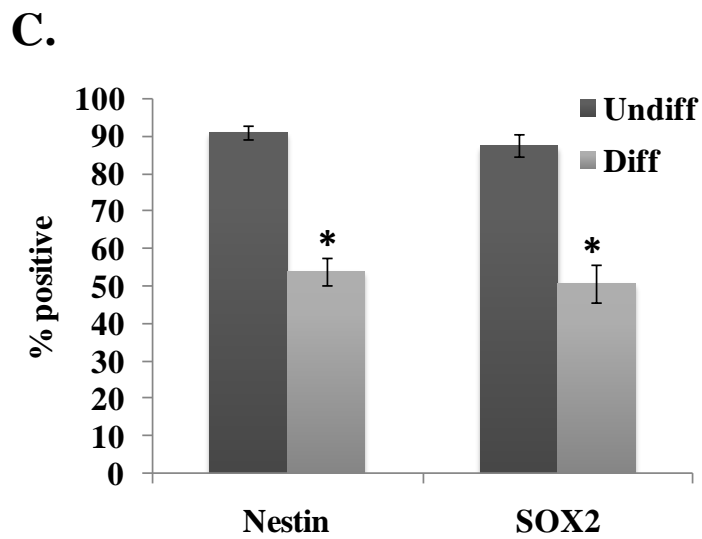
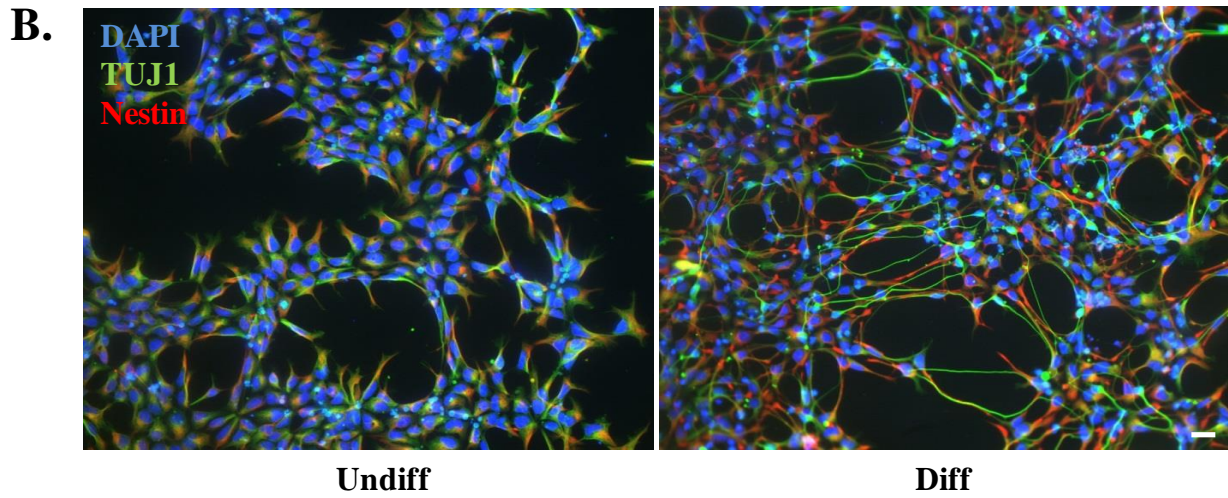
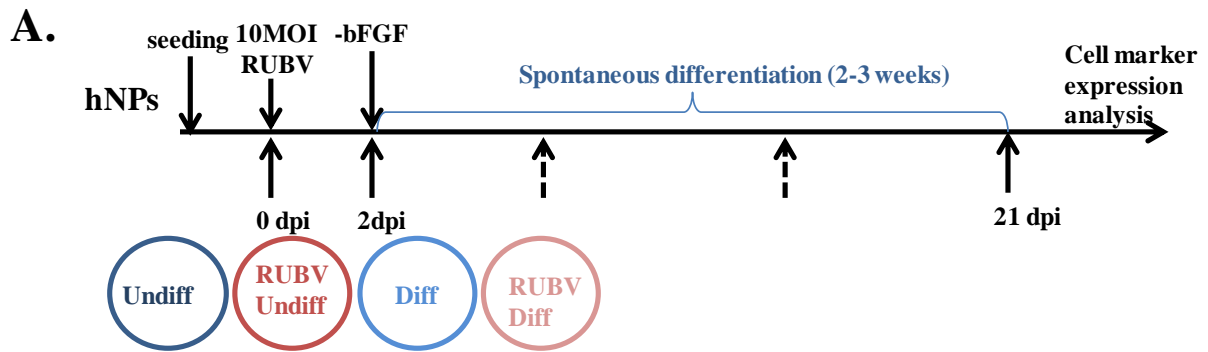


Figure 4.1 hNPC spontaneous differentiation is primarily into neurons.

(A) Scheme of hNPC differentiation protocol: Following seeding, hNPC's were left uninfected or infected with RUBV (MOI= 10) on the next day. After two days of recovery in expansion medium, differentiation was initiated by growth factor withdrawal (control, undifferentiated cells were maintained in expansion medium with growth factor. Cells were passaged twice during the three-week differentiation process, at which time analyses were performed. Four experimental conditions were thus generated as shown: differentiated cells (Diff), RUBV-infected differentiated cells (RUBV Diff), undifferentiated cells (Undiff), and RUBV-infected undifferentiated cells (RUBV Undiff). (B) Immunofluorescence staining of undifferentiated and differentiated hNPCs by antibodies against Nestin (red)(a protein indicative of multipotency) and Tuj-1 (β -tubulin-III, green)(a protein indicative of neuronal differentiation), Hoechst stain (blue) denotes nuclei. Note the neurites cell extensions in the differentiated cells. Bars: 10 μ m. (C) Expression of stemness (multipotency) markers Nestin and SOX2 analyzed by flow cytometry. The experiment was repeated 3 times. Error bars indicate SDs. *: statistical difference from the undifferentiated control at a 95% confidence interval ($P < 0.05$).

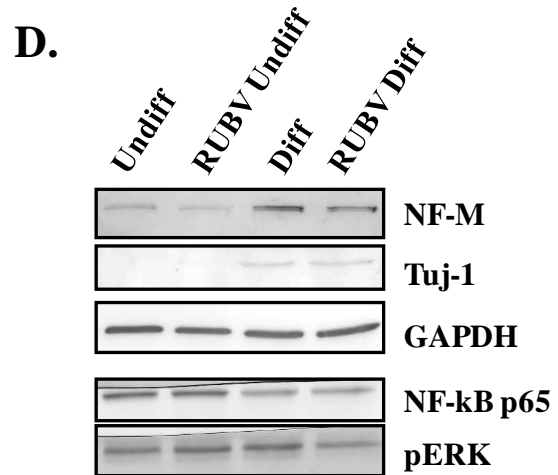
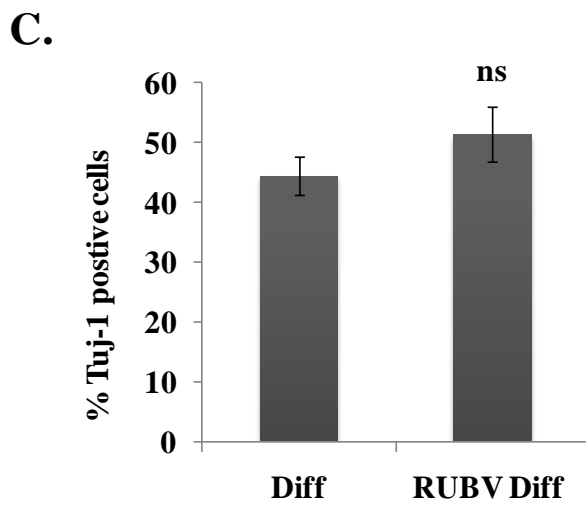
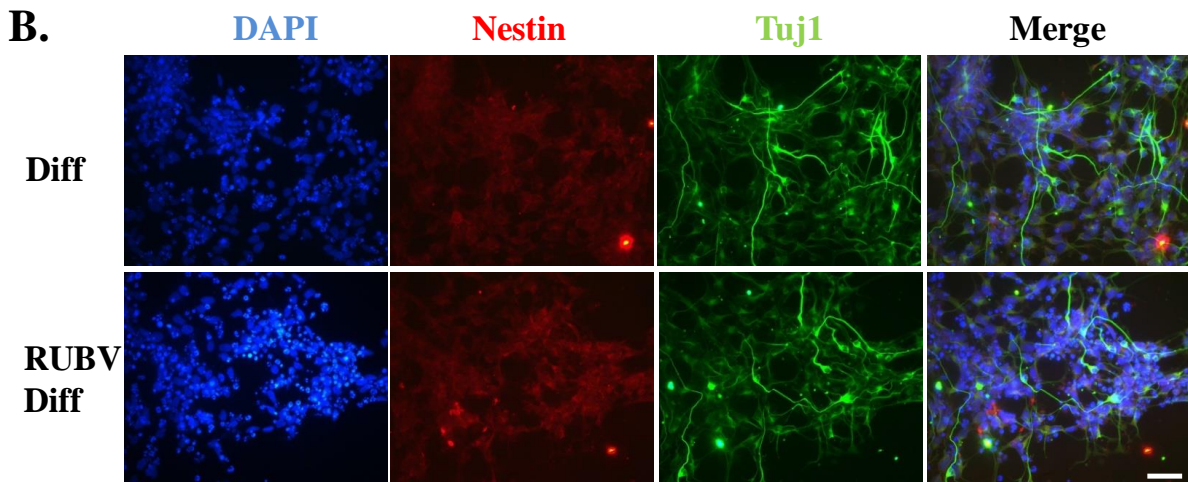
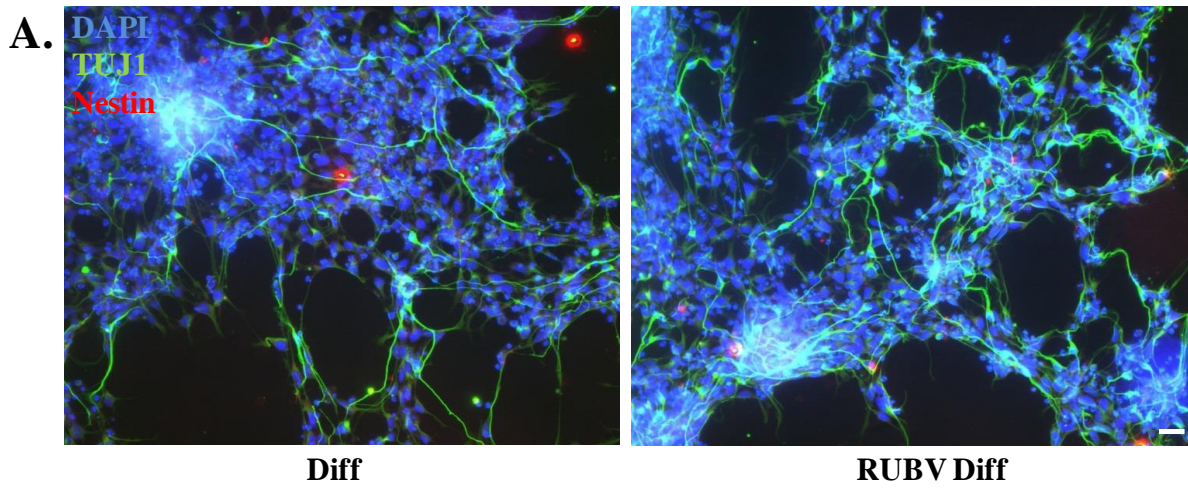


Figure 4.2 Effect of RUBV infection on spontaneous differentiation of hNPCs.

(A)hNPCs, either uninfected or infected with RUBV were induced to differentiate and analyzed by fluorescence microscopy 21 days post differentiation. Cells were stained for Nestin (red) or -Tuj-1 antibody (green); nuclei were visualized with Hoechst dye (blue). Merged images are shown. Bars: 10 μ m. (B) Morphology comparison of diff and diff RUBV culture. (C) The percentage of Tuj-1 positive in each culture was determined. The experiment was repeated 3 times and in each experiment, at least 3 fields of view were counted. Error bars indicate SDs ns, no statistical significance compared to the uninfected control at a 95% confidence interval ($P < 0.05$). (D) Western Blot analysis of expression of neuronal markers, neurofilament-M (NF-M) and Tuj-1, and key regulators of differentiation, pERK and NF-kB p65 at the end of differentiation course. Each experiment was performed at least twice. A representative blot is shown. GAPDH: loading control.

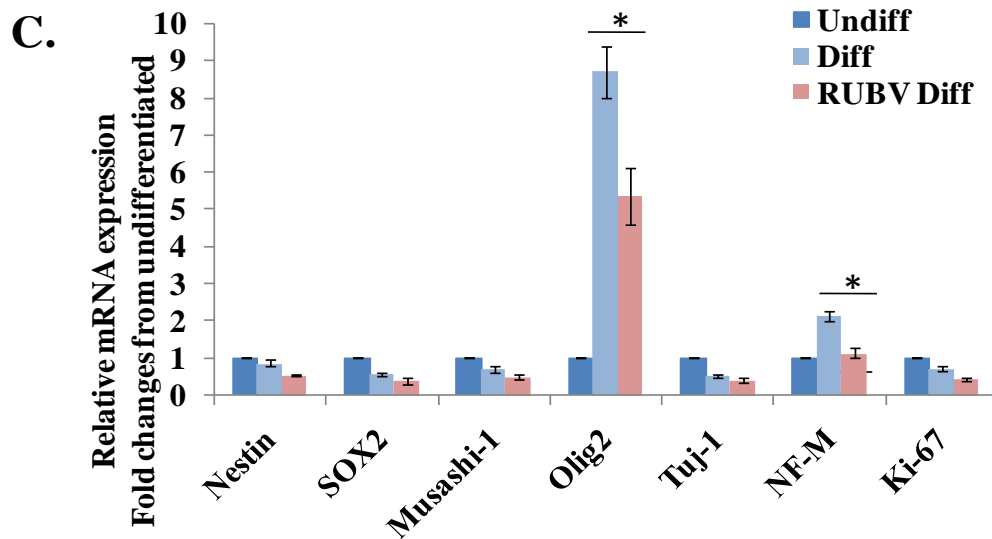
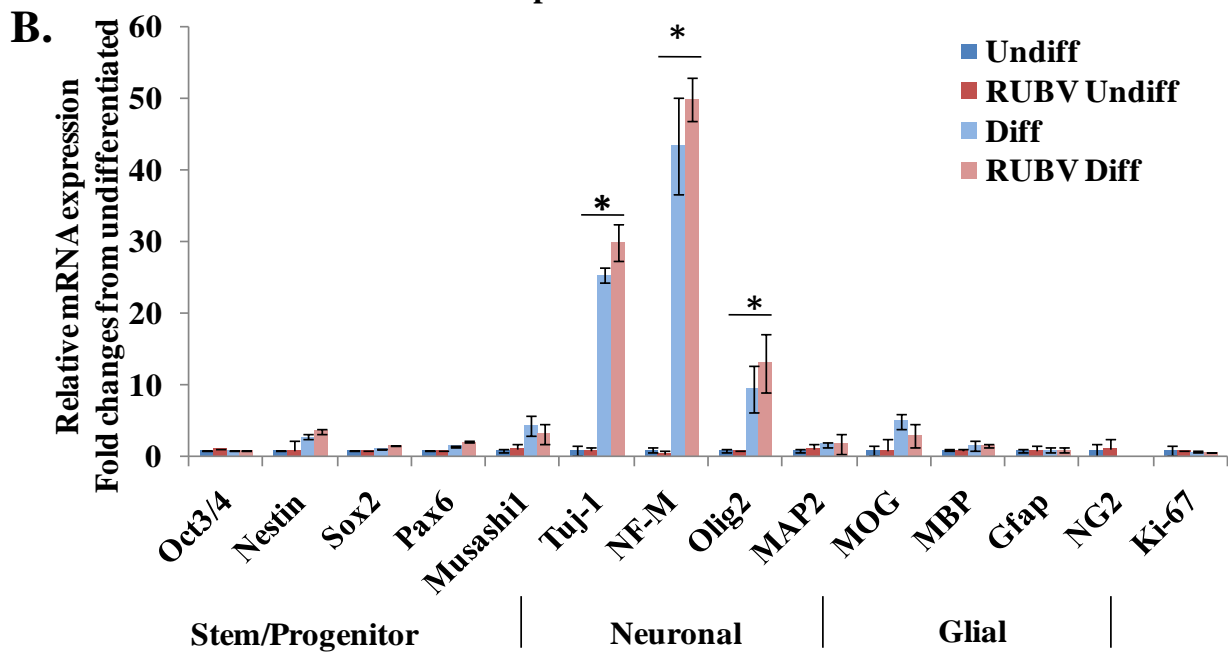
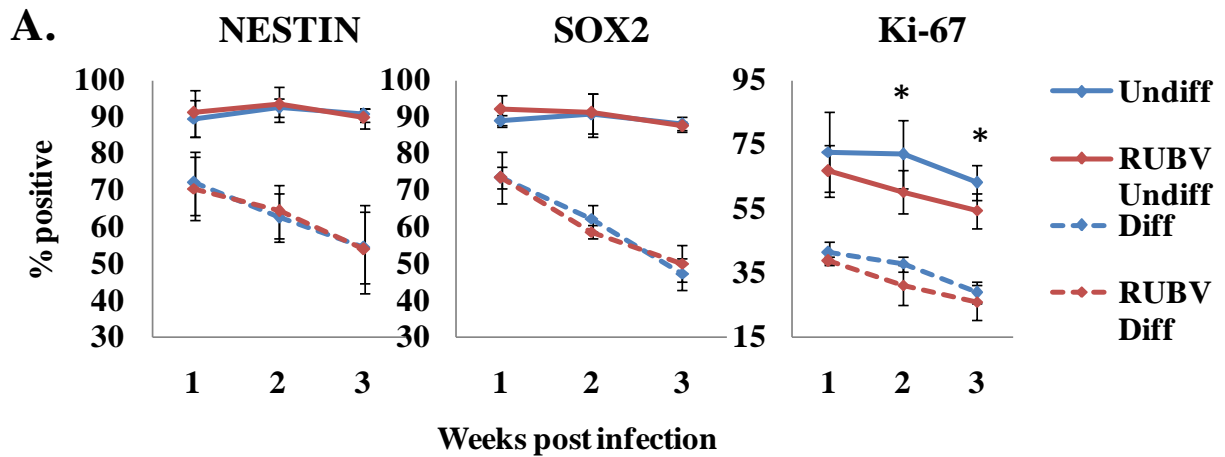


Figure 4.3 RUBV infection did not impair hNPC neurogenesis.

(A) Expression of the stemness markers Nestin and SOX2 as well as the proliferation marker Ki-67 in each of the four experimental groups was analyzed by flow cytometry at each week during the spontaneous differentiation protocol. Each data point is the average from three experiments, each a duplicate titration. Error bars indicate SDs. *, statistical significance ($P < 0.05$) in comparison with the Undiff control (B,C) RNA isolated from each of the four experimental groups either 4 days (C) or at the end of the differentiation protocol (B) were used for a real-time qRT-PCR of several stemness and differentiation-specific genes. Each experiment was done in triplicate and repeated at least twice, and representative data from one experiment are shown. The gene expression levels were normalized to GAPDH mRNA in the same sample and are shown as fold change over the amount in the Undiff at same time point. Error bars represent standard deviations. *, statistical significance ($P < 0.05$) in comparison with the Undiff control

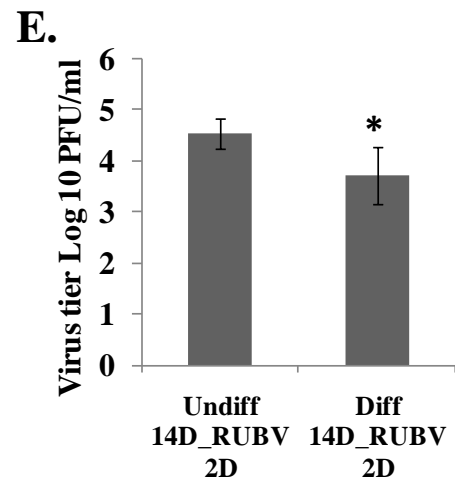
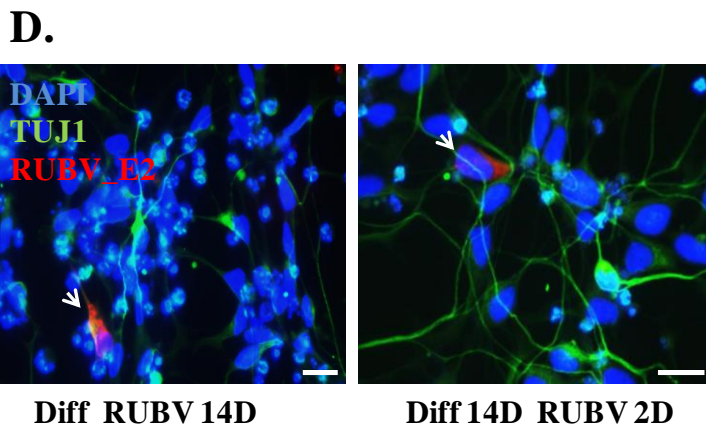
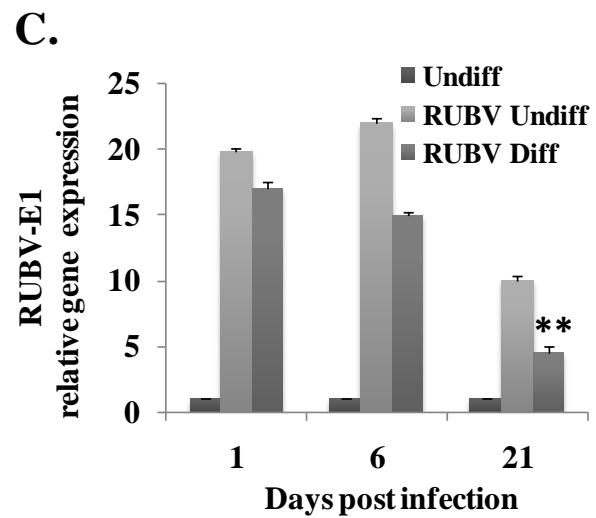
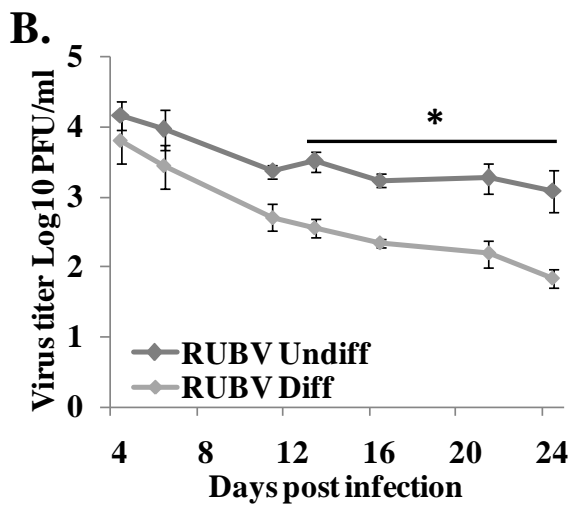
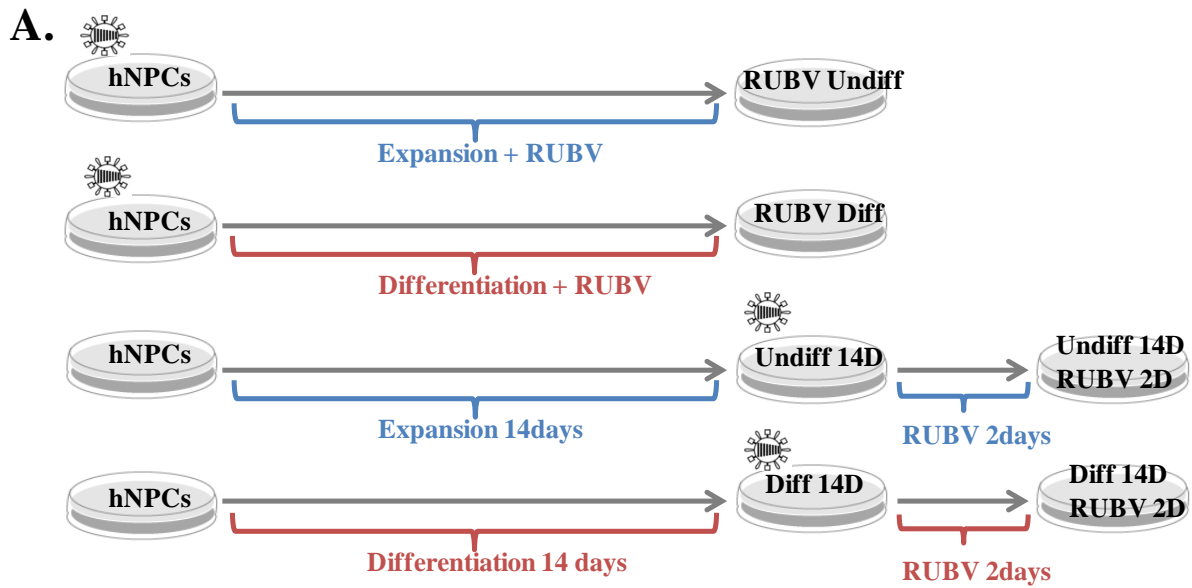


Figure 4.4 Lack of permissivity to the RUBV infection of hNPCs under spontaneous differentiation.

(A) Illustration of permissiveness experiment design. The RUBV Undiff and RUBV Diff are as described in Fig. 1. In addition, Undiff or Diff cells were infected with RUBV 14 days post differentiation and virus titer and the presence of virus infected cells were assayed two days later. These two groups were designated (Diff 14D_RUBV 2D) and (Undiff 14D_RUBV 2D), respectively. **(B)** Virus titer from RUBV infected hNPCs under differentiation vs the RUBV infected undifferentiated control. *, statistical significance ($P < 0.05$) compared to virus titer from undifferentiated hNPCs at same time point. **(C)** The amount of the viral genomic RNA was analyzed by real-time qRT-PCR in Undiff, RUBV Undiff, and RUBV Diff cells at the indicated days post differentiation. **, statistically highly significant ($p < 0.01$) in comparison with RUBV Undiff on the same day post differentiation. **(D)** Left: RUBV Diff cells were fixed after 14 days of differentiation and immunostained with antibodies directed against viral antigen E2 (red) and Tuj-1 (green). Nuclei were stained with DAPI (blue). The white arrow indicates infected cells and the bolded arrow indicates neurons. Bars: 10 μ m. Right: Diff hNPCs at day 14 post differentiation were infected with RUBV (MOI = 10) and two days after infection the culture was fixed and immunostained for E2 (red) and Tuj-1 (green), arrow indications are the same as in the left panel. Bars, 10 μ m. **(E)** Comparison of virus titer from hNPCs infected with RUBV (MOI = 10) following differentiation for 14 days and undifferentiated hNPCs maintained for 14 days (medium was harvested 2 days post-infection). Error bars indicate SDs. The experiment was conducted twice. *, statistical significance in comparison to the undifferentiated culture ($P < 0.05$)

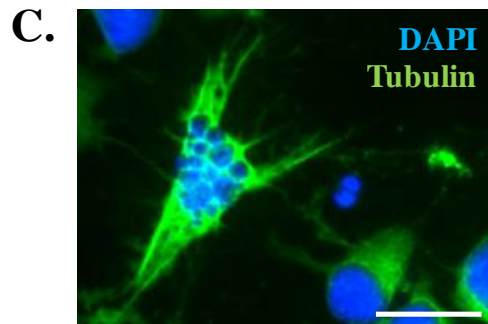
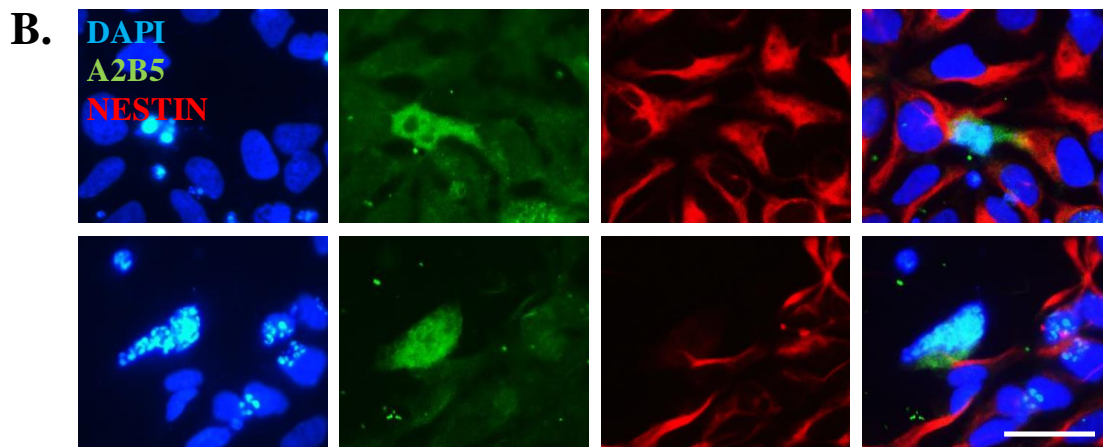
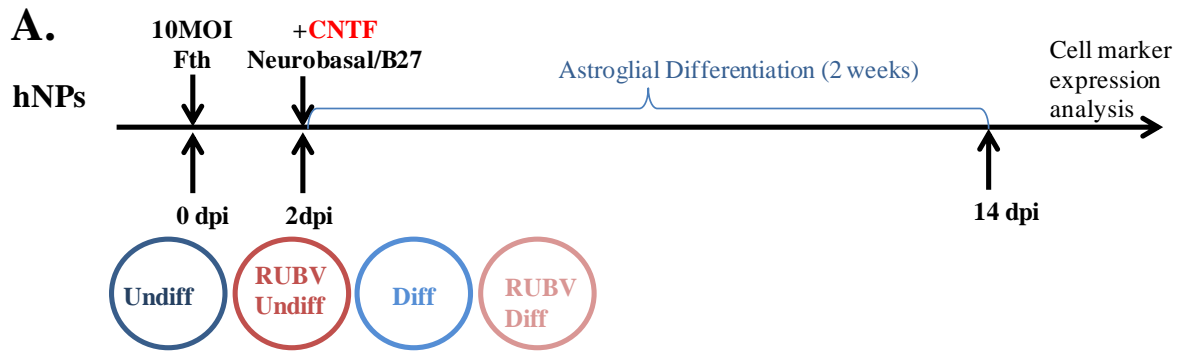


Figure 4.5 Differentiation of hNPCs into astroglial cells.

(A) Scheme of hNPC astroglial differentiation protocol: Following seeding, hNPC's were left uninfected or infected with RUBV (MOI= 10) on the next day. After two days of recovery in expansion medium, differentiation was initiated by adding cell growth factor CNTF (control, undifferentiated cells were maintained in expansion medium without this growth factor). Cells were passaged twice during the two-week differentiation process, at which time analyses were performed. Four experimental conditions were thus generated as shown: differentiated cells (Diff), RUBV-infected differentiated cells (RUBV Diff), undifferentiated cells (Undiff), and RUBV-infected undifferentiated cells (RUBV Undiff) (B) Immunofluorescence labeling of hNPCs after astroglial differentiation by antibodies against the stemness marker Nestin (red) and astroglial marker A2B5 (green), Hoechst stain (blue) denote nuclei. Pictures of two representative cells were shown. Bars: 10 μ m. (C) Immunofluorescence labeling of a representative cell after astroglial differentiation by antibodies against Tubulin (green), Hoechst stain (blue) denotes nuclei. Pictures of one representative cell were shown. Note that the cell has a different shape than undifferentiated hNPCs. Bars: 10 μ m.

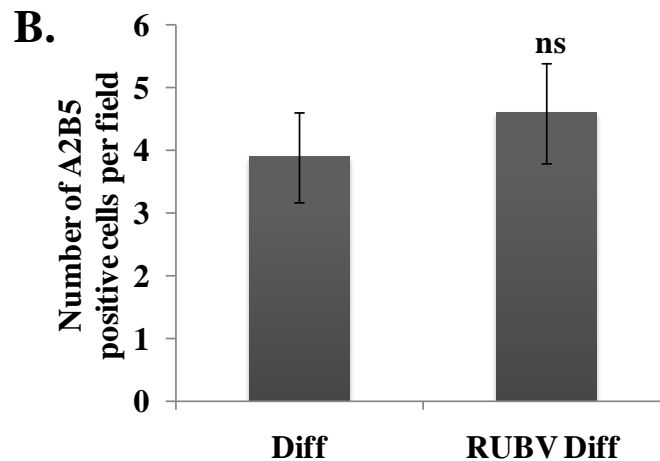
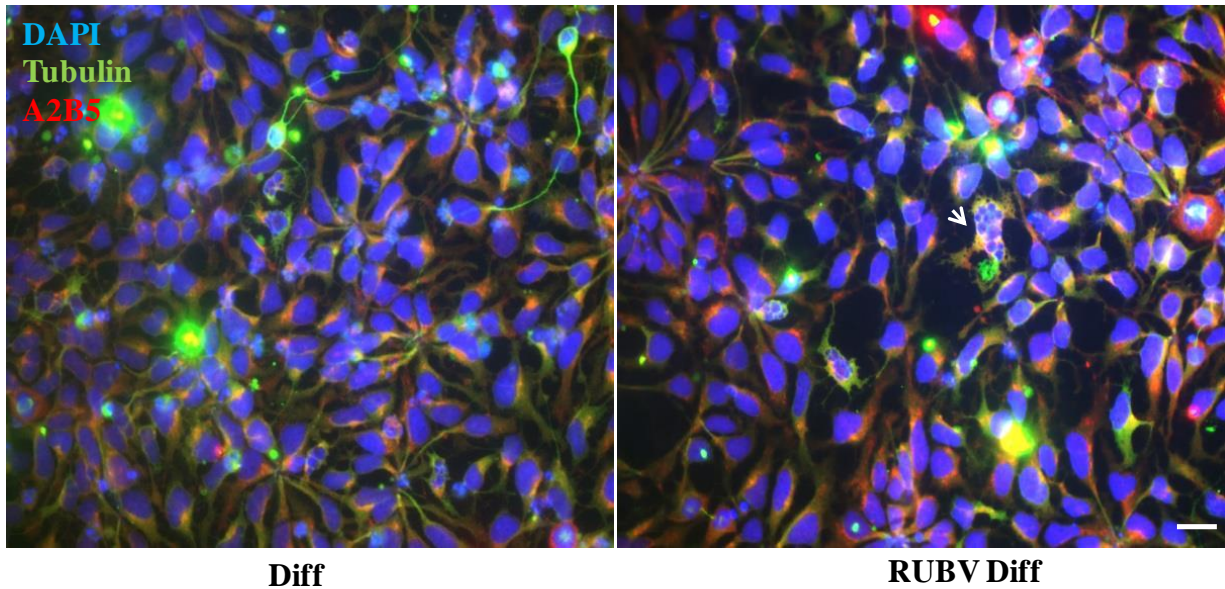
A.

Figure 4.6 Effect of RUBV infection on hNPCs astroglial differentiation.

(**A,B**) hNPCs were left uninfected Diff or infected with RUBV at an m.o.i of 10 (RUBV Diff), differentiated as described in Figure 4.5, and processed at 14 days after differentiation for analysis by fluorescence microscopy. A2B5, an astroglial marker was detected with anti-A2B5 antibody (red), Tubulin with anti-Tubulin antibody (green), and nuclei with Hoechst dye (blue). Merged images are shown in A. Bars: 10 μ m. (**B**) The mean number of A2B5 positive cells per field of view was determined. The experiment was repeated 3 times and at least 3 fields of view were examined in each experiment. Error bars indicate SDs. ns, no statistical significance ($p > .05$)

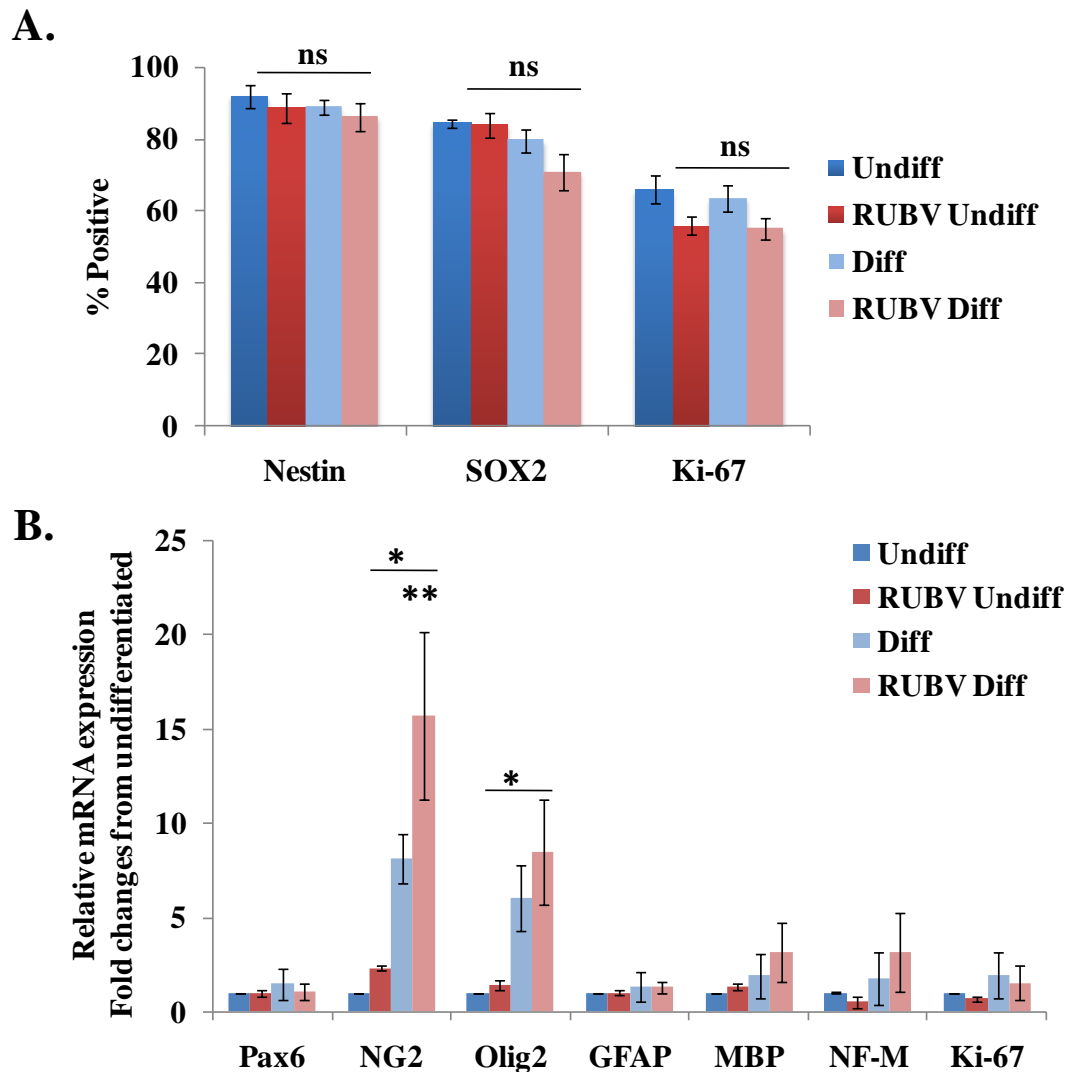


Figure 4.7 Effect of RUBV infection of gene expression during hNPC astroglial differentiation.

(A) Percentage of cells expressing the stemness markers Nestin and SOX2 as well as the proliferation marker Ki-67 was measured in each of the four experimental groups by flow cytometry at the end of the differentiation protocol. Each data point is the average of duplicate titrations from three independent experiments. Error bars indicate SDs. ns, no statistical significance in comparison with the Undiff control ($p > 0.05$). (B) RNA isolated from the four experimental groups at the end of the differentiation protocol was used to perform real-time qRT-PCR to quantify expression of several stemness and differentiation genes. Each experiment was done in triplicate and repeated at least twice, and representative data from one experiment are shown. The gene expression levels were normalized to GAPDH mRNA in the same sample and are shown as fold change over the amount of RNA present in the Undiff control at the same time point. Error bars indicate SDs; *, statistical significance ($p < 0.05$) in comparison to the Undiff control. **, highly statistical significance ($P < 0.01$ in comparison with the Diff control.)

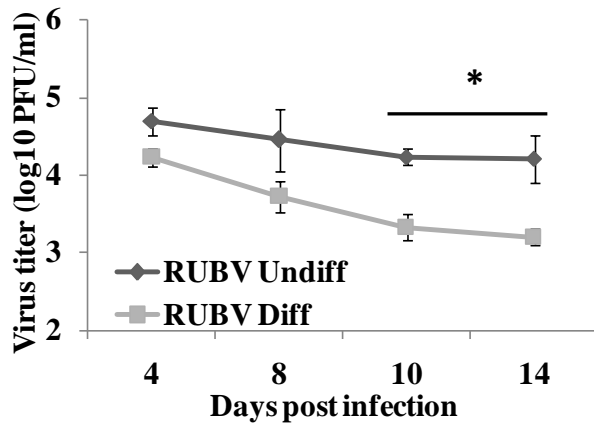
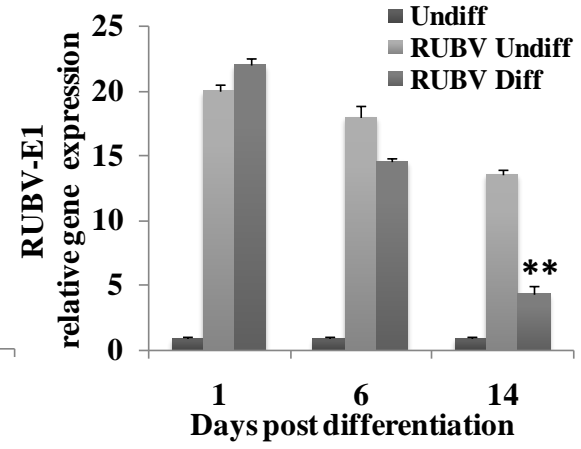
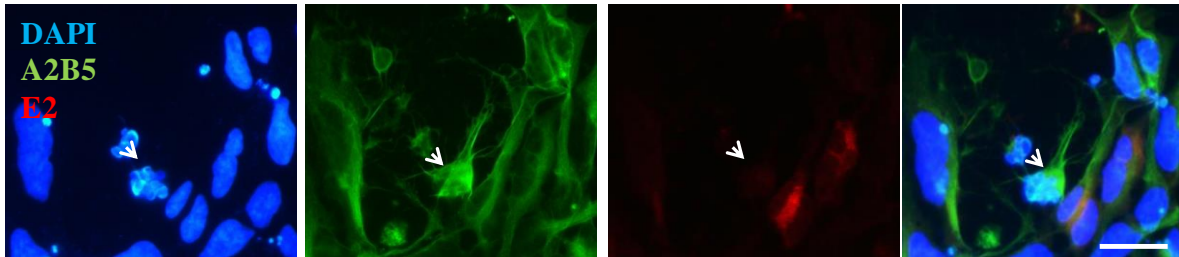
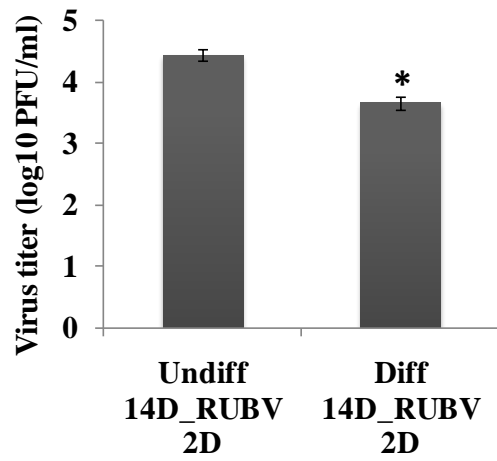
A.**B.****C.****D.**

Figure 4.8 Lack of permissivity to RUBV infection of hNPCs following astroglial differentiation..

(A) Virus titer in culture fluid from RUBV Diff hNPCs vs culture fluid from RUBV Undiff at indicated days of the astroglial differentiation protocol. The means of 3 independent experiments are shown; error bars indicate SDs; *, statistical significance ($P < 0.05$) between the two cultures. **(B)** The expression of the viral genomic RNA was assayed by real-time qRT-PCR in Undiff, RUBV Undiff, and RUBV Diff at the indicated time points post-differentiation. The experiment was repeated 3 times, error bars indicate SDs, **, highly statistical significance compared to RUBV Undiff control on the same day post differentiation. **(C)** After completion of the differentiation protocol (14 days), RUBV Diff cells were immunostained with antibodies directed against viral antigen E2 (red) and A2B5, an astroglial marker (green). Nuclei were stained with DAPI (blue). Bolded arrow show astroglial lineage cell. Bars: $10\mu\text{m}$. **(D)** Comparison of virus produced following infection of Undiff and Diff hNPCs after completion of the astroglial differentiation protocol. Cells were infected after 14 days of differentiation and medium was collected and titered 2 days post-infection. This experiment was conducted three times, error bars indicate SDs, *, statistical significance ($P < 0.05$).

CHAPTER 5 : SINDBIS VIRUS INFECTION INDUCES APOPTOSIS AND TRIGGERS PREMATURE DIFFERENTIATION OF HUMAN NEURAL PROGENITORS

5.1 INTRODUCTION

In this last research chapter, we investigated the effect of SINV on hNPCs to contrast the difference between its effect on hNPCs with RUBV to determine whether the observations on RUBV infection of hNPCs are general among viruses or unique to RUBV. SINV was chosen because it is also a member of the *Togaviridae* family. SINV causes rash and fever in humans and age-dependent encephalitis in mice, therefore it serves as a model to study viral encephalitis induced by viruses in the *Togaviridae* family [3, 4]. In addition, SINV is widely used as a vector for the delivery of genes into selected stem cells; however, the toxicity as well as other side effects of such viral vectors has rarely been discussed. In a recent study, a SINV vector expressing HIV gp120 was used to infected hNPCs and showed a lytic infection while others using wild-type HIV did not [120, 286]. Therefore, it is worthwhile this virus to compare and contrast its effect to that of RUBV on hNPCs.

Not unsurprisingly, as a known neurotropic virus, SINV induced a lytic replication cycle in hNPCs with CPE observed at 24h.p.i. and few cells remained adherent at 48h.p.i. In contrast to RUBV, SINV replicated and disseminated effectively as virus titer increased by 100 fold in hNPC cells and the percentage of infected cells reached over 85% at later time points. SINV attenuated cell proliferation by triggering apoptosis instead of inducing cell mitotic inhibition, a mechanism different than RUBV. Under close scrutiny, this could due to the virus induction of strong inflammatory responses as key regulators of such pathways are highly induced upon virus infection. Interestingly, the virus also seems to induce a premature differentiation of hNPCs at early times, which could due to abnormal expression of key regulators, such as pSTAT3 during the inflammatory responses. The SINV infection of hNPCs clearly contrasts with

that of RUBV infection in that a slow virus such as RUBV affects maturation and function of the brain in a different way than a quick neurotropic virus such as SINV.

5.2 MATERIAL AND METHODS

5.2.1 Cell culture

hNP1™ Neural Progenitor cells (hNPC's) (ArunA Biomedical) derived from the WA09 hESCs were cultured in Matrigel™ (BD Bioscience) coated tissue culture dishes as described in Chapter 2. For experiments in this part of the study, passage 7 to 10 cells were used.

Baby hamster kidney (BHK-21) cells for preparing SINV stock were obtained from the American Type Culture Collection (ATCC) and grown and maintained at 35°C in Dulbecco's Modified Eagle Medium (D-MEM, Cellgro) with 5% fetal bovine serum (FBS), as described previously[287].

5.2.2 Virus stock preparation and infection

The Sindbis virus (SINV, HR strain) used in this study was a laboratory strain routinely used in the Frey laboratory. For making SINV stock, BHK cells at 80% confluence were infected with SINV at an m.o.i of 0.1. At 2 dpi the development of cytopathic effects (CPE) was present in nearly 100% of the cells and at that time the supernatant was collected and stored at -80°C. Cell free virus stock was prepared by centrifugation of the medium at 2000 rpm and collection of the supernatant. Each batch of virus stock was titered by plaque assay. Medium for mock infection was similarly prepared from uninfected BHK cells. To infect NPCs: cells were seeded in 2×10^6 cell/cm² (a high density) and changed with complete neural expansion medium the next day. For the infection, SINV stock was added directly to the plate at m.o.i of 1pfu/cell. Infected plates underwent analysis through 2 dpi without additional medium changing.

5.2.3 SINV growth curve characterization

To characterize SINV growth kinetics, hNP1 cells at 60-70% confluence were infected with SINV at an m.o.i of 1 and medium was collected at 4, 8, 12, 24, and 48 hours post infection. The amount of infectious SINV produced was titered by plaque assay. For plaque assay, serial ten-fold dilutions of SINV were inoculated onto semi-confluent Vero cell monolayers. After adsorption (1hr, 35°C), the inocula were removed and the cells were overlaid with MEM containing 0.7% agarose (Miles) and incubated for 2 days at 35°C, as described in Chapter 2. at which time the plaques were visualized by crystal violet staining.

5.2.4 Live-cell morphology changes

Cell morphology changes were monitored on an inverted Nikon TMS-F microscope (using a 20× objective). Uninfected and infected cells were monitored in parallel to compare changes in cell morphology and the presence of CPE.

5.2.5 Immunofluorescent assay (IFA)

Standard immunofluorescence was performed as described in Chapter 2. Primary antibodies used were directed against nestin (a neural stem marker; 1:450; Neuromics), SINV-NSP (a SINV antigen against SINV non-structural protein NSP1:100, Eptomics), active-caspase 3 (1:500; Cell signaling) and β -tubulin (cytoskeleton marker, 1:200, Abcam). Secondary antibodies were anti-rabbit/mouse Alexa Fluor 488 and anti-rabbit/mouse Alexa Fluor 594 (1:2000-4000; Molecular Probes-Invitrogen Life Technologies). Fluorescence images were acquired on a Zeiss Axioplan epifluorescence wide-field microscope and processed with AxioVision software. For image quantification, at least three fields of view under each experimental condition were analyzed. CellProfiler software was used for the automatic image processing and quantification, as described in Chapter 2.

5.2.6 Proliferation assay

For the assessment of the effect of SINV on hNPC differentiation, hNPCs were seeded onto 60 mm² plates in a density of 2×10^6 cells/plate and infected with SINV at an m.o.i of 1. Mock infected and SINV infected samples were collected at 12, 24 and 48 hours post infection and subjected to the following analyses: (1) EdU incorporation assay for assessment of cell cycle and proliferation (2) Active-caspase 3 staining for apoptosis induction. (3) Living cell PI staining for detection of cell death events. All techniques were done as described in Chapter 3.

5.2.7 Flow cytometry

The percentage of cells expressing virus antigens or lineage specific markers was determined by flow cytometry. hNPCs were harvested and washed twice with 2%FBS/PBS staining buffer and then fixed by BD Cytofix/Cytoperm solution according to the manufacturer's instructions (BD Bioscience) in aliquots of 100,000 cells in replicate for each antigen. Each aliquot was stained with one or two of the selected cell marker antibodies for 1 hr on ice. Antibodies used were: anti active Caspase 3(conjugated with V450, BD Pharmingen) and anti-nestin (conjugated with PE, BD Pharmingen). Cells were then washed twice with staining buffer and labeled with secondary antibody, if appropriate. Flow cytometry was performed using a BD LSR Fortessa or FACS Canto, both from BD Bioscience. Forward and side-scatter plots were used to exclude dead cells and debris from the histogram analysis. Data analysis was performed using FACS Diva software (BD Bioscience). The percentage of cells expressing fluorescence intensity greater than the control cells was calculated using the FlowJo program (Tree Star, Inc., Ashland, Oregon).

5.2.8 Western Blot

Western Blot analysis was performed on cell lysates of hNPCs either mock infected or SINV infected (moi = 1) at 4, 12, 24, 36, 48 hours post infections, using protocols described in Chapter 2. Primary

antibodies used were anti-GAPDH (1:5000; Abcam), anti-NF- κ B p65 (1:200; Santa Cruz); anti-phospho-STAT3 (1:200; Cell signaling), anti-phospho-IRF3 (1:1000; Eptomics); anti-Nestin (1:500; Neuromics); anti-neuro-filament M (NF-M; 1:500; Neuromics); anti-Tuj1 (1:1000; Abcam); anti-PCNA (1:1000, Santa Cruz) and anti-cleaved-caspase 3 (1:1000; Cell Signaling).

5.3 RESULTS

5.3.1 hNPCs are fully permissive to SINV infection

To determine the permissiveness of hNPCs to SINV infection, we plated them onto Matrigel-coated plates and infected them with SINV at an m.o.i of 1. The capacity of the virus to infect, to replicate, and to disseminate in hNPCs then was evaluated by immunofluorescence at 4, 8, 12, 24, and 48 hours following infection using an antibody directed toward the viral nonstructural proteins, SINV-NSP. In addition, we also used an antibody against tubulin to monitor cell morphology changes during the infection (Figure.5.1.A). At 4 hours following infection, a number of cells, albeit a small number, stained positive for SINV-NSP, revealing their permissiveness to SINV infection. No significant changes in cell shape/morphology were detected at this point. The observation of cultures from 4 to 24 hours after infection showed that while only $3.8\% \pm 0.32\%$ of the cells were expressing virus antigen at 4h.p.i, a large proportion of cells, $86.8\% \pm 0.8\%$, did so by 24h.p.i (Figure.5.1.B), thus demonstrating that the virus replicates in hNPCs and disseminates in a very efficient manner. CPE (i.e. presence of floaters, elongation of adherent cell bodies) was detected at 24 hours post infection and at 48 hours few cells remain attached to the plate compared to the uninfected control. The percentage of infected cells no longer increased at 48 h.p.i, probably due to the massive loss of proliferating hNPCs upon SINV infection. Interestingly, an elongated cell morphology was noticed in infected cells at this time point, indicating that SINV may induce premature differentiation of hNPCs. The extracellular virus yield was examined as a measurement of SINV replication efficiency (Figure.5.1.C). Virus titer increased by 100 fold from 4 h.p.i (10^3 pfu/ml) to

24 h.p.i (10^5 pfu/ml), at which time the virus had disseminated throughout most of the culture. The viral titer achieved by SINV in hNPCs is 2-3 log lower than those seen in BHK cells (10^7 or 10^8 pfu/cell)[288].

5.3.2 SINV inhibits hNPCs proliferation by inducing apoptosis but not cell cycle arrest

Since SINV infection led to massive cell loss, we investigated whether the diminished hNPC population was due to SINV induced cell death or cell cycle arrest. The effect of SINV on hNPC proliferation was quantitatively analyzed by EdU incorporation, which demonstrated significantly reduced cell growth in the infected cultures (Figure.5.2.A). At 12 h.p.i, no significant change in EdU labeling was noticed, however, at 24 h.p.i, this reduced drastically from $74.7\% \pm 3.2\%$ in uninfected control cells to $33.4\% \pm 1.25\%$ in SINV infected hNPCs. This negative effect on cell proliferation was not demonstrated until 24 hours after infection, in correlation with virus replication kinetics.

To investigate the induction of apoptosis upon SINV infection, at 24 h.p.i mock infected and SINV infected cells were fixed, stained for active-caspase 3 and analyzed by flow cytometry. Compared to uninfected cells, a 2-fold increase in the percentage of active-caspase 3 positive cells in the SINV infected culture was observed (uninfected: $17.5\% \pm 0.25\%$ positive vs. SINV infected: $35\% \pm 0.33\%$ positive) (Figure.5.2.B). To further characterize apoptotic events in hNPCs upon SINV infection, the expression of active-caspase 3 was monitored at the protein level by Western Blot throughout the infection time course (Figure.5.2.C). Expression of active-caspase 3 was significantly elevated at 24-48h.p.i, consistent with our observations of CPE. This result clearly showed that SINV induces apoptosis as a means of cell death in hNPCs.

To address whether SINV mediated growth inhibition in hNPCs results from attenuated cell cycle progression, cell lysates from 4 to 48 h.p.i were used to probe the expression of proliferation cell nuclear antigen (PCNA) by Western Blot (Figure.5.2.C). PCNA is an accessory factor for DNA polymerase δ in eukaryotic cells and therefore is only expressed in proliferating cells which have robust DNA synthesis. Infections of hNPCs with SINV did not result in significant loss in the expression of PCNA, especially at

24 h.p.i when strong apoptosis was induced. The reduction seen at 48 h.p.i could possibly be due to massive reduction in cell number, as illustrated by the expression of the internal control, GAPDH.

Thus, SINV limited hNPCs proliferation primarily by inducing cell death/apoptosis instead of triggering cell cycle arrest.

5.3.3 Proliferating hNPCs lost cellular multipotency/stemness upon SINV infection

As hNPCs exhibited a neuron-like elongated cell shape at the end of SINV infection time course, we wanted to investigate whether SINV induces premature differentiation or loss of cellular multipotency upon infection. The percentage of Nestin positive cells was analyzed at 24 hours after SINV infection (Figure.5.2.B). SINV infection decreased Nestin positive cells by 30% compared to the uninfected control ($91\% \pm 1.3\%$ of uninfected vs. $62.2\% \pm 3.33\%$ of SINV infected were positive). Expression of Nestin was also monitored on the protein level by Western Blot (Figure.5.2.C). A similar decrease in Nestin expression was noticed, clearly suggested that proliferating hNPCs lost their multipotency/stemness during SINV infection. Reduction of Nestin levels was not seen until 24 h.p.i, which is the time point SINV reached its highest infection rate, indicating that alteration in cell multipotency was also correlated with virus replication. To investigate if a premature differentiation was initiated, we probed the cells against lineage specific markers such as Tuj-1, A2B5 and NF-M, however, none of these markers showed a positive staining compared to uninfected hNPCs at 48 h.p.i (data not shown). It is possible that the time course of this experiment was too short for infected hNPCs to exhibit differentiated cell markers at the protein level. On the other hand, it is also possible that SINV infection impaired hNPC differentiation potential.

5.3.4 SINV modulates multiple cell signaling pathways of hNPCs during infection

Finally, we wanted to investigate the mechanism behind SINV modulation of hNPCs morphology, proliferation and multipotency/stemness. Expression of multiple signaling molecules (NF-kB p65,

pSTAT3, pIRF3 and pERK1/2) on crucial regulation pathways during SINV infection course were analyzed by Western Blot (Figure.5.2.D). The expression of active phosphorylated (Y705) STAT3 (pSTAT3) was down-regulated by SINV at 24h.p.i, suggesting a negative regulation of JAK/STAT pathway upon infection. pSTAT3 is required for normal hNPC differentiation, and the reduction in this protein possibly led to impaired differentiation potential[289]. Expression of Phospho-p44/42 MAPK (pERK1/2) was similarly down-regulated by SINV at 24h.p.i. The MAPK pathway regulates multiple phosphorylation events including those involved in cell proliferation. Robust expression of pERK1/2 was shown to be pro-survival[290]. Therefore, it is highly possible that SINV impairs hNPC proliferation by repressing pERK1/2 expression and therefore the regulation of MAPK pathway. Expression of NF-kB p65 and phospho-interferon regulation factor 3 (pIRF3) were not significantly altered upon SINV infection. As both proteins serve as signaling molecules in IL-6 and IFN induction, it was plausible to suggest SINV did not induce high expression of cytokines and therefore the inflammatory response.

5.4 DISCUSSION

In this last part of our study, we addressed the susceptibility of hNPCs and their cellular responses to SINV infection. Although SINV does not produce CNS anomalies in humans, there are still multiple reasons why we studied infection of this virus in to hNPCs: (1), SINV is a model alphavirus that produces age-dependent encephalitis in mice, providing a parallel reference for viral induced human CNS degenerative disease and, most importantly, the study of neurological aspects of infection by its close relative RUBV [291, 292]. (2), SINV has been used to infection rat neural progenitors and these results provide the closest relevant references to our studies, considering SINV and RUBV are classified in *Togaviridae*[161]. (3), SINV is a common test analyte in the class of viral agents for various *in vitro* models [161]. hESC-derived hNPCs are rarely used in viral pathogenesis studies and another goal of our studies is to assess the feasibility of hNPCs as a model to study viral infection. We have shown that RUBV is a poor inducer of cytokine responses in hNPCs ; we therefore utilized SINV as a complementary agent to evaluate the cell signaling profile of hNPCs e. (4), SINV-based vectors have been widely employed in

stem cell infections and tumor therapies in humans , however, little is known about the toxicity of the vector itself. Therefore in the current study, we evaluated the potential effect of using SINV as a vector in the studies of human cells as well as in therapies for cancer[293].

Here, for the first time for a member of the Alphavirus genus y, we report that SINV can infect hNPCs and significantly attenuate cell proliferation. The virus induces robust cell death and abruptly terminates hNPCs multipotency. The results of our studies could shed light on multiple aspects discussed above.

hNPC is highly susceptible to SINV infection

We have shown that hNPCs are fully permissive for SINV infection. The virus is able to establish productive replication and dissemination in culture since over 90% of cells were infected at the time peak virus titer was achieved, which corresponds to its neurotropic nature. Highly-efficient cell entry of SINV is probably due to the abundant availability of the cell surface receptor laminin on hNPCs, which has been shown as a receptor for SINV in mammalian cells [294]. SINV infection of human cell has not been extensively studied; however, there are several reports that human brain cells are susceptible to SINV infection. In a comparison of oncolytic potential with eight other viruses, SINV was shown infect nearly 100% of human glioblastoma cells (U-87MG) and induce apoptosis immediately upon its entry[293]. The spread of SINV has also been demonstrated in human brain microvascular endothelial cells (HBMECs), where the virus infection renders cells hypersensitive to the inflammatory inducer Bradykinin [162]. Here we also demonstrated sufficient virus replication of SINV in hNPCs and its potential to deplete the said cell pool. Therefore, it is intriguing why the virus is not neurovirulent in the human CNS. SINV has also been shown to replicate in human peripheral mononuclear cells (PBMC), decreasing cell adhesion [161]. Thus, it is highly possible that the virus is eliminated by immune system before entering the CNS as the virus was shown enter the brain through the hematogenous route in a mouse model [3].

SINV triggered apoptosis of hNPCs

Several viruses actively induce apoptosis at late stages of infection, thus allowing the dissemination of progeny viruses, while avoiding host inflammatory and immune responses[295]. In a mouse model, NPCs are very susceptible to SINV induced apoptosis as cell death was detected as early as one day post infection [161]. It has been recently shown that certain viruses like CVB3 and CMV can either induce apoptosis in hNPCs thus achieve optimal viral dissemination[204, 221]. Consistent with these reports, we observed a strong induction of apoptosis in SINV infected hNPCs, as illustrated by an increase in the active-caspase 3 positive cell population and protein expression at late stage of infection. Further validation of proliferation damage in hNPCs with progressive infection was obtained by EdU incorporation analysis, which clearly demonstrated that SINV impacted cell metabolism since there was a significant decrease in EdU uptake compared the uninfected control. Interestingly, we did not observe any reduction of cell cycle progression in hNPCs as the relative expression of PCNA was consistent even at a later time points of infection, indicating that cell cycle arrest does not contribute to the reduced NPC population following infection. This is in sharp contrast to the situation of JEV and RUBV infection of hNPCs in which both viruses attenuate cell proliferation by inducing cell cycle arrest. As mentioned in Chapter 3 discussion, inhibition of apoptosis is also a mechanism by which the virus sustains its replication in the infected cell. Thus, our studies with SINV and RUBV illustrated the difference of hNPCs response to different pathogens. Considering similarities between human NPCs and murine NPCs in their response to SINV infection, our study also emphasized virus induced apoptosis as a possible mechanism of diminishing the NPC pool following infection in the pathogenesis of encephalitis.

SINV decrease expression of Nestin in hNPCs

Next, we sought to determine if SINV impacted differentiation of hNPCs. However, as the virus almost depleted the hNPC pools in 2 days, it is thus impossible to initiate any type of differentiation in presence of the virus. But still, we were able to detect a significant reduction of stemness marker Nestin expression in proliferating hNPCs after infection, indicating the virus infection triggered premature differentiation of the cells or at least, abnormal neural precursor development. Reduced Nestin expression

has been highlighted in a recent relevant study: the researchers reported that a Sindbis virus vector expressing HIV envelope protein (SIN-HIVenv) could impair murine neural stem cell survival and expression of Nestin [120]. The role of HIVenv in damaging NPCs was ruled out by other groups as it was reported that few apoptosis or TUNEL positive NPCs were detected following exposure of the cells to either a high concentration of gp120 or in the subgranular zone (SGZ) of gp120 transgenic mice [146, 199]. Thus, it is the SINV vector that disturbs Nestin expression observed in the neural stem cells. Taking these studies together with ours, we showed that SINV impacts the multipotency of NPCs and therefore the proper development of CNS. Further studies should focus on determining if the reduced expression of Nestin is directly triggered by SINV or by a bystander effect and to characterize the cell lineage to which hNPCs tend to differentiate after SINV infection.

SINV upset the dedicated balance of hNPCs cell signaling

In last part of our study, we took advantage of the strong cell responses that SINV triggered to investigate cell signaling profile of hNPCs, which regulates their response to diverse pathogens.

The JAK/STAT pathway plays a pivotal role in balancing hNPCs lineage specific differentiation. Activation of phosphorylated (Y705) STAT3 and the accumulation of this form inside cells is required for normal astrocyte differentiation [289]. The reduced pSTAT3 level in SINV infected hNPCs indicates that the virus probably impaired cell specific differentiation into this cell type. In addition, the pSTAT3 is also associated with expression of cytokines such as IL-6 in the developing CNS [296], thus, the pSTAT3 reduction could also be a mechanism by which SINV avoids inflammatory responses in NPCs. Reduced pSTAT3 expression has also been reported in JEV infection of hNPCs [205].

Extracellular signal-regulated kinases (ERK1/2) participates in modulation of genes that regulate multiple cell events in neural progenitors: proliferation, differentiation, cell fate, and synaptic plasticity [297]. The protein also has been shown to regulate apoptosis in a pAKT independent manner in hNPCs [290]. In our study, we observed that SINV infection induced the phosphorylation of both ERK at

early time points p.i. and this phosphorylation was decreased later on, suggesting a virus interplay with cellular apoptosis signaling with progression of infection, possibly to achieve optimal replication and dissemination in culture. Consistent with our study, such changes of ERK1/2 expression upon SINV infection was also reported in HMBCs [161]. Not uncommon, this important control center of cellular responses is differently employed to support the replication of several important human pathogenic RNA viruses including influenza virus, Ebola virus, hepatitis C virus and SARS coronavirus[298].

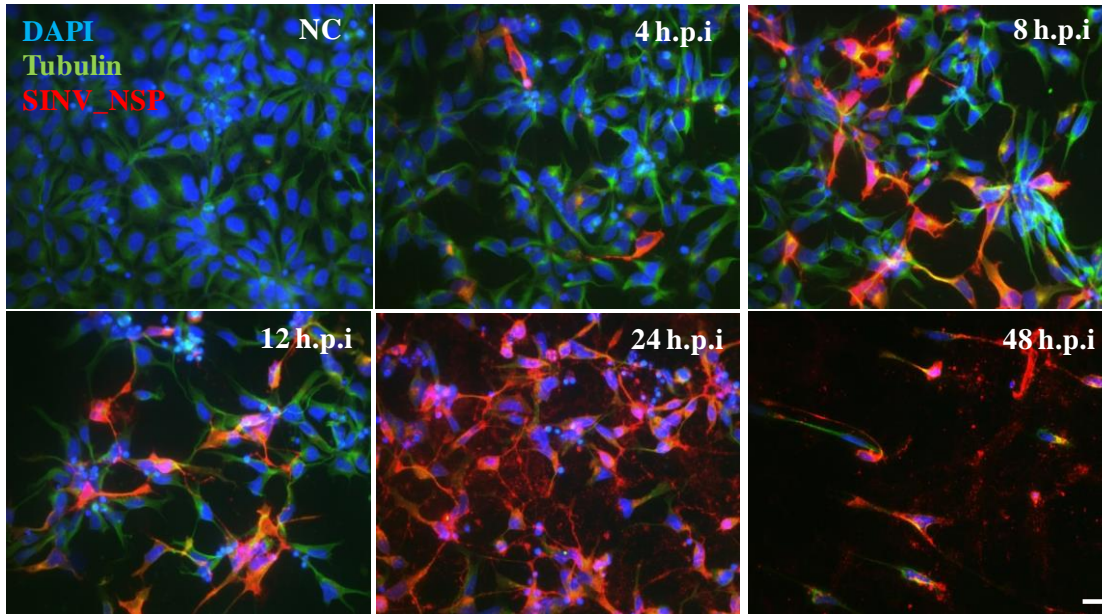
NF- κ B is another central signaling molecule in hNPCs: *in vivo*, the protein regulates neural plasticity, learning, memory, neuroprotection and neurodegeneration; *in vitro*, this molecule controls the proliferation, migration, differentiation of hNPCs [299]. More importantly, NF- κ B plays a central role in cellular stress responses and in inflammation by controlling the expression of a network of inducers and effectors; in this way it defines the response to a specific pathogen[300]. Surprisingly, our results showed that expression was not affected by SINV infection, an indication of lack of an inflammatory response during infection. In addition, the pro-apoptotic role of NF- κ B may be compensated for by the significant decrease of pERK1/2/. Finally, the binding site of NF- κ B is down stream of pSTAT3 on the target differentiation regulator gene promoter, therefore, a modulation of NF- κ B besides STAT3 maybe redundant for the virus.

Interferon regulatory gene 3 (IRF3) mediates Type I-IFN induction and signaling. Type-I IFN signaling was enhanced during hNPCs differentiation, suggesting maturation of the innate immune system during fetal development[301]. However, in our study, we did not observe any changes of IRF3 induction upon virus infection, implying a lack of IFN responses to SINV infection; but on the other hand, we may have simply verified the immaturity of innate immune system in hNPCs. The neuronal differentiation-dependent Type I IFN activity and SINV susceptibility provides a plausible explanation for clinical observation that several neurotropic arbovirus infection are particularly severe in pediatric patients where immature neurons or NPCs may be more susceptible to virus-induced damage due to reduced innate immune responses, even in the setting of adequate systemic or local type I IFN production-[291].

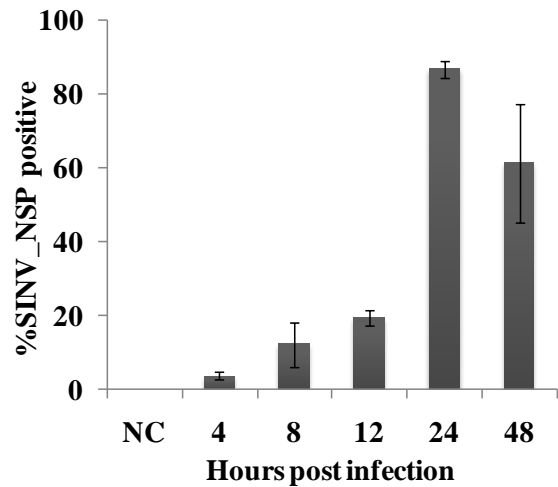
Conclusion

Back to our original questions for this part of study: here we showed that (a) SINV establishes a productive infection to hNPCs induces massive apoptosis/ cell death and altered cell stem cell marker expression. This is in combination with the virus' ability to avoid cell inflammatory responses by upsetting specific cell signaling pathways and taking advantage of the hNPCs' intrinsic immaturity in innate immune system. In the particular, the latter may contribute to the age dependence of neurological disease seen in the SINV-mouse model, (b) the robust and versatile signaling, proliferation and other cell responses of hNPCs to virus infection demonstrated that it is a good model for study pathogenesis of teratogens or other neurovirulent pathogens. (c) We are adding hNPCs as a novel type of human cells that are susceptible to SINV infection and have proved its cytopathic effect in stem cell lineages. Therefore, extra care should carry out when utilizing SINV vector for human disease gene therapy and stem cell infection.

A.



B.



C.

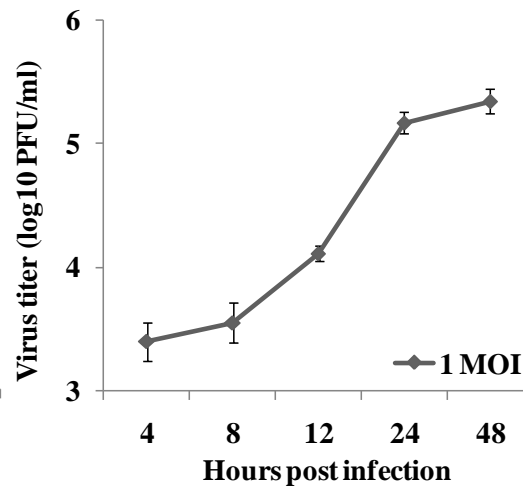


Figure 5.1 hNPCs are highly susceptible to SINV infection.

hNPCs were infected with SINV at an m.o.i. of 1(A) At 4, 8, 12, 24, and 48 hours after infection, cells were immunostained with antibodies against tubulin (green) and the SINV nonstructural proteins (NSP, red). Nuclei were counterstained with DAPI (blue). Bars: 10 μ m. (B) Medium collected at the same time points was titered for infectious virus. Each data point is the average of duplicate titration from three experiments. Error bars indicate SDs. (C) Based on SINV_NSIP immunostaining as shown in figure 5.1, the percentage of infected hNPCs was determined at each time point. The results are the means of two independent experiments; at least 200 cells from three different fields were counted at each time point. Error bars indicate SDs.

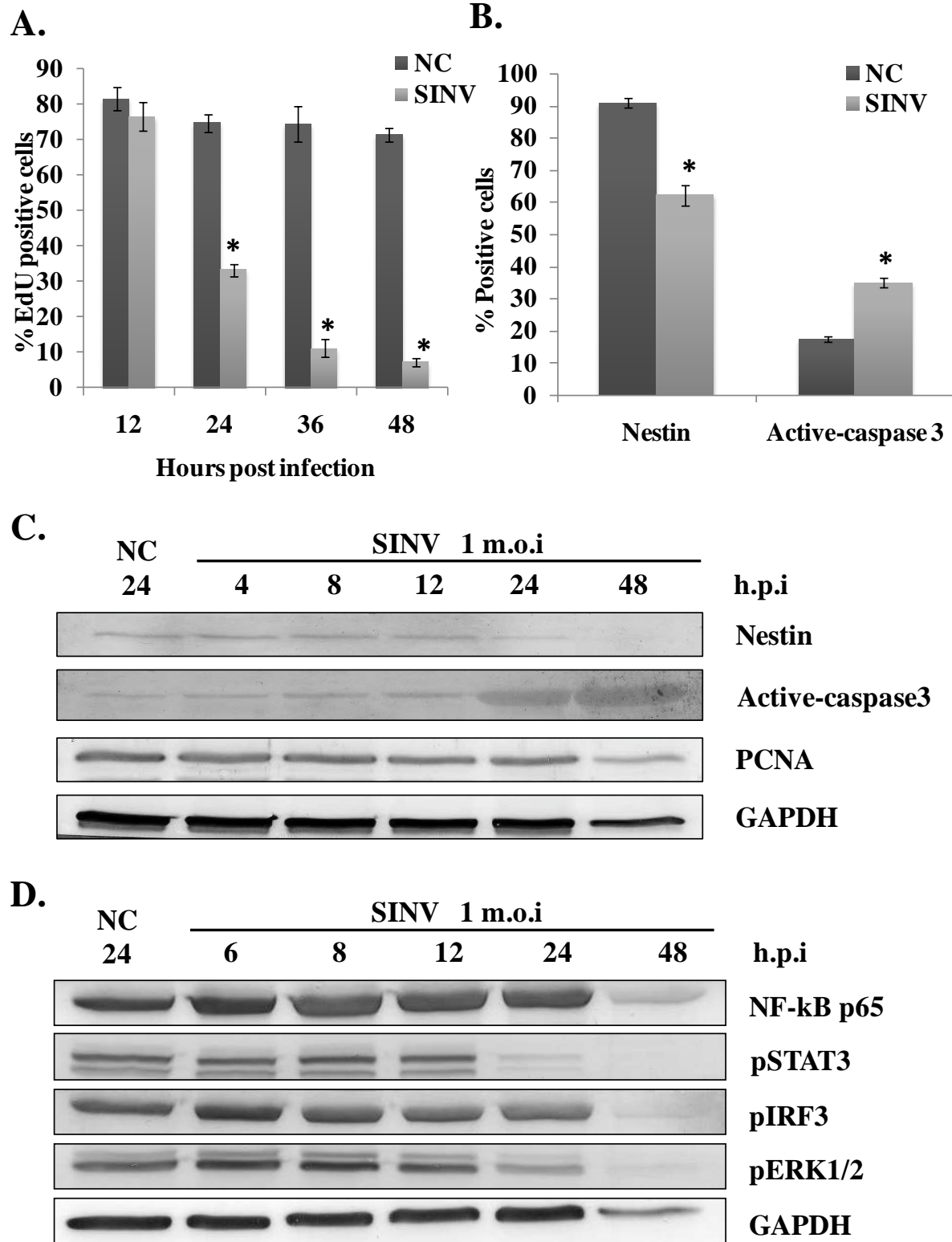


Figure 5.2 Effect of SINV infection on hNPCs proliferation and undifferentiated phenotype.

hNPCs were mock infected or infected with SINV (MOI = 1) **(A)** Cell proliferation was analyzed by flow cytometry using an EdU incorporation assay. **(B)** At 48 hours after infection, expression of the stemness marker Nestin as well as the apoptotic marker active caspase 3 was analyzed by flow cytometry. In both A and B, the experiments were repeated at least twice, two titrations per experiment. Error bars indicate SDs. *, statistical significance ($P < 0.05$) compared to the mock infected control at same time point **(C)** Western Blot analysis of the expression of Nestin, active caspase 3 and proliferating cell marker PCNA during the infection time course. Each experiment was performed at least twice. A representative blot is shown. GAPDH: loading control. **(D)** Western Blot analyses of the expression of key innate immune response regulators during SINV infection. The expression of cellular proteins that regulate key event during differentiation as well as early inflammation responses were analyzed during infection time course. Each experiment was performed at least twice. A representative blot was shown. GAPDH: loading control.

CHAPTER 6 : GENERAL CONCLUSION, SIGNIFICANCE AND FUTURE DIRECTION

6.1 GENERAL CONCLUSIONS AND SIGNIFICANCE

6.1.1 Working model for CRS and RUBV induced neurological diseases

The overarching goal of this dissertation was to elucidate the mechanism underlying the development of neurological abnormalities in CRS. Since the primary time in gestation when RUBV exhibits profound teratogenicity (i.e, the first trimester) coincides with organogenesis in the developing fetus, the favored hypothesis is that alterations induced in infected fetal stem/progenitor cells ultimately affect organ development. The attractiveness of this hypothesis increased, especially in CNS complications, considering the recently developed “schizophrenia hypothesis” which stated that schizophrenia results from a disruption in programmed maturation of the brain in prenatal and early neonatal life [109]. Meanwhile, RUBV specific antibody can be detected in the CNS of infants with CRS for a prolonged time after birth and in PRP with onset of disease in the second-decade of life in individuals with CRS, indicating the infectious process continues within in brain even after birth and that virus persistence may play an important role for the pathogenesis of RUBV-associated neurological diseases. Our model is that hNPCs are the major cell type that RUBV impacts in the developing of CNS. The cells support RUBV replication and persistence and therefore it serves as a reservoir for long-term viral residence in brain RUBV limits hNPCs cell doubling potential and deactivates the genetic program of cell death in infected cells, albeit in a small number of cells. Overall, however, this explains the general features of CRS-induced disease, namely reduced cell number and aberrations, but not to the extent that fetal death occurs, Since hNPCs still function in adult brain, it is highly possible that the depletion of hNPCs over the years would significantly hamper the local brain tissue repair and regeneration ability and thus contribute partially to the later onset neurological diseases, such as autism or schizophrenia. Our model is also proposed in conjunction with the studies in this dissertation, which found that viral persistency may play an important role for the disease development: the non-productive replication of RUBV in hNPCs may serve as a mechanism to

avoid local cytokine/inflammatory responses in brain at early embryonic development. However, with the progressive maturity of adaptive immune response and increased humoral competency, virus can be detected and therefore trigger massive immune responses that contribute to CRS late-onset diseases. The neuronal and glial cell damages could possibly be triggered by viral mediated demyelination (molecular mimicry between viral envelope protein and MOG) and cytokine mediated local necrosis. Our results may complement the clonal hypothesis by Simons (REF), which posits that viral persistence in congenital rubella could be explained by the effect of many interacting factors: the intracellular location of RUBV may avoid the activity of specific antibodies; the impossibility of activating the genetic program of cell death by at least part of the infected cells during embryogenesis; the slower growth rate and limited doubling potential observed in clones of infected cells.

6.1.2 hESC derived neural progenitors as a model to study viral teratogenesis

Numerous attempts have been made to establish a model of RUBV and other teratogenic viruses both *in vitro* and *in vivo*. Overall, definitive conclusions cannot be drawn for mechanisms of teratogenesis of RUBV since none of the previous studies was performed in a human lineage that mimics early stages of fetal development. hNPCs derived from hESCs presumably mimic the *in utero* progression from the pluripotent cells of the inner cell mass to differentiated neuronal phenotype. Thus, the first advantage of using such cells to study RUBV and other viral teratogens is that they well reflect the most important developmental events during first trimester of pregnancy the time period in which the fetus is most vulnerable to the malformations. Indeed, in our study, the results of RUBV infection of hNPCs are consistent with earlier *in vitro* and *in vivo* CRS studies in brain suggesting that hNPCs provide a reliable model for RUBV-induced teratogenesis research. Another advantage we can obviously point out after all these experiments is that: hESC derived hNPCs have uniform performance over proliferation and differentiation, However, this is hard to achieve in hNPCs isolated from abortuses; the performance of the cells largely depend on the gestational age of fetus and genetic background. Finally, the diverse cell responses of hNPCs to different virus infections (SINV and RUBV in our study and VZV by Goldstein) supports that

hESC-derived progenitor cultures have potential broad application for detailed pathogenesis studies with RUBV and other clinically important teratogenic viruses.

Taken together, our work demonstrates the utility of hESCs derived culture systems as a platform to study the interactions between embryonic development, virus infection and pathogenesis in CNS. Future work should focus on broadening the genetic background of the cells, which can be achieved by employing other hESC lines and reprogramming cells of interested individuals (see NIH hESCs cell line registry for a complete list of hESC lines eligible for NIH funding). Also, additional work has to be done by stem cell biologists to further explore the multipotency of those progenitor cells such as to characterize specific lineages that can be derived from progenitor cells. Thus, moving to more efficient protocols for complete terminal differentiation of hNPCs would be a great step-forward in the field.

6.1.3 Significance

The work described in this dissertation adds to the expanding breath of knowledge concerning the CNS disorders associated with RUBV infection. It is important to continue this work, as important parallels could be drawn between RUBV and other teratogenic/ neurotropic viruses in the pathogenesis of various brain anomalies. In comparison and contrast with another neurotropic virus, SINV, our study also illustrated how multiple factors come together to influence the final outcome of an infection in same type of cells therefore the neuropathological manifestations. It is intriguing that RUBV, although inducing a wide spectrum of neurological disease throughout life of congenitally infected individuals is not particularly neurovirulent to the brain. As similarly seen in VZV, this represents a category of neuropathogenesis associated with teratogenic viruses that requires further exploration. RUBV infected hNPCs could further serves as a model of chronic viral infections in perinatal/postnatal period which via disruptions of NPCs growth and neurogenesis, which might lead to the onset of neurobehavioral abnormalities.

6.2 FUTURE DIRECTIONS

Although strides have been reported in this dissertation to understand the basis of RUBV teratogenesis, more work need to be done to address the problem. We were able to demonstrate a limited replication of RUBV in hNPCs. However, little is known about the mechanism behind this phenomenon. The outcome of virus infection to a specific cell type is a combined result of virus-host interactions. Therefore, future studies should first focus on identifying cellular factors that restrict RUBV entry and/or limit viral replication. To this end, differences in global gene expression between the RUBV infected and uninfected hNPCs should be assayed and thus specific information as to mechanisms involved in the inability of RUBV to enter and replicate in hNPCs may be obtained. This experimental model may provide insight into the mechanisms and host factors required for the specificity of productive RUBV infection. In addition, it is also necessary to explore viral components that are subjected to this restriction. The exact step during RUBV cycle that is restricted by hNPCs will be first determined, for example: RUBV genome will be introduced into hNPCs directly by transfection to determine if viral entry is the case.

Further investigation of the fate of infected hNPCs would be another extension of this study. Particularly, it would be interesting if we can capture and track the infection on a single cell basis. In this regards, state-of-the-art techniques may employed including laser-capture, living cell antigen staining, etc. Whether those infected cells retained this differentiation after RUBV goes persistent or gradually be selected out ould thus be determined. In addition to that, it would also be interesting to investigate RUBV infection in terminally differentiated human neuronal and glial cell lines such as U87-MG and M059J to get a more comprehensive evaluation of RUBV replication in brain.

Finally, to provide additional support to our final model, we would first expand the virus strains used to include clinical isolates and the cells used to include those from different genetic backgrounds. It is of critical importance of investigate the ability of RUBV to infect pluripotent hESCs to see if RUBV-induced teratogenesis includes infection of cells at a stage earlier than the precursor stage.

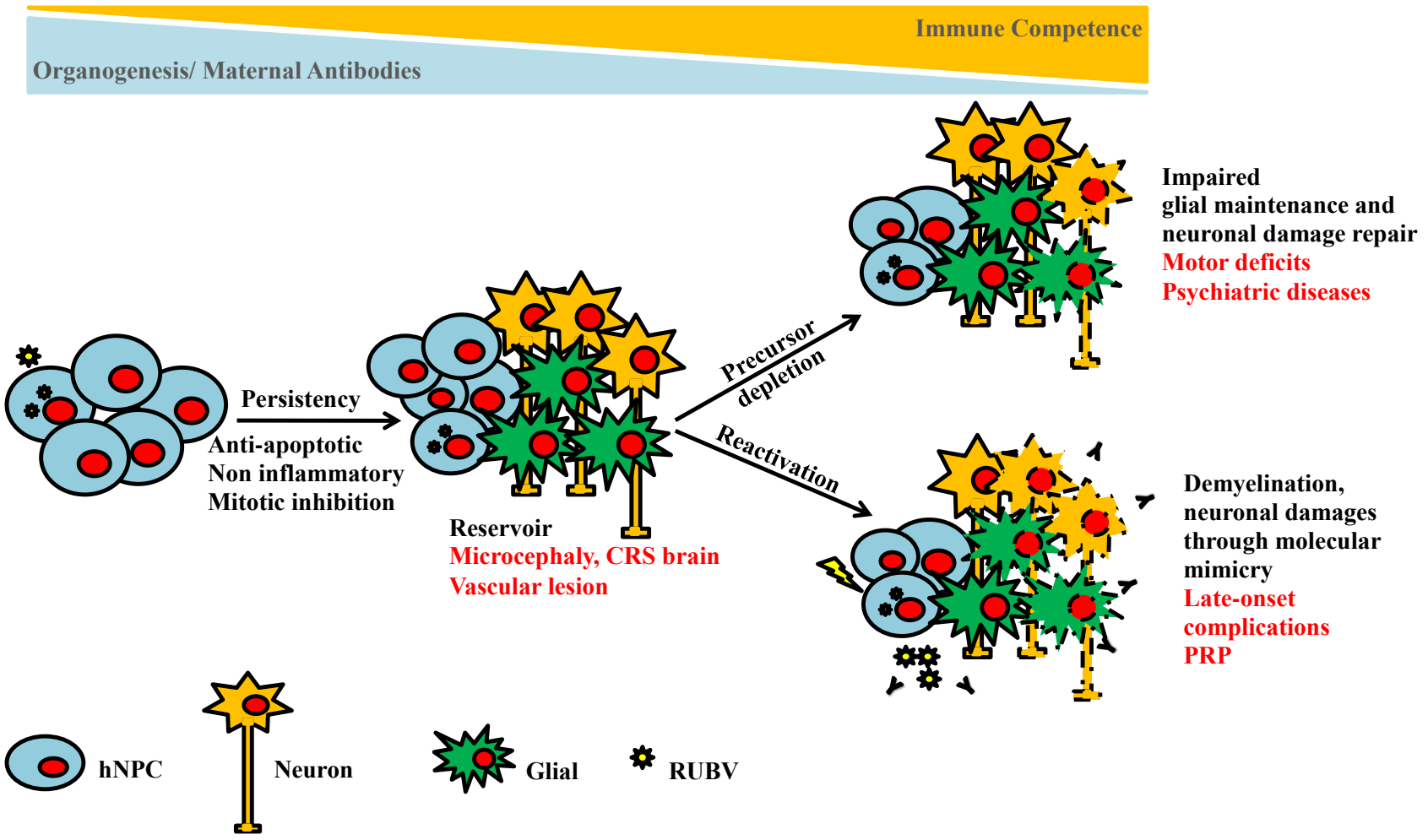


Figure 6.1 Proposed model for RUBV teratogenesis in the central nervous system.

REFERENCES

1. Frey, T.K. and S. Katow, *Rubella Virus*, in *eLS*. 2001, John Wiley & Sons, Ltd.
2. Jose, J., J.E. Snyder, and R.J. Kuhn, *A structural and functional perspective of alphavirus replication and assembly*. *Future Microbiol*, 2009. **4**(7): p. 837-56.
3. Lewis, J., et al., *Alphavirus-induced apoptosis in mouse brains correlates with neurovirulence*. *J Virol*, 1996. **70**(3): p. 1828-35.
4. Nargi-Aizenman, J.L. and D.E. Griffin, *Sindbis Virus-Induced Neuronal Death Is both Necrotic and Apoptotic and Is Ameliorated by N-Methyl-D-Aspartate Receptor Antagonists*. *Journal of Virology*, 2001. **75**(15): p. 7114-7121.
5. Hearne, A.M., M.A. O'Sullivan, and G.J. Atkins, *Infection of cultured early mouse embryos with Semliki Forest and rubella viruses*. *J Gen Virol*, 1986. **67** (Pt 6): p. 1091-8.
6. Hovi, T., *Release of rubella virus ribonucleic acid from ribonucleoprotein by polyanions*. *J Virol*, 1972. **9**(5): p. 879-82.
7. Frey, T.K., *Molecular biology of rubella virus*. *Adv Virus Res*, 1994. **44**: p. 69-160.
8. Lee, J.Y., D.S. Bowden, and J.A. Marshall, *Membrane junctions associated with rubella virus infected cells*. *J Submicrosc Cytol Pathol*, 1996. **28**(1): p. 101-8.
9. Lee, J.Y. and D.S. Bowden, *Rubella virus replication and links to teratogenicity*. *Clin Microbiol Rev*, 2000. **13**(4): p. 571-87.
10. Cong, H., Y. Jiang, and P. Tien, *Identification of the Myelin Oligodendrocyte Glycoprotein as a Cellular Receptor for Rubella Virus*. *Journal of Virology*, 2011. **85**(21): p. 11038-11047.
11. Lee, J.Y., J.A. Marshall, and D.S. Bowden, *Replication complexes associated with the morphogenesis of rubella virus*. *Arch Virol*, 1992. **122**(1-2): p. 95-106.
12. Hemphill, M.L., et al., *Time course of virus-specific macromolecular synthesis during rubella virus infection in Vero cells*. *Virology*, 1988. **162**(1): p. 65-75.
13. Garoff, H., M. Sjoberg, and R.H. Cheng, *Budding of alphaviruses*. *Virus Res*, 2004. **106**(2): p. 103-16.
14. Wesselhoeft, C., *Rubella (German measles)*. *N Engl J Med*, 1947. **236**(26): p. 978-88.
15. Duszak, R.S., *Congenital rubella syndrome--major review*. *Optometry*, 2009. **80**(1): p. 36-43.
16. Gregg, N.M., *Congenital cataract following German measles in the mother. 1941*. *Epidemiol Infect*, 1991. **107**(1): p. iii-xiv; discussion xiii-xiv.
17. Centers for Disease, C. and Prevention, *Progress toward control of rubella and prevention of congenital rubella syndrome --- worldwide, 2009*. *MMWR Morb Mortal Wkly Rep*, 2010. **59**(40): p. 1307-10.
18. Reef, S.E., et al., *Progress toward control of rubella and prevention of congenital rubella syndrome--worldwide, 2009*. *J Infect Dis*, 2011. **204 Suppl 1**: p. S24-7.
19. Meissner, H.C., S.E. Reef, and S. Cochi, *Elimination of rubella from the United States: a milestone on the road to global elimination*. *Pediatrics*, 2006. **117**(3): p. 933-5.

20. Slater, P.E., et al., *Control of rubella in Israel: progress and challenge*. Public Health Rev, 1996. **24**(2): p. 183-92.
21. Ma, J., L.X. Hao, and H.M. Luo, [*Progress on rubella control and immunization strategies*]. Zhongguo Yi Miao He Mian Yi, 2010. **16**(1): p. 69-71.
22. Plotkin, S.A., *Rubella eradication*. Vaccine, 2001. **19**(25-26): p. 3311-9.
23. Parkman, P.D., E.L. Buescher, and M.S. Artenstein, *Recovery of rubella virus from army recruits*. Proc Soc Exp Biol Med, 1962. **111**: p. 225-30.
24. West, R. and P.M. Roberts, *Measles, mumps and rubella vaccine: current safety issues*. BioDrugs, 1999. **12**(6): p. 423-9.
25. Plotkin, S.A., et al., *Attenuation of RA 27-3 rubella virus in WI-38 human diploid cells*. Am J Dis Child, 1969. **118**(2): p. 178-85.
26. Weibel, R.E., et al., *Clinical and laboratory studies of live attenuated RA 27/3 and HPV 77-DE rubella virus vaccines*. Proc Soc Exp Biol Med, 1980. **165**(1): p. 44-9.
27. Hofmann, J., et al., *Persistent fetal rubella vaccine virus infection following inadvertent vaccination during early pregnancy*. J Med Virol, 2000. **61**(1): p. 155-8.
28. Lindegren, M.L., et al., *Update: rubella and congenital rubella syndrome, 1980-1990*. Epidemiol Rev, 1991. **13**: p. 341-8.
29. Cutts, F.T., et al., *Control of rubella and congenital rubella syndrome (CRS) in developing countries, Part 1: Burden of disease from CRS*. Bull World Health Organ, 1997. **75**(1): p. 55-68.
30. Robertson, S.E., et al., *Control of rubella and congenital rubella syndrome (CRS) in developing countries, Part 2: Vaccination against rubella*. Bull World Health Organ, 1997. **75**(1): p. 69-80.
31. Nossal, G.J., *Vaccines and future global health needs*. Philos Trans R Soc Lond B Biol Sci, 2011. **366**(1579): p. 2833-40.
32. Tipple, M. and E. Saxon, *Diagnostic virology in clinical practice*. Prim Care, 1979. **6**(1): p. 195-209.
33. Dudgeon, J.A., *Maternal rubella and its effect on the foetus*. Arch Dis Child, 1967. **42**(222): p. 110-25.
34. Tingle, A.J., et al., *Rubella-associated arthritis. I. Comparative study of joint manifestations associated with natural rubella infection and RA 27/3 rubella immunisation*. Ann Rheum Dis, 1986. **45**(2): p. 110-4.
35. Singh, V.K., A.J. Tingle, and M. Schulzer, *Rubella-associated arthritis. II. Relationship between circulating immune complex levels and joint manifestations*. Ann Rheum Dis, 1986. **45**(2): p. 115-9.
36. Webster, W.S., *Teratogen update: congenital rubella*. Teratology, 1998. **58**(1): p. 13-23.
37. Best, J.M. and J.E. Banatvala, *Rubella*, in *Principles and Practice of Clinical Virology*. 2002, John Wiley & Sons, Ltd. p. 387-418.
38. Forrest, J.M., M.A. Menser, and J.D. Harley, *Diabetes mellitus and congenital rubella*. Pediatrics, 1969. **44**(3): p. 445-7.
39. McIntosh, E.D. and M.A. Menser, *A fifty-year follow-up of congenital rubella*. Lancet, 1992. **340**(8816): p. 414-5.
40. Tondury, G. and D.W. Smith, *Fetal rubella pathology*. J Pediatr, 1966. **68**(6): p. 867-79.

41. South, M.A. and J.L. Sever, *Teratogen update: the congenital rubella syndrome*. *Teratology*, 1985. **31**(2): p. 297-307.
42. Cooper, L.Z., et al., *Neonatal thrombocytopenic purpura and other manifestations of rubella contracted in utero*. *Am J Dis Child*, 1965. **110**(4): p. 416-27.
43. Rausen, A.R., et al., *Generalized Bone Changes and Thrombocytopenic Purpura in Association with Intrauterine Rubella*. *Pediatrics*, 1965. **36**: p. 264-8.
44. Giles, J.P., L.Z. Cooper, and S. Krugman, *The Rubella Syndrome*. *J Pediatr*, 1965. **66**: p. 434-7.
45. Holt, P.G. and C.A. Jones, *The development of the immune system during pregnancy and early life*. *Allergy*, 2000. **55**(8): p. 688-697.
46. Lebon, P., et al., *Presence of an acid-labile alpha-interferon in sera from fetuses and children with congenital rubella*. *J Clin Microbiol*, 1985. **21**(5): p. 775-8.
47. Rawls, W.E., et al., *Persistent virus infection in congenital rubella*. *Arch Ophthalmol*, 1967. **77**(4): p. 430-3.
48. Menser, M.A., et al., *Persistence of virus in lens for three years after prenatal rubella*. *Lancet*, 1967. **2**(7512): p. 387-8.
49. Rawls, W.E. and J.L. Melnick, *Rubella virus carrier cultures derived from congenitally infected infants*. *J Exp Med*, 1966. **123**(5): p. 795-816.
50. Kenrick, K.G., et al., *Immunoglobulins and rubella-virus antibodies in adults with congenital rubella*. *Lancet*, 1968. **1**(7542): p. 548-51.
51. Alford, C.A., Jr., *Studies on antibody in congenital rubella infections. I. Physicochemical and immunologic investigations of rubella neutralizing antibody*. *Am J Dis Child*, 1965. **110**(4): p. 455-63.
52. Rawls, W.E., *Congenital rubella: the significance of virus persistence*. *Prog Med Virol*, 1968. **10**: p. 238-85.
53. Holmes, L.B., *Human teratogens: update 2010*. *Birth Defects Res A Clin Mol Teratol*, 2011. **91**(1): p. 1-7.
54. *TORCH syndrome and TORCH screening*. *Lancet*, 1990. **335**(8705): p. 1559-61.
55. Nahmias, A.J., et al., *Perinatal risk associated with maternal genital herpes simplex virus infection*. *Am J Obstet Gynecol*, 1971. **110**(6): p. 825-37.
56. Rasmussen, S.A., et al., *Teratology: from science to birth defects prevention*. *Birth Defects Res A Clin Mol Teratol*, 2009. **85**(1): p. 82-92.
57. Fabiyi, A., G.L. Gitnick, and J.L. Sever, *Chronic rubella virus infection in the ferret (*Mustela putorius fero*) puppy*. *Proc Soc Exp Biol Med*, 1967. **125**(3): p. 766-71.
58. Harris, R.E., *Viral teratogenesis: a review with experimental and clinical perspectives*. *Am J Obstet Gynecol*, 1974. **119**(7): p. 996-1008.
59. Wolinsky, J.S., et al., *An antibody- and synthetic peptide-defined rubella virus E1 glycoprotein neutralization domain*. *J Virol*, 1993. **67**(2): p. 961-8.
60. Zausmer, E., *Congenital rubella: pathogenesis of motor deficits*. *Pediatrics*, 1971. **47**(1): p. 16-26.
61. Plotkin, S.A., A. Boue, and J.G. Boue, *The in Vitro Growth of Rubella Virus in Human Embryo Cells*. *Am J Epidemiol*, 1965. **81**: p. 71-85.

62. Kay, H.E., et al., *Congenital Rubella Infection of a Human Embryo*. Br Med J, 1964. **2**(5402): p. 166-7.
63. Best, J.M., J.E. Banatvala, and M.E. Smith, *Further studies on the growth of rubella virus in human embryonic organ cultures: preliminary observations on interferon production in these cultures*. J Hyg (Lond), 1971. **69**(2): p. 223-32.
64. Yoneda, T., et al., *Altered growth, differentiation, and responsiveness to epidermal growth factor of human embryonic mesenchymal cells of palate by persistent rubella virus infection*. J Clin Invest, 1986. **77**(5): p. 1613-21.
65. Naeye, R.L. and W. Blanc, *Pathogenesis of congenital rubella*. JAMA, 1965. **194**(12): p. 1277-83.
66. Adamo, P., et al., *Rubella virus does not induce apoptosis in primary human embryo fibroblast cultures: a possible way of viral persistence in congenital infection*. Viral Immunol, 2004. **17**(1): p. 87-100.
67. Boué A, B.J.G., *Effects of rubella virus infection on the division of human cells*. Am J Dis Child, 1969. **118**(1): p. 45-48.
68. Plotkin, S.A. and A. Vaheri, *Human fibroblasts infected with rubella virus produce a growth inhibitor*. Science, 1967. **156**(3775): p. 659-61.
69. Atreya, C.D., S. Kulkarni, and K.V. Mohan, *Rubella virus P90 associates with the cytokinesis regulatory protein Citron-K kinase and the viral infection and constitutive expression of P90 protein both induce cell cycle arrest following S phase in cell culture*. Arch Virol, 2004. **149**(4): p. 779-89.
70. Atreya, C.D., K.V. Mohan, and S. Kulkarni, *Rubella virus and birth defects: molecular insights into the viral teratogenesis at the cellular level*. Birth Defects Res A Clin Mol Teratol, 2004. **70**(7): p. 431-7.
71. Monif, G.R., et al., *Postmortem Isolation of Rubella Virus from Three Children with Rubella-Syndrome Defects*. Lancet, 1965. **1**(7388): p. 723-4.
72. Korones, S.B., et al., *Congenital rubella syndrome: study of 22 infants. Myocardial damage and other new clinical aspects*. Am J Dis Child, 1965. **110**(4): p. 434-40.
73. Duncan, R., et al., *Rubella virus capsid protein induces apoptosis in transfected RK13 cells*. Virology, 2000. **275**(1): p. 20-9.
74. Duncan, R., et al., *Rubella virus-induced apoptosis varies among cell lines and is modulated by Bcl-XL and caspase inhibitors*. Virology, 1999. **255**(1): p. 117-28.
75. Ilkow, C.S., I.S. Goping, and T.C. Hobman, *The Rubella virus capsid is an anti-apoptotic protein that attenuates the pore-forming ability of Bax*. PLoS Pathog, 2011. **7**(2): p. e1001291.
76. Pugachev, K.V. and T.K. Frey, *Rubella virus induces apoptosis in culture cells*. Virology, 1998. **250**(2): p. 359-70.
77. Hofmann, J., M.W. Pletz, and U.G. Liebert, *Rubella virus-induced cytopathic effect in vitro is caused by apoptosis*. J Gen Virol, 1999. **80** (Pt 7): p. 1657-64.
78. Domegan, L.M. and G.J. Atkins, *Apoptosis induction by the Therien and vaccine RA27/3 strains of rubella virus causes depletion of oligodendrocytes from rat neural cell cultures*. J Gen Virol, 2002. **83**(Pt 9): p. 2135-43.
79. Natale, V.A., et al., *Effect of infection with rubella virus on the development of rat cerebellar cells in culture*. Neuropathol Appl Neurobiol, 1993. **19**(6): p. 530-4.
80. Van Alstyne, D. and D.W. Paty, *The effect of dibutyryl cyclic AMP on restricted replication of rubella virus in rat glial cells in culture*. Virology, 1983. **124**(1): p. 173-80.

81. Singer, D.B., et al., *Pathology of the congenital rubella syndrome*. J Pediatr, 1967. **71**(5): p. 665-75.
82. Banatvala, J.E., J.E. Potter, and J.M. Best, *Interferon response to sendai and rubella viruses in human foetal cultures, leucocytes and placental cultures*. J Gen Virol, 1971. **13**(2): p. 193-201.
83. Schneider-Schaulies, J., S. Schneider-Schaulies, and V. Ter Meulen, *Differential induction of cytokines by primary and persistent measles virus infections in human glial cells*. Virology, 1993. **195**(1): p. 219-28.
84. Kansagra, S.M. and W.B. Gallentine, *Cytokine storm of acute necrotizing encephalopathy*. Pediatr Neurol, 2011. **45**(6): p. 400-2.
85. Coyle, P.K., et al., *Rubella-specific immune complexes after congenital infection and vaccination*. Infect Immun, 1982. **36**(2): p. 498-503.
86. Williams, M.P., et al., *Characteristics of a persistent rubella infection in a human cell line*. J Gen Virol, 1981. **52**(Pt 2): p. 321-8.
87. Abernathy, E.S., C.Y. Wang, and T.K. Frey, *Effect of antiviral antibody on maintenance of long-term rubella virus persistent infection in Vero cells*. J Virol, 1990. **64**(10): p. 5183-7.
88. Joklik, W.K., *The mechanism of action of interferon*. Ann N Y Acad Sci, 1977. **284**: p. 711-6.
89. Bowden, D.S., et al., *Distribution by immunofluorescence of viral products and actin-containing cytoskeletal filaments in rubella virus-infected cells*. Arch Virol, 1987. **92**(3-4): p. 211-9.
90. Lee, J.Y., J.A. Marshall, and D.S. Bowden, *Localization of rubella virus core particles in vero cells*. Virology, 1999. **265**(1): p. 110-9.
91. Claus, C., et al., *Involvement of p32 and microtubules in alteration of mitochondrial functions by rubella virus*. J Virol, 2011. **85**(8): p. 3881-92.
92. Suppiah, S., et al., *Binding of cellular p32 protein to the rubella virus P150 replicase protein via PxxPxR motifs*. J Gen Virol, 2012. **93**(Pt 4): p. 807-16.
93. Kujala, P., et al., *Intracellular distribution of rubella virus nonstructural protein P150*. J Virol, 1999. **73**(9): p. 7805-11.
94. Brown, A.S., et al., *Nonaffective psychosis after prenatal exposure to rubella*. Am J Psychiatry, 2000. **157**(3): p. 438-43.
95. Chess, S., *Autism in children with congenital rubella*. J Autism Child Schizophr, 1971. **1**(1): p. 33-47.
96. Lim, K.O., et al., *Brain dysmorphology in adults with congenital rubella plus schizophrenialike symptoms*. Biol Psychiatry, 1995. **37**(11): p. 764-76.
97. Pearce, B.D., *Schizophrenia and viral infection during neurodevelopment: a focus on mechanisms*. Mol Psychiatry, 2001. **6**(6): p. 634-46.
98. Cremer, N.E., et al., *Isolation of rubella virus from brain in chronic progressive panencephalitis*. J Gen Virol, 1975. **29**(2): p. 143-53.
99. Monif, G.R. and J.L. Sever, *Chronic infection of the central nervous system with rubella virus*. Neurology, 1966. **16**(1): p. 111-2.
100. Dwyer, D.E., et al., *Acute encephalitis complicating rubella virus infection*. Pediatr Infect Dis J, 1992. **11**(3): p. 238-40.
101. Frey, T.K., *Neurological aspects of rubella virus infection*. Intervirology, 1997. **40**(2-3): p. 167-75.
102. Lau, K.K., et al., *Acute encephalitis complicating rubella*. Hong Kong Med J, 1998. **4**(3): p. 325-328.

103. Date, M., et al., [A case of rubella encephalitis: rubella virus genome was detected in the cerebrospinal fluid by polymerase chain reaction]. *No To Hattatsu*, 1995. **27**(4): p. 286-90.
104. Nomura, K., et al., [A case report of subacute panencephalitis associated with specific T cells sensitized to proteolipid protein (PLP) synthetic peptides identified with rubella virus]. *Rinsho Shinkeigaku*, 1996. **36**(9): p. 1074-8.
105. Atkins, M.C. and T.F. Esmonde, *Guillain-Barre syndrome associated with rubella*. *Postgrad Med J*, 1991. **67**(786): p. 375-6.
106. Rorke, L.B., *Nervous system lesions in the congenital rubella syndrome*. Vol. 98. 1973. 249-51.
107. Atkins, G.J., et al., *Multiplication of rubella and measles viruses in primary rat neural cell cultures: relevance to a postulated triggering mechanism for multiple sclerosis*. *Neuropathol Appl Neurobiol*, 1991. **17**(4): p. 299-308.
108. Chantler, J.K., L. Smyrnis, and G. Tai, *Selective infection of astrocytes in human glial cell cultures by rubella virus*. *Lab Invest*, 1995. **72**(3): p. 334-40.
109. Brown, A.S. and E.S. Susser, *In utero infection and adult schizophrenia*. *Ment Retard Dev Disabil Res Rev*, 2002. **8**(1): p. 51-7.
110. Weil, M.L., et al., *Chronic progressive panencephalitis due to rubella virus simulating subacute sclerosing panencephalitis*. *N Engl J Med*, 1975. **292**(19): p. 994-8.
111. Townsend, J.J., J.S. Wolinsky, and J.R. Baringer, *The neuropathology of progressive rubella panencephalitis of late onset*. *Brain*, 1976. **99**(1): p. 81-90.
112. Mocsny, N., *Slow virus diseases of the central nervous system*. *Rehabil Nurs*, 1989. **14**(3): p. 130-2.
113. Townsend, J.J., et al., *Neuropathology of progressive rubella panencephalitis after childhood rubella*. *Neurology*, 1982. **32**(2): p. 185-90.
114. Vandvik, B., et al., *Progressive rubella virus panencephalitis: synthesis of oligoclonal virus-specific IgG antibodies and homogeneous free light chains in the central nervous system*. *Acta Neurol Scand*, 1978. **57**(1): p. 53-64.
115. Townsend, J.J., et al., *Progressive rubella panencephalitis. Late onset after congenital rubella*. *N Engl J Med*, 1975. **292**(19): p. 990-3.
116. ter Meulen, V. and W.W. Hall, *Slow virus infections of the nervous system: virological, immunological and pathogenetic considerations*. *J Gen Virol*, 1978. **41**(1): p. 1-25.
117. Kemper, T.L., et al., *Retardation of the myelo- and cytoarchitectonic maturation of the brain in the congenital rubella syndrome*. *Res Publ Assoc Res Nerv Ment Dis*, 1973. **51**: p. 23-62.
118. Daston, G.P., *Laboratory models and their role in assessing teratogenesis*. *Am J Med Genet C Semin Med Genet*, 2011. **157**(3): p. 183-7.
119. Odeberg, J., et al., *Human cytomegalovirus inhibits neuronal differentiation and induces apoptosis in human neural precursor cells*. *J Virol*, 2006. **80**(18): p. 8929-39.
120. van Marle, G., et al., *Aberrant cortical neurogenesis in a pediatric neuroAIDS model: neurotrophic effects of growth hormone*. *AIDS*, 2005. **19**(16): p. 1781-91.
121. Delahunt, C.S. and N. Rieser, *Rubella-induced embryopathies in monkeys*. *Am J Obstet Gynecol*, 1967. **99**(4): p. 580-8.
122. Menser, M.A., J.M. Forrest, and R.D. Bransby, *Rubella infection and diabetes mellitus*. *Lancet*, 1978. **1**(8055): p. 57-60.

123. Avila, L., W.E. Rawls, and P.B. Dent, *Experimental infection with rubella virus. I. Acquired and congenital infection in rats*. J Infect Dis, 1972. **126**(6): p. 585-92.
124. Swarup, V., et al., *Tumor necrosis factor receptor-1-induced neuronal death by TRADD contributes to the pathogenesis of Japanese encephalitis*. J Neurochem, 2007. **103**(2): p. 771-83.
125. Cooray, S., L. Jin, and J.M. Best, *The involvement of survival signaling pathways in rubella-virus induced apoptosis*. Virol J, 2005. **2**: p. 1.
126. Thomson, J.A., et al., *Embryonic stem cell lines derived from human blastocysts*. Science, 1998. **282**(5391): p. 1145-7.
127. Zychlinska, M., et al., *Restricted expression of Epstein-Barr virus latent genes in murine B cells derived from embryonic stem cells*. PLoS One, 2008. **3**(4): p. e1996.
128. Wash, R., et al., *Permissive and restricted virus infection of murine embryonic stem cells*. J Gen Virol, 2012. **93**(Pt 10): p. 2118-30.
129. Verlinsky, Y., et al., *Human embryonic stem cell lines with genetic disorders*. Reprod Biomed Online, 2005. **10**(1): p. 105-10.
130. Dukhovny, A., et al., *Varicella-Zoster Virus Infects Human Embryonic Stem Cell-Derived Neurons and Neurospheres but Not Pluripotent Embryonic Stem Cells or Early Progenitors*. Journal of Virology, 2012. **86**(6): p. 3211-3218.
131. Conti, L. and E. Cattaneo, *Neural stem cell systems: physiological players or in vitro entities?* Nat Rev Neurosci, 2010. **11**(3): p. 176-87.
132. Dhara, S.K. and S.L. Stice, *Neural differentiation of human embryonic stem cells*. J Cell Biochem, 2008. **105**(3): p. 633-40.
133. Kalyani, A., K. Hobson, and M.S. Rao, *Neuroepithelial stem cells from the embryonic spinal cord: isolation, characterization, and clonal analysis*. Dev Biol, 1997. **186**(2): p. 202-23.
134. Kennea, N.L. and H. Mehmet, *Neural stem cells*. The Journal of Pathology, 2002. **197**(4): p. 536-550.
135. Young, A., et al., *Ion channels and ionotropic receptors in human embryonic stem cell derived neural progenitors*. Neuroscience, 2011. **192**: p. 793-805.
136. Shin, S., et al., *Long-Term Proliferation of Human Embryonic Stem Cell-Derived Neuroepithelial Cells Using Defined Adherent Culture Conditions*. Stem Cells, 2006. **24**(1): p. 125-138.
137. Dhara, S.K., et al., *Human neural progenitor cells derived from embryonic stem cells in feeder-free cultures*. Differentiation, 2008. **76**(5): p. 454-464.
138. Muller, F.J., et al., *Regulatory networks define phenotypic classes of human stem cell lines*. Nature, 2008. **455**(7211): p. 401-5.
139. Breier, J.M., et al., *Neural progenitor cells as models for high-throughput screens of developmental neurotoxicity: State of the science*. Neurotoxicology and Teratology, 2010. **32**(1): p. 4-15.
140. Lai, B., et al., *Endothelium-induced proliferation and electrophysiological differentiation of human embryonic stem cell-derived neuronal precursors*. Stem Cells Dev, 2008. **17**(3): p. 565-72.
141. Acharya, M.M., et al., *Consequences of ionizing radiation-induced damage in human neural stem cells*. Free Radic Biol Med, 2010. **49**(12): p. 1846-55.
142. Cheng, K. and W.S. Kisaalita, *Exploring cellular adhesion and differentiation in a micro-/nano-hybrid polymer scaffold*. Biotechnol Prog, 2010. **26**(3): p. 838-46.

143. Dodla, M.C., J. Mumaw, and S.L. Stice, *Role of astrocytes, soluble factors, cells adhesion molecules and neurotrophins in functional synapse formation: implications for human embryonic stem cell derived neurons*. *Curr Stem Cell Res Ther*, 2010. **5**(3): p. 251-60.
144. Wu, Z.Z., et al., *Effects of topography on the functional development of human neural progenitor cells*. *Biotechnol Bioeng*, 2010. **106**(4): p. 649-59.
145. Jin, K., et al., *Effect of human neural precursor cell transplantation on endogenous neurogenesis after focal cerebral ischemia in the rat*. *Brain Res*, 2011. **1374**: p. 56-62.
146. Das, S. and A. Basu, *Viral infection and neural stem/progenitor cell's fate: implications in brain development and neurological disorders*. *Neurochem Int*, 2011. **59**(3): p. 357-66.
147. Tsutsui, Y., *Effects of cytomegalovirus infection on embryogenesis and brain development*. *Congenit Anom (Kyoto)*, 2009. **49**(2): p. 47-55.
148. Lokensgard, J.R., et al., *Human cytomegalovirus replication and modulation of apoptosis in astrocytes*. *J Hum Virol*, 1999. **2**(2): p. 91-101.
149. Luo, M.H., et al., *Human cytomegalovirus infection causes premature and abnormal differentiation of human neural progenitor cells*. *J Virol*, 2010. **84**(7): p. 3528-41.
150. Luo, M.H., P.H. Schwartz, and E.A. Fortunato, *Neonatal neural progenitor cells and their neuronal and glial cell derivatives are fully permissive for human cytomegalovirus infection*. *J Virol*, 2008. **82**(20): p. 9994-10007.
151. Brnic, D., et al., *Borna disease virus infects human neural progenitor cells and impairs neurogenesis*. *J Virol*, 2012. **86**(5): p. 2512-22.
152. Krathwohl, M.D. and J.L. Kaiser, *HIV-1 promotes quiescence in human neural progenitor cells*. *J Infect Dis*, 2004. **190**(2): p. 216-26.
153. Scassa, M.E., et al., *Human embryonic stem cells and derived contractile embryoid bodies are susceptible to Cocksakievirus B infection and respond to interferon I β treatment*. *Stem Cell Research*, 2011. **6**(1): p. 13-22.
154. Peng, H., et al., *HIV-1-infected and immune-activated macrophages induce astrocytic differentiation of human cortical neural progenitor cells via the STAT3 pathway*. *PLoS One*, 2011. **6**(5): p. e19439.
155. Peng, H., et al., *HIV-1-infected and/or immune-activated macrophage-secreted TNF-alpha affects human fetal cortical neural progenitor cell proliferation and differentiation*. *Glia*, 2008. **56**(8): p. 903-16.
156. Chiodo, F., et al., *Infective diseases during pregnancy and their teratogenic effects*. *Ann Ist Super Sanita*, 1993. **29**(1): p. 57-67.
157. Touze, E., et al., *Hepatitis B vaccination and first central nervous system demyelinating event: a case-control study*. *Neuroepidemiology*, 2002. **21**(4): p. 180-6.
158. Gerna, G., et al., *[Nuclear DNA content of human embryonal fibroblasts (RU-1) in cultures infected with virulent and attenuated strains of rubella virus]*. *Riv Istochim Norm Patol*, 1975. **19**(1-4): p. 125.
159. Heggie, A.D., *Growth inhibition of human embryonic and fetal rat bones in organ culture by rubella virus*. *Teratology*, 1977. **15**(1): p. 47-55.
160. Burdeinick-Kerr, R. and D.E. Griffin, *Gamma interferon-dependent, noncytolytic clearance of sindbis virus infection from neurons in vitro*. *J Virol*, 2005. **79**(9): p. 5374-85.
161. Thach, D.C., et al., *Assessing the feasibility of using neural precursor cells and peripheral blood mononuclear cells for detection of bioactive Sindbis virus*. *Biosens Bioelectron*, 2003. **18**(8): p. 1065-72.

162. Rust, N.M., et al., *Bradykinin enhances Sindbis virus infection in human brain microvascular endothelial cells*. *Virology*, 2012. **422**(1): p. 81-91.
163. Tzeng, W.P., J. Xu, and T.K. Frey, *Characterization of cell lines stably transfected with rubella virus replicons*. *Virology*, 2012. **429**(1): p. 29-36.
164. Becroft, D.M., *Prenatal cytomegalovirus infection: epidemiology, pathology and pathogenesis*. *Perspect Pediatr Pathol*, 1981. **6**: p. 203-41.
165. Frenkel, L.D., et al., *Unusual eye abnormalities associated with congenital cytomegalovirus infection*. *Pediatrics*, 1980. **66**(5): p. 763-6.
166. Adler, S.P., G. Nigro, and L. Pereira, *Recent advances in the prevention and treatment of congenital cytomegalovirus infections*. *Semin Perinatol*, 2007. **31**(1): p. 10-8.
167. Tardieu, M., et al., *Circulating immune complexes containing rubella antigens in late-onset rubella syndrome*. *J Pediatr*, 1980. **97**(3): p. 370-3.
168. Atkins, G.J., et al., *Mechanisms of viral teratogenesis*. *Reviews in Medical Virology*, 1995. **5**(2): p. 75-86.
169. Carter, C.J., *Schizophrenia susceptibility genes directly implicated in the life cycles of pathogens: cytomegalovirus, influenza, herpes simplex, rubella, and Toxoplasma gondii*. *Schizophr Bull*, 2009. **35**(6): p. 1163-82.
170. McCarthy, M., D. Auger, and S.R. Whitemore, *Human cytomegalovirus causes productive infection and neuronal injury in differentiating fetal human central nervous system neuroepithelial precursor cells*. *J Hum Virol*, 2000. **3**(4): p. 215-28.
171. Spiller, O.B., L.K. Borysiewicz, and B.P. Morgan, *Development of a model for cytomegalovirus infection of oligodendrocytes*. *J Gen Virol*, 1997. **78** (Pt 12): p. 3349-56.
172. Gonczol, E., P.W. Andrews, and S.A. Plotkin, *Cytomegalovirus replicates in differentiated but not in undifferentiated human embryonal carcinoma cells*. *Science*, 1984. **224**(4645): p. 159-61.
173. Perelygina, L., et al., *Persistent infection of human fetal endothelial cells with rubella virus*. *PLoS One*, 2013. **8**(8): p. e73014.
174. Chantler, J.K. and A.J. Tingle, *Replication and expression of rubella virus in human lymphocyte populations*. *J Gen Virol*, 1980. **50**(2): p. 317-28.
175. Fortunato, E.A., M.L. Dell'Aquila, and D.H. Spector, *Specific chromosome 1 breaks induced by human cytomegalovirus*. *Proc Natl Acad Sci U S A*, 2000. **97**(2): p. 853-8.
176. Chang, T.H., et al., *Chromosome studies of human cells infected in utero and in vitro with rubella virus*. *Proc Soc Exp Biol Med*, 1966. **122**(1): p. 236-43.
177. Ansari, B.M. and M.K. Mason, *Chromosomal abnormality in congenital rubella*. *Pediatrics*, 1977. **59**(1): p. 13-5.
178. Odeberg, J., et al., *Human cytomegalovirus inhibits neuronal differentiation and induces apoptosis in human neural precursor cells*. *J Virol*, 2006. **80**(18): p. 8929-8939.
179. Skaletskaya, A., et al., *A cytomegalovirus-encoded inhibitor of apoptosis that suppresses caspase-8 activation*. *Proc Natl Acad Sci U S A*, 2001. **98**(14): p. 7829-34.
180. Reboredo, M., R.F. Greaves, and G. Hahn, *Human cytomegalovirus proteins encoded by UL37 exon 1 protect infected fibroblasts against virus-induced apoptosis and are required for efficient virus replication*. *J Gen Virol*, 2004. **85**(Pt 12): p. 3555-67.

181. Odeberg, J., et al., *Late human cytomegalovirus (HCMV) proteins inhibit differentiation of human neural precursor cells into astrocytes*. J Neurosci Res, 2007. **85**(3): p. 583-593.
182. Adamo, M.P., M. Zapata, and T.K. Frey, *Analysis of gene expression in fetal and adult cells infected with rubella virus*. Virology, 2008. **370**(1): p. 1-11.
183. Koontz, T., et al., *Altered development of the brain after focal herpesvirus infection of the central nervous system*. J Exp Med, 2008. **205**(2): p. 423-35.
184. Hayflick, L. and P.S. Moorhead, *The serial cultivation of human diploid cell strains*. Exp Cell Res, 1961. **25**: p. 585-621.
185. Pope, D.D. and D. Van Alstyne, *Evidence for restricted replication of Rubella virus in rat glial cells in culture*. Virology, 1981. **113**(2): p. 776-80.
186. Kosugi, I., et al., *Cytomegalovirus infection of the central nervous system stem cells from mouse embryo: a model for developmental brain disorders induced by cytomegalovirus*. Lab Invest, 2000. **80**(9): p. 1373-1383.
187. Tsutsui, Y., H. Kawasaki, and I. Kosugi, *Reactivation of latent cytomegalovirus infection in mouse brain cells detected after transfer to brain slice cultures*. J Virol, 2002. **76**(14): p. 7247-7254.
188. Cheeran, M.C.J., et al., *Neural precursor cell susceptibility to human cytomegalovirus diverges along glial or neuronal differentiation pathways*. J Neurosci Res, 2005. **82**(6): p. 839-850.
189. Tsutsui, Y., I. Kosugi, and H. Kawasaki, *Neuropathogenesis in cytomegalovirus infection: indication of the mechanisms using mouse models*. Rev Med Virol, 2005. **15**(5): p. 327-345.
190. Matsukage, S., et al., *Mouse embryonic stem cells are not susceptible to cytomegalovirus but acquire susceptibility during differentiation*. Birth Defects Research Part A: Clinical and Molecular Teratology, 2006. **76**(2): p. 115-125.
191. Goodwin, T.J., et al., *Three-Dimensional Normal Human Neural Progenitor Tissue-Like Assemblies: A Model of Persistent Varicella-Zoster Virus Infection*. PLoS Pathog, 2013. **9**(8): p. e1003512.
192. Dukhovny, A., et al., *Varicella-zoster virus infects human embryonic stem cell-derived neurons and neurospheres but not pluripotent embryonic stem cells or early progenitors*. J Virol, 2012. **86**(6): p. 3211-8.
193. Markus, A., et al., *Varicella-zoster virus (VZV) infection of neurons derived from human embryonic stem cells: direct demonstration of axonal infection, transport of VZV, and productive neuronal infection*. J Virol, 2011. **85**(13): p. 6220-33.
194. Yu, X., et al., *Varicella zoster virus infection of highly pure terminally differentiated human neurons*. J Neurovirol, 2013. **19**(1): p. 75-81.
195. Lee, K.S., et al., *Human Sensory Neurons Derived from Induced Pluripotent Stem Cells Support Varicella-Zoster Virus Infection*. PLoS ONE, 2012. **7**(12): p. e53010.
196. Rotschafer, J.H., et al., *Modulation of neural stem/progenitor cell proliferation during experimental Herpes Simplex encephalitis is mediated by differential FGF-2 expression in the adult brain*. Neurobiology of Disease, 2013. **58**(0): p. 144-155.
197. De Filippis, L., et al., *Differentiated human neural stem cells: a new ex vivo model to study HHV-6 infection of the central nervous system*. J Clin Virol, 2006. **37 Suppl 1**: p. S27-32.
198. Lawrence, D.M., et al., *Human immunodeficiency virus type 1 infection of human brain-derived progenitor cells*. J Virol, 2004. **78**(14): p. 7319-28.

199. Okamoto, S.-i., et al., *HIV/gp120 decreases adult neural progenitor cell proliferation via checkpoint kinase-mediated cell-cycle withdrawal and G1 arrest*. *Cell Stem Cell*, 2007. **1**(2): p. 230-236.
200. Rothenaigner, I., et al., *Long-term HIV-1 infection of neural progenitor populations*. *AIDS*, 2007. **21**(17): p. 2271-81.
201. Kaul, M., G.A. Garden, and S.A. Lipton, *Pathways to neuronal injury and apoptosis in HIV-associated dementia*. *Nature*, 2001. **410**(6831): p. 988-994.
202. Tabor-Godwin, J.M., et al., *The role of autophagy during coxsackievirus infection of neural progenitor and stem cells*. *Autophagy*, 2012. **8**(6): p. 938-953.
203. Honda, T., et al., *The coxsackievirus-adenovirus receptor protein as a cell adhesion molecule in the developing mouse brain*. *Brain Res Mol Brain Res*, 2000. **77**(1): p. 19-28.
204. Feuer, R., et al., *Coxsackievirus targets proliferating neuronal progenitor cells in the neonatal CNS*. *J Neurosci*, 2005. **25**(9): p. 2434-2444.
205. Ariff, I.M., et al., *Japanese encephalitis virus infection alters both neuronal and astrocytic differentiation of neural stem/progenitor cells*. *J Neuroimmune Pharmacol*, 2013. **8**(3): p. 664-76.
206. Das, S. and A. Basu, *Inflammation: a new candidate in modulating adult neurogenesis*. *J Neurosci Res*, 2008. **86**(6): p. 1199-1208.
207. Das, S. and A. Basu, *Japanese encephalitis virus infects neural progenitor cells and decreases their proliferation*. *J Neurochem*, 2008. **106**(4): p. 1624-1636.
208. Das, S., D. Ghosh, and A. Basu, *Japanese encephalitis virus induce immuno-competency in neural stem/progenitor cells*. *PLoS One*, 2009. **4**(12): p. e8134.
209. Hans, A., et al., *Persistent, noncytolytic infection of neurons by Borna disease virus interferes with ERK 1/2 signaling and abrogates BDNF-induced synaptogenesis*. *FASEB J*, 2004. **18**(7): p. 863-5.
210. Metcalf, T.U., et al., *Recruitment and retention of B cells in the central nervous system in response to alphavirus encephalomyelitis*. *J Virol*, 2013. **87**(5): p. 2420-9.
211. Schaumburg, C., et al., *Human embryonic stem cell-derived oligodendrocyte progenitor cells express the serotonin receptor and are susceptible to JC virus infection*. *J Virol*, 2008. **82**(17): p. 8896-9.
212. Ferenczy, M.W., et al., *Differentiation of human fetal multipotential neural progenitor cells to astrocytes reveals susceptibility factors for JC virus*. *J Virol*, 2013. **87**(11): p. 6221-31.
213. Besson Duvanel, C., P. Honegger, and J.-M. Matthieu, *Antibodies directed against rubella virus induce demyelination in aggregating rat brain cell cultures*. *Journal of Neuroscience Research*, 2001. **65**(5): p. 446-454.
214. Domegan, L.M. and G.J. Atkins, *Apoptosis induction by the Therien and vaccine RA27/3 strains of rubella virus causes depletion of oligodendrocytes from rat neural cell cultures*. *Journal of General Virology*, 2002. **83**(9): p. 2135-2143.
215. Natale, V.A.I., et al., *Effect of infection with rubella virus on the development of rat cerebellar cells in culture*. *Neuropathology and Applied Neurobiology*, 1993. **19**(6): p. 530-534.
216. Tosh, P.K., et al., *Correlation between rubella antibody levels and cytokine measures of cell-mediated immunity*. *Viral Immunol*, 2009. **22**(6): p. 451-6.
217. PetruzzIELLO, R., et al., *Pathway of rubella virus infectious entry into Vero cells*. *Journal of General Virology*, 1996. **77**(2): p. 303-308.

218. Baumann, N. and D. Pham-Dinh, *Biology of oligodendrocyte and myelin in the mammalian central nervous system*. *Physiol Rev*, 2001. **81**(2): p. 871-927.
219. Dukhovny, A., et al., *VZV infects human embryonic stem cell-derived neurons and neurospheres, but not pluripotent embryonic stem cells or early progenitors*. *Journal of Virology*, 2012.
220. Davis, H.E., et al., *Charged polymers modulate retrovirus transduction via membrane charge neutralization and virus aggregation*. *Biophys J*, 2004. **86**(2): p. 1234-42.
221. Penkert, R.R. and R.F. Kalejta, *Human embryonic stem cell lines model experimental human cytomegalovirus latency*. *MBio*, 2013. **4**(3): p. e00298-13.
222. D'Aiuto, L., et al., *Human induced pluripotent stem cell-derived models to investigate human cytomegalovirus infection in neural cells*. *PLoS One*, 2012. **7**(11): p. e49700.
223. Simons, M.J., *Congenital rubella: an immunological paradox?* *Lancet*, 1968. **2**(7581): p. 1275-8.
224. Atkins, G.J., et al., *Transient virus infection and multiple sclerosis*. *Rev Med Virol*, 2000. **10**(5): p. 291-303.
225. Godec, M.S., et al., *Absence of measles, mumps, and rubella viral genomic sequences from multiple sclerosis brain tissue by polymerase chain reaction*. *Ann Neurol*, 1992. **32**(3): p. 401-4.
226. van den Pol, A.N., *Viral infection leading to brain dysfunction: more prevalent than appreciated?* *Neuron*, 2009. **64**(1): p. 17-20.
227. Oker-Blom, C., et al., *Rubella virus contains one capsid protein and three envelope glycoproteins, E1, E2a, and E2b*. *J Virol*, 1983. **46**(3): p. 964-73.
228. Wang, D. and T. Shenk, *Human cytomegalovirus UL131 open reading frame is required for epithelial cell tropism*. *J Virol*, 2005. **79**(16): p. 10330-8.
229. Gerna, G., et al., *Human Cytomegalovirus Replicates Abortively in Polymorphonuclear Leukocytes after Transfer from Infected Endothelial Cells via Transient Microfusion Events*. *Journal of Virology*, 2000. **74**(12): p. 5629-5638.
230. Preece, M.A., P.J. Kearney, and W.C. Marshall, *Growth-hormone deficiency in congenital rubella*. *Lancet*, 1977. **2**(8043): p. 842-4.
231. Scholzen, T. and J. Gerdes, *The Ki-67 protein: from the known and the unknown*. *J Cell Physiol*, 2000. **182**(3): p. 311-22.
232. Wang, L. and W.S. Kisaalita, *Characterization of micropatterned nanofibrous scaffolds for neural network activity readout for high-throughput screening*. *J Biomed Mater Res B Appl Biomater*, 2010. **94**(1): p. 238-49.
233. Rowe, J., et al., *Heterogeneity in Diphtheria-Tetanus-Acellular Pertussis Vaccine-Specific Cellular Immunity during Infancy: Relationship to Variations in the Kinetics of Postnatal Maturation of Systemic Th1 Function*. *Journal of Infectious Diseases*, 2001. **184**(1): p. 80-88.
234. Marzi, M., et al., *Characterization of type 1 and type 2 cytokine production profile in physiologic and pathologic human pregnancy*. *Clinical & Experimental Immunology*, 1996. **106**(1): p. 127-133.
235. Tamayo-Sarver, J.H., et al., *Advanced statistics: how to determine whether your intervention is different, at least as effective as, or equivalent: a basic introduction*. *Acad Emerg Med*, 2005. **12**(6): p. 536-42.
236. Plotkin, S.A., *ROutes of fetal infection and mechanisms of fetal damage*. *American Journal of Diseases of Children*, 1975. **129**(4): p. 444-449.

237. Frisch, S.M. and R.A. Screaton, *Anoikis mechanisms*. *Curr Opin Cell Biol*, 2001. **13**(5): p. 555-62.
238. Chang, Y.C., C.C. Huang, and C.C. Liu, *Frequency of linear hyperechogenicity over the basal ganglia in young infants with congenital rubella syndrome*. *Clin Infect Dis*, 1996. **22**(3): p. 569-71.
239. Golstein, P. and G. Kroemer, *Cell death by necrosis: towards a molecular definition*. *Trends Biochem Sci*, 2007. **32**(1): p. 37-43.
240. Martinez, L.D. and M.T. Zapata, *Apoptosis induction by the infection with Gilchrist strain of rubella virus*. *J Clin Virol*, 2002. **25**(3): p. 309-15.
241. Peng, H., et al., *Cellular IAP1 regulates TRAIL-induced apoptosis in human fetal cortical neural progenitor cells*. *J Neurosci Res*, 2005. **82**(3): p. 295-305.
242. Ellis, R.E., J.Y. Yuan, and H.R. Horvitz, *Mechanisms and functions of cell death*. *Annu Rev Cell Biol*, 1991. **7**: p. 663-98.
243. Levine, B., et al., *Conversion of lytic to persistent alphavirus infection by the bcl-2 cellular oncogene*. *Nature*, 1993. **361**(6414): p. 739-42.
244. Yuan, S.H., et al., *Cell-surface marker signatures for the isolation of neural stem cells, glia and neurons derived from human pluripotent stem cells*. *PLoS One*, 2011. **6**(3): p. e17540.
245. Salvant, B.S., E.A. Fortunato, and D.H. Spector, *Cell cycle dysregulation by human cytomegalovirus: influence of the cell cycle phase at the time of infection and effects on cyclin transcription*. *J Virol*, 1998. **72**(5): p. 3729-3741.
246. Krathwohl, M.D. and J.L. Kaiser, *Chemokines promote quiescence and survival of human neural progenitor cells*. *Stem Cells*, 2004. **22**(1): p. 109-118.
247. Krathwohl, M.D. and J.L. Kaiser, *HIV-1 promotes quiescence in human neural progenitor cells*. *J Infect Dis*, 2004. **190**(2): p. 216-226.
248. Tran, P.B. and R.J. Miller, *Chemokine receptors: signposts to brain development and disease*. *Nat Rev Neurosci*, 2003. **4**(6): p. 444-455.
249. Mahomed, A. and R. Chetty, *HUMAN immunodeficiency virus infection, bcl-2, p53 protein, and ki-67 analysis in ocular surface squamous neoplasia*. *Archives of Ophthalmology*, 2002. **120**(5): p. 554-558.
250. Zheng, X., et al., *Expression of Ki67 antigen, epidermal growth factor receptor and Epstein-Barr virus-encoded latent membrane protein (LMP1) in nasopharyngeal carcinoma*. *Eur J Cancer B Oral Oncol*, 1994. **30b**(5): p. 290-5.
251. Rawls, W.E., *Viral persistence in congenital rubella*. *Prog Med Virol*, 1974. **18**(0): p. 273-88.
252. Hoskins, J.M. and S.A. Plotkin, *Behaviour of rubella virus in human diploid cell strains. II. Studies of infected cells*. *Arch Gesamte Virusforsch*, 1967. **21**(3): p. 296-308.
253. Atreya, C.D., et al., *The rubella virus putative replicase interacts with the retinoblastoma tumor suppressor protein*. *Virus Genes*, 1998. **16**(2): p. 177-83.
254. Efklidou, S., et al., *vFLIP from KSHV inhibits anoikis of primary endothelial cells*. *J Cell Sci*, 2008. **121**(Pt 4): p. 450-7.
255. Iwakiri, D., T. Minamitani, and M. Samanta, *Epstein-Barr virus latent membrane protein 2A contributes to anoikis resistance through ERK activation*. *J Virol*, 2013. **87**(14): p. 8227-34.
256. Xu, J., et al., *Hepatitis B virus X protein confers resistance of hepatoma cells to anoikis by up-regulating and activating p21-activated kinase 1*. *Gastroenterology*, 2012. **143**(1): p. 199-212.e4.

257. Pukhalsky, A.L., et al., *Cytokine profile after rubella vaccine inoculation: evidence of the immunosuppressive effect of vaccination*. *Mediators of Inflammation*, 2003. **12**(4): p. 203-207.
258. Gealy, C., et al., *Posttranscriptional suppression of interleukin-6 production by human cytomegalovirus*. *J Virol*, 2005. **79**(1): p. 472-85.
259. Miller, M.T. and K. Stromland, *Teratogen update: thalidomide: a review, with a focus on ocular findings and new potential uses*. *Teratology*, 1999. **60**(5): p. 306-21.
260. Das, S. and A. Basu, *Viral infection and neural stem/progenitor cell's fate: Implications in brain development and neurological disorders*. *Neurochemistry International*, 2011. **59**(3): p. 357-366.
261. Lane, B., et al., *White matter MR hyperintensities in adult patients with congenital rubella*. *AJNR Am J Neuroradiol*, 1996. **17**(1): p. 99-103.
262. Dewhurst, S., et al., *Persistent productive infection of human glial cells by human immunodeficiency virus (HIV) and by infectious molecular clones of HIV*. *J Virol*, 1987. **61**(12): p. 3774-82.
263. Zurbriggen, A. and M. Vandevelde, *Canine distemper virus-induced glial cell changes in vitro*. *Acta Neuropathol*, 1983. **62**(1-2): p. 51-8.
264. Knutton, S. and T. Bachi, *The role of cell swelling and haemolysis in Sendai virus-induced cell fusion and in the diffusion of incorporated viral antigens*. *J Cell Sci*, 1980. **42**: p. 153-67.
265. Stohlman, S.A. and D.R. Hinton, *Viral induced demyelination*. *Brain Pathol*, 2001. **11**(1): p. 92-106.
266. Besson Duvanel, C., P. Honegger, and J.M. Matthieu, *Antibodies directed against rubella virus induce demyelination in aggregating rat brain cell cultures*. *J Neurosci Res*, 2001. **65**(5): p. 446-54.
267. Gaber, Z.B. and B.G. Novitch, *All the embryo's a stage, and Olig2 in its time plays many parts*. *Neuron*, 2011. **69**(5): p. 833-5.
268. Georgieva, L., et al., *Convergent evidence that oligodendrocyte lineage transcription factor 2 (OLIG2) and interacting genes influence susceptibility to schizophrenia*. *Proc Natl Acad Sci U S A*, 2006. **103**(33): p. 12469-74.
269. Buffo, A., et al., *Expression pattern of the transcription factor Olig2 in response to brain injuries: implications for neuronal repair*. *Proc Natl Acad Sci U S A*, 2005. **102**(50): p. 18183-8.
270. Buffo, A., et al., *Origin and progeny of reactive gliosis: A source of multipotent cells in the injured brain*. *Proc Natl Acad Sci U S A*, 2008. **105**(9): p. 3581-6.
271. Young, R.A., *Control of the embryonic stem cell state*. *Cell*, 2011. **144**(6): p. 940-54.
272. Ivanova, N.B., et al., *A Stem Cell Molecular Signature*. *Science*, 2002. **298**(5593): p. 601-604.
273. Zhou, J., et al., *High-efficiency induction of neural conversion in human ESCs and human induced pluripotent stem cells with a single chemical inhibitor of transforming growth factor beta superfamily receptors*. *Stem Cells*, 2010. **28**(10): p. 1741-50.
274. Mayer-Proschel, M., et al., *Human neural precursor cells – an in vitro characterization*. *Clinical Neuroscience Research*, 2002. **2**(1–2): p. 58-69.
275. Kalcheva, N., et al., *Genomic structure of human microtubule-associated protein 2 (MAP-2) and characterization of additional MAP-2 isoforms*. *Proc Natl Acad Sci U S A*, 1995. **92**(24): p. 10894-8.
276. Mariani, M., et al., *Class III beta-tubulin (TUBB3): more than a biomarker in solid tumors?* *Curr Mol Med*, 2011. **11**(9): p. 726-31.
277. Lalonde, R. and C. Strazielle, *Neurobehavioral characteristics of mice with modified intermediate filament genes*. *Rev Neurosci*, 2003. **14**(4): p. 369-85.

278. Maurer, H.a.K., W, *Towards a molecular signature of neural stem cells*, in *Neural stem cell research*, E.V. Greer, Editor. 2006, Nova Science Publishers: New York. p. xi, 185 p.
279. Raff, M.C., R.H. Miller, and M. Noble, *A glial progenitor cell that develops in vitro into an astrocyte or an oligodendrocyte depending on culture medium*. *Nature*, 1983. **303**(5916): p. 390-6.
280. Ziskin, J.L., et al., *Vesicular release of glutamate from unmyelinated axons in white matter*. *Nat Neurosci*, 2007. **10**(3): p. 321-30.
281. Nishiyama, A., et al., *Polydendrocytes (NG2 cells): multifunctional cells with lineage plasticity*. *Nat Rev Neurosci*, 2009. **10**(1): p. 9-22.
282. Wang, H., et al., *Myelin oligodendrocyte glycoprotein antibodies and multiple sclerosis in healthy young adults*. *Neurology*, 2008. **71**(15): p. 1142-6.
283. Tejada-Simon, M.V., et al., *Cross-reactivity with myelin basic protein and human herpesvirus-6 in multiple sclerosis*. *Ann Neurol*, 2003. **53**(2): p. 189-97.
284. Sakamoto, Y., et al., *Complete amino acid sequence of PO protein in bovine peripheral nerve myelin*. *J Biol Chem*, 1987. **262**(9): p. 4208-14.
285. Bullwinkel, J., et al., *Ki-67 protein is associated with ribosomal RNA transcription in quiescent and proliferating cells*. *J Cell Physiol*, 2006. **206**(3): p. 624-35.
286. Schwartz, L. and E.O. Major, *Neural progenitors and HIV-1-associated central nervous system disease in adults and children*. *Curr HIV Res*, 2006. **4**(3): p. 319-327.
287. Frolova, E.I., et al., *Functional Sindbis virus replicative complexes are formed at the plasma membrane*. *J Virol*, 2010. **84**(22): p. 11679-95.
288. Matthews, J.D., et al., *Do viruses require the cytoskeleton?* *Viol J*, 2013. **10**(121): p. 10-121.
289. Rajan, P., *STATus and Context within the Mammalian Nervous System*. *Mol Med*, 2011. **17**(9-10): p. 965-73.
290. Shioda, N., F. Han, and K. Fukunaga, *Role of Akt and ERK signaling in the neurogenesis following brain ischemia*. *Int Rev Neurobiol*, 2009. **85**: p. 375-87.
291. Reinartz, A.B., M.G. Broome, and B.P. Sagik, *Age-dependent resistance of mice to sindbis virus infection: viral replication as a function of host age*. *Infect Immun*, 1971. **3**(2): p. 268-273.
292. Griffin, D.E., *Role of the immune response in age-dependent resistance of mice to encephalitis due to Sindbis virus*. *J Infect Dis*, 1976. **133**(4): p. 456-464.
293. Wollmann, G., P. Tattersall, and A.N. van den Pol, *Targeting Human Glioblastoma Cells: Comparison of Nine Viruses with Oncolytic Potential*. *Journal of Virology*, 2005. **79**(10): p. 6005-6022.
294. Wang, K.S., et al., *High-affinity laminin receptor is a receptor for Sindbis virus in mammalian cells*. *J Virol*, 1992. **66**(8): p. 4992-5001.
295. Levine, B., *Apoptosis in viral infections of neurons: a protective or pathologic host response?* *Curr Top Microbiol Immunol*, 2002. **265**: p. 95-118.
296. Taga, T. and S. Fukuda, *Role of IL-6 in the neural stem cell differentiation*. *Clin Rev Allergy Immunol*, 2005. **28**(3): p. 249-56.
297. Nuttall, J.R. and P.I. Oteiza, *Zinc and the ERK kinases in the developing brain*. *Neurotox Res*, 2012. **21**(1): p. 128-41.
298. Pleschka, S., *RNA viruses and the mitogenic Raf/MEK/ERK signal transduction cascade*. *Biol Chem*, 2008. **389**(10): p. 1273-82.

299. Widera, D., et al., *Potential role of NF-kappaB in adult neural stem cells: the underrated steersman?* Int J Dev Neurosci, 2006. **24**(2-3): p. 91-102.
300. Vitiello, M., et al., *NF-kappaB as a potential therapeutic target in microbial diseases.* Mol Biosyst, 2012. **8**(4): p. 1108-20.
301. Farmer, J.R., et al., *Activation of the Type I Interferon Pathway Is Enhanced in Response to Human Neuronal Differentiation.* PLoS ONE, 2013. **8**(3): p. e58813.

APPENDICES

APPENDIX A. HYPOTHETICAL STATISTIC TEST

14	STATIS	NC						Fth						
15		1	2	3	Hypo4	average	SD	1	2	3	Hypo4	average	SD	ttest
16	0						0						0	
17	3	4.95	4.275	6.716667	4.95	5.313889	1.260851	5	4.6	5.55	5	5.05	0.47697	0.616948
18	5	9.82	7.8	14.2	9.82	10.60667	3.271717	10.4	8.3	10.36667	10.4	9.688889	1.202929	0.654354
19	7	37.8	23.55	25.5	37.8	28.95	7.726092	33.4	23.7	18.06667	33.4	25.05556	7.756025	0.082354
20	9	62	37.325	47.33333	62	48.88611	12.41057	50.8	30.9	42.33333	50.8	41.34444	9.986788	0.013455
21	11	72.4	58.575	48.33333	72.4	59.76944	12.07771	51.8	48.025	45	51.8	48.275	3.406886	0.046716